ON THE USE OF EXTENDED X-RAY ABSORPTION FINE STRUCTURE

SPECTROSCOPY TO DETERMINE THE BONDING CONFIGURATIONS OF

ORTHOPHOSPHATE SURFACE COMPLEXES AT THE

GOETHITE/WATER INTERFACE

by

Dalton Belchior Abdala

A dissertation submitted to the Faculty of the University of Delaware in partial fulfillment of the requirements for the degree of Doctor of Philosophy in Plant and Soil Sciences

Fall 2012

ON THE USE OF EXTENDED X-RAY ABSORPTION FINE STRUCTURE

SPECTROSCOPY TO DETERMINE THE BONDING CONFIGURATIONS OF

ORTHOPHOSPHATE SURFACE COMPLEXES AT THE

GOETHITE/WATER INTERFACE

by

Dalton Belchior Abdala

Approved: _____
Blake C. Meyers, Ph.D.
Chair of the Department of Plant and Soil Sciences

Approved: _____
Mark Rieger, Ph.D.
Dean of the College of Agriculture and Natural Resources

Approved: _____
Charles G. Riordan, Ph.D.
Vice Provost for Graduate and Professional Education

I certify that I have read this dissertation and that in my opinion it meets the academic and professional standard required by the University as a dissertation for the degree of Doctor of Philosophy.

Signed: _____

Donald L. Sparks, Ph.D.
Professor in charge of dissertation

I certify that I have read this dissertation and that in my opinion it meets the academic and professional standard required by the University as a dissertation for the degree of Doctor of Philosophy.

Signed: _____

Paul Andrews Northrup, Ph.D.
Member of dissertation committee

I certify that I have read this dissertation and that in my opinion it meets the academic and professional standard required by the University as a dissertation for the degree of Doctor of Philosophy.

Signed: _____

Peter Leinweber, Ph.D.
Member of dissertation committee

I certify that I have read this dissertation and that in my opinion it meets the academic and professional standard required by the University as a dissertation for the degree of Doctor of Philosophy.

Signed: _____

Yuji Arai, Ph.D.
Member of dissertation committee

DEDICATION

Having met Matt Siebecker (Papa), Quenita (Mama) and Gabi (hermanita) was worthy of every moment I spent in Delaware during my four years of graduate studies at the University of Delaware. I am thankful to the opportunity of coming to the United States to pursue my Ph.D. because it gave me the chance to meet a part of my family that I would not have met otherwise. Together with my mom, you guys are to whom I dedicate all the efforts I put into this work.

ACKNOWLEDGMENTS

I can still remember the moment the train dropped me off at the train station near the Farm House. I must confess that my first feeling was to take the train back home immediately. Relentlessly, I decided to walk on and, with my luggage and my pigeon English, I looked for 30th Lovett Ave., where the Office of Foreign Student & Scholars was then located. That was the only address in Delaware I had in my mind and where I knew that I would have to stop by eventually.

I would like to start out this acknowledgments session by thanking Matt Ginder-Vogel for finding me a place at the Farm House to stay until I found an apartment to live. Notwithstanding, my deepest thanks go to Matt Siebecker and Quenita for having found me a place in their lives since my very first days here until the very last ones. I'll never forget Matt introducing me to Quenita and saying that I was Brazilian; she started speaking to me in Spanish…

I recognize that without the patience and assistance of Dr. Paul Northrup in this work, it would not be possible to be completed. For this, I am grateful to him for the time he spent on this project, for his dedication and intense involvement in my research. I will certainly remember him when doing any XAS analysis.

I am most appreciative to Dr. Sparks for the opportunity of pursuing my Ph.D. in his renowned research group. He was always there to help me with whatever I needed from him and I'm aware that if he didn't do more it was only because it was certainly out of his reach. I am also thankful to the "all-purpose" Jerry Hendricks for

TABLE OF CONTENTS

viii

LIST OF TABLES

LIST OF FIGURES

ABSTRACT

Phosphate transport, cycling and availability in soils are strongly affected by sorption reactions with Al- and Fe- (hydr)oxides, 1:1 silicate clays and with some components of soil organic matter. The importance of these reactions lies in the fact that phosphorus (P) can be a limiting nutrient in terrestrial ecosystems, and sorptive removal of natural or fertilizer P can impact the health and the production levels of agriculture. Notwithstanding, sorption/desorption reactions controlling excess P concentrations in soils, particularly as a result of anthropogenic activity, are also important to ensure soil and water quality. A great deal of research on P retention mechanisms in soils and soil components has been conducted over the last decades. However, in spite of the large amount of literature garnered from the decades of research on this subject, studies addressing P sorption mechanisms, particularly on goethite, have resulted in countless conflicting interpretations of binding mechanisms. With the advent of more sophisticated molecular-scale techniques, such as Extended X-Ray Absorption Fine Structure (EXAFS) spectroscopy, one is now able to measure interatomic distances between an X-ray absorbing atom and its nearest neighbors and to assign sorption mechanisms based on the bonding distances between the two entities. In this study, we employed EXAFS spectroscopy to examine the effects that some environmental conditions impart on P surface complexation at the goethite/water

interface. Three sets of experiments were performed in order to obtain detailed structural information on the P structures formed on goethite as a function of (i) surface loading, (ii) pH and (iii) residence time. The first set of experiments (chapter 2) was intended to address the surface loading effects of P on the sorption mechanisms in which goethite was reacted with orthophosphate at P concentrations of 0.1, 0.2, and 0.8 mmol L^{-1} at pH 4.5 for 5 days. EXAFS analysis revealed a continuum between adsorption and surface precipitation, with bidentate mononuclear (^{2}E), bidentate binuclear (^{2}C) and monodentate mononuclear (^{1}V) surface complexes as well as surface precipitates forming at the goethite/water interface under the studied conditions. It was also shown that the coexistence of different surface complexes or the predominance of one sorption mechanism over others was directly related to surface loading. The second and third sets of experiments (chapter 3) were carried out to provide information on how the local chemical environment of sorbed P changes as an effect of pH and time. Goethite was reacted with orthophosphate at a P concentration of 0.8 mmol L^{-1} P at pH 3.0, 4.5 and 6.0. The residence time effect on the mechanisms of P sorption on goethite was also evaluated for two different reaction times, 5 and 18 days, on goethite suspensions reacted at pH 4.5. The monodentate surface complex was shown to be the predominant mechanism by which P sorbs at the goethite surface under the experimental conditions. The lack of a discrete Fe − P shell and the presence of highly disordered structures, particularly, at R-space $\geq$ 4 suggested the formation of P surface precipitates at the goethite/water interface.

In the last set of experiments, soils from a field-scale experiment were sampled and analyzed in order to assess the long-term effects of consecutive application of swine and cattle manures (M) on P reactivity and distribution in highly weathered agricultural lands of Paraná state, Brazil. Phosphorus K-edge spectroscopy was employed along with sequential P chemical fractionation and desorption kinetics experiments to provide macro and micro-scale information on the long-term fate of M application on those soils. The M rates applied to those soils over the years were typical of intensive agricultural areas in Brazil, varying from approximately 25 to 90 ton ha^{-1} year^{-1} on a dry weight basis. The soils have been cropped year round for 10, 20 and 40 years with different land managements, namely Tifton pastureland, no-tillage and conventional agriculture, respectively.

Soil test P (STP) values ranged from 3.7 up to 4.3 times as much higher than the reference soil. A sharp increase in amorphous Fe and Al amounts were observed as an effect of the consecutive application of M. Whereas our results showed that the P sorption capacity of some manured soils remained unchanged, P risk assessment indices such as DPS_{M-3}, DPS_{Ox}, PSS and PSR-II indicated that P losses should be expected, likely due to the excessive M rates applied to those soils. The much higher contents of amorphous Fe and Al (hydr)oxides in manured soils seem to have counterbalanced the inhibiting effect of SOM on P sorption by creating additional P sorbing sites. Accordingly, the newly created P sorbing surfaces were important to prevent an even larger P loss potential. This observation was in good agreement with desorption kinetics data, which showed that higher half-lives of P in manured soils

might have been due to an enhanced P sorption due to higher amorphous Fe and Al (hydr)oxide contents. Additionally, P in manured soils was shown to be associated with less labile pools. The shortest half-life and thus fastest P turnover in the adjacent forest soil might have been related to more labile P pools in the untreated soil. Although manure application led to an overall enlargement of P pools, reactive P was mainly associated with the less bioavailable ones, as evidenced by sequential P fractionation data. The consecutive application of animal manures was shown to have an effect on the transformation of crystalline into amorphous Fe- and Al-containing minerals, as evidenced by ammonium oxalate extractions of Fe and Al and confirmed by visual inspection of XANES spectra, showing the presence of the diagnostic pre-edge feature of crystalline Fe(III)-minerals in the adjacent area and its absence in manured soils. Accordingly, the highly reactive non-crystalline Fe-containing minerals formed are presumably the main surfaces to which P from the animal manures is held.

Chapter 1

INTRODUCTION

1.1.1 Phosphorus in the Environment

Phosphorus (P) is a naturally occurring element that can be found in the earth's crust and cycled in the environment as a result of weathering of geologic materials. In the biosphere, P can be found in all living organisms and in water. Vegetation, plankton and microbes are all active participants in the biotic phosphorus pool. Biotic maintenance is ultimately dependent upon P cycling through abiotic mechanisms, including sorption by soils and sediments, mineral precipitation, and sedimentation in aquatic systems.

Phosphorus is an essential element for life. As phosphate, it is a component of DNA, RNA, ATP and the phospholipids that form all cell membranes. Demonstrating the link between phosphorus and life, elemental phosphorus was historically first isolated from human urine, and bone ash was an important early phosphate source. The chief commercial use of phosphorus compounds is in the fertilizer industry (up to 80%) for crop fertilizer production, due to the need to replace the phosphorus that plants remove from the soil. Other applications include the role of organo-phosphorus compounds in pesticides and detergents (Diskowski & Hoffmann, 2005).

Because P is a vital nutrient for plants and animals, low phosphate levels are important limiting factors to growth in terrestrial and aquatic systems.
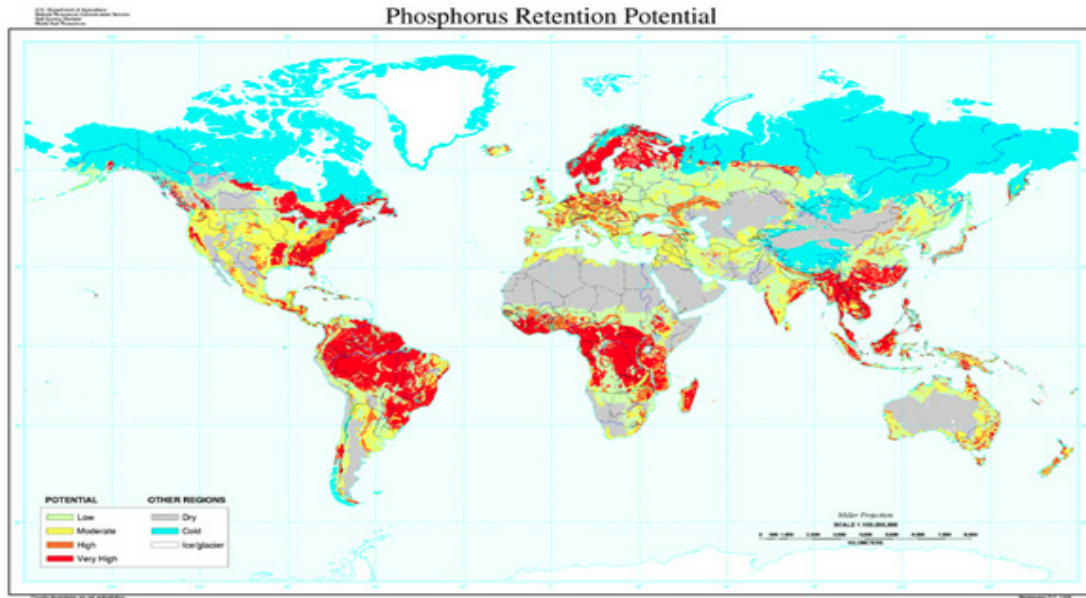
Figure 1.1a. Global P retention potential. Source: USDA, World Soil Resources Map Index, 2011
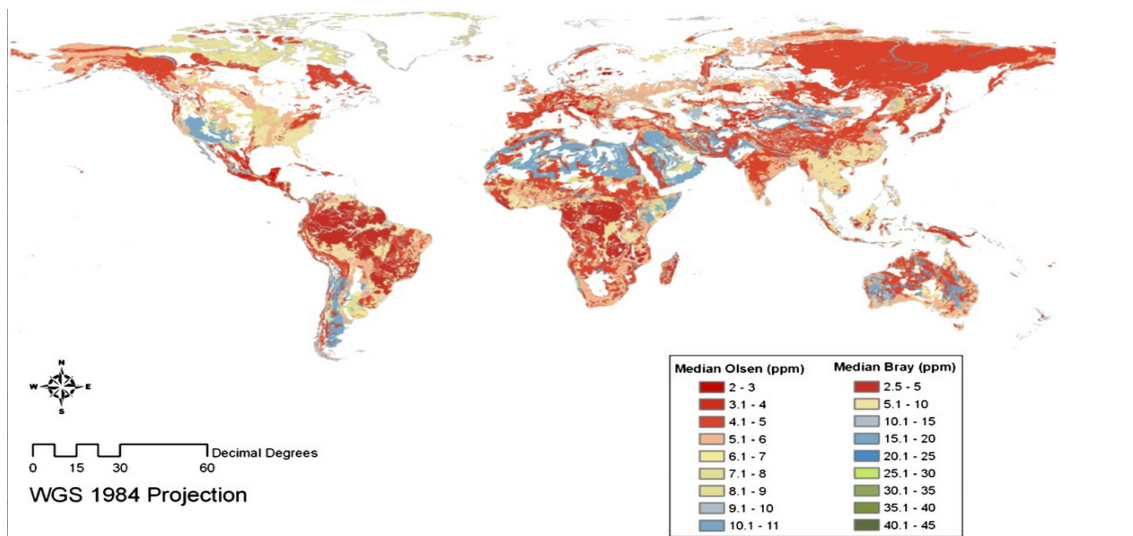
Figure 1.1b. Worldwide soil P depletion zones as a measure of P availability provided by Olsen and Bray plant available P extractant solutions. Source: WGS, 1984

Acid soils represent about 50% of the total arable land area in the world, being mostly found in the tropical and subtropical regions (Uexkull & Mutert, 1995). They constitute about 68, 38 and 27% of the soils in Tropical America, Tropical Asia and Tropical Africa, respectively (Pandey & Gardener, 1992). Figure 1a shows that P retention potential is high, particularly, in inherently P deficient tropical soils. Soils of these regions are extremely P-deficient, partly as a result of high P sorption associated with elevated levels of Fe- and Al-(hydr)oxides. Therefore, substantial P inputs are required for optimum growth and adequate food production (Sanchez & Buol, 1975).

Whereas agricultural areas of the tropics are threatened by inherently poor and P depleted soils (Figure 1b), global reserves of P are running out and, since plants need P to grow, this poses an enormous challenge for global food production in the foreseeable future. A shortage of phosphate could ultimately result in large-scale famine and social-political turmoil.

As long as there is no substitute for P, solutions to the problem of P scarcity include improving the efficiency of nutrient management in agriculture and the recovery of nutrients from waste, like biosolids and manures. This means that P shortage creates opportunities related to the increasing demand for technological innovation in recycling P from P-rich materials, improving agricultural waste use efficiency and recycling industries.

Phosphorus is one of 16 elements that is essential for plant growth. As a macronutrient (second only to nitrogen), massive amounts of phosphate-based fertilizers are used in agriculture. This is also because agricultural soils around the world are naturally low in

3

phosphorus, and most cropping systems on these soils require supplemental phosphorus to maximize yield potential.

Research has documented that applying fertilizer phosphorus increases crop growth and yields on soils that are naturally low in phosphorus and in soils that have been depleted through crop removal (Mullins, 2000).

Although the economic benefits of phosphorus fertilization on crop production are well documented, too much P can have negative effects on the environment. Phosphorus is a somewhat unique pollutant in that it is an essential element. It is a limiting factor in terms of biological production not only in soil environments, but also in aquatic systems. However, excessively fertilized soils, generally represented by agricultural soils with intensive farming, have been frequently associated with the build up of soil P and subsequent P losses to surface waters. As a result, P has been recognized as the main culprit in the eutrophication of natural waters. Accordingly, there has been an increasing demand to better understand P speciation in soils. Over the last two decades, spectroscopic techniques have been of particular interest to soil and environmental chemists for speciating P in soils.

The objective of this research is to obtain insights into the mechanisms that control P sorption on an Fe bearing mineral oxide – goethite – at environmentally relevant pHs over a range of residence times. The information obtained in our studies is important in modeling P sorption/desorption reactions on mineral oxide surfaces and obtaining insights into the fate and reactivity of inorganic P in highly weathered soils.

1.1.2   Phosphorus Chemistry

P belongs to the Group 5A in the periodic table with an electronic configuration of ([Ne] $4s^2$ $4p^3$). Although P is widely distributed in nature, it is not found by itself in the elemental form. Elemental P in its pentavalent state is extremely reactive and will combine with Oxygen when exposed to the oxidizing atmosphere. It results in the formation of phosphate (PO_4^{3-}) and usually displays tetrahedral sp3 hybridization. The phosphate anion is holosymmetric, with the 3 negative charges equally distributed over the 4 Oxygens by resonance.

In natural systems, like soil and water, P will exist predominantly as the ion phosphate. Orthophosphate, the simplest phosphate, has the chemical formula PO_4^{-3}. In water, orthophosphate mostly exists as $H_2PO_4^-$ in acidic conditions or as HPO_4^{2-} in alkaline conditions. The diagram below shows the fractional distribution of P species in aqueous solution as a function of pH.
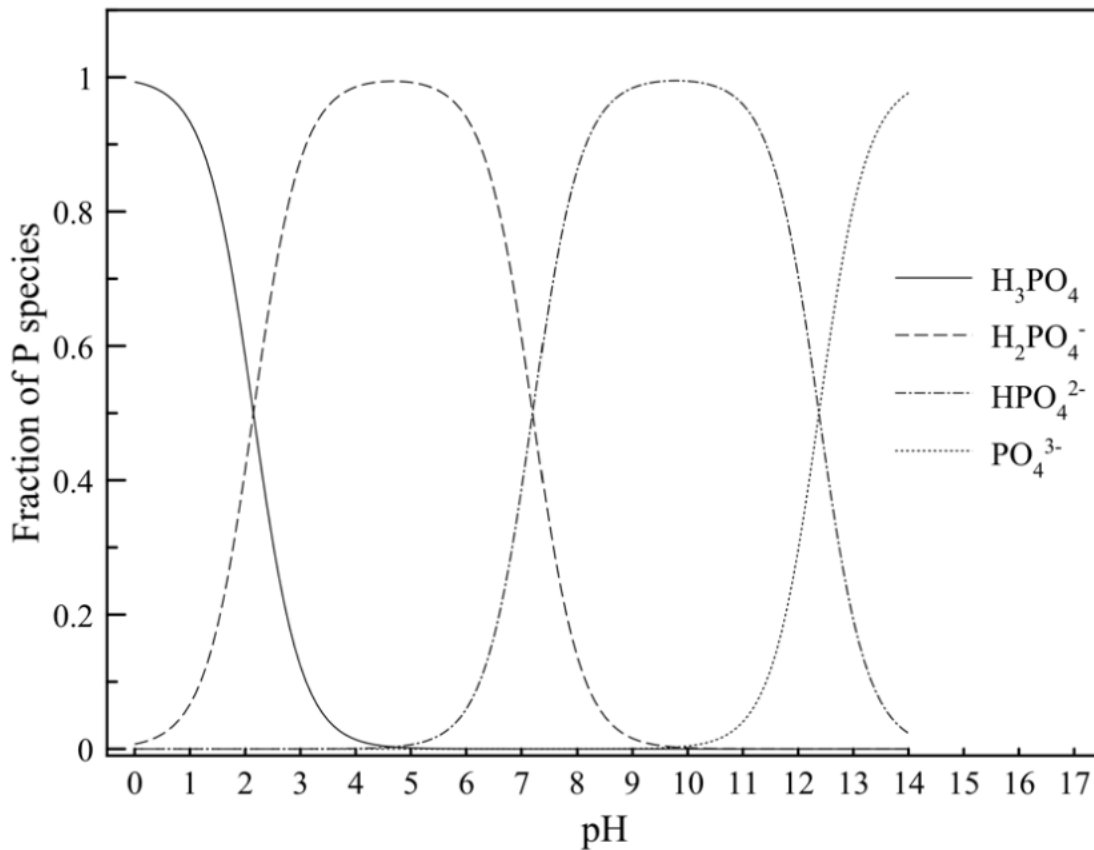
Figure 1.2. Fractional distribution of P species in aqueous solution as a function of pH.

When P_2O_5 is dissolved in water, the tribasic H_3PO_4 is formed. The deprotonation of H_3PO_4 yields its three anions with respective log Kp's, $H_2PO_4^-$ (2.12), HPO_4^{2-} (7.21) and PO_4^{3-} (12.6). The conjugate bases phosphate can produce are:

$[H_3PO_4] \leftrightarrow [H^+] + [H_2PO_4^-]$ $\qquad\qquad$ $pK_{a1} = 2.12$

$[H_2PO_4^-] \leftrightarrow [H^+] + [HPO_4^{2-}]$ $\qquad\qquad$ $pK_{a2} = 7.21$

$[HPO_4^{2-}] \leftrightarrow [H^+] + [PO_4^{3-}]$ $\qquad\qquad$ $pK_{a3} = 12.6$
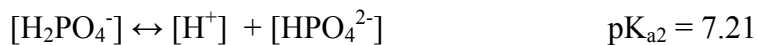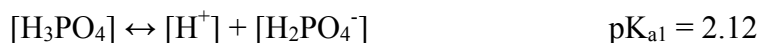
At the typical soil pH range, phosphate is found as the ion $H_2PO_4^-$. Therefore, this is the most important phosphate species involved in reactions that control its cycling in natural settings.

1.1.3   Phosphorus in Soil Environments

Soil phosphorus may exist in different forms, including orthophosphate, phosphorus in organic compounds (commonly referred to as organic phosphorus) and condensed phosphate. Despite orthophosphate being the most bioavailable P form in soils, it is not the only P fraction present. According to Harrison (1987), the organic pool of P may be large, accounting for as much as 30 to 65% of the total P in soils, but it must otherwise be hydrolyzed before being taken up by plants.

Given the high adsorption capacity of tropical soils for inorganic phosphate and, therefore, the limited P availability to plants, the delivery of P from organic matter is an important mechanism by which plants may acquire this nutrient (Giaveno et al., 2008).

The mechanisms of P sorption in soils and sediments are complicated because they vary from one form to another. Celi et al. (1999) and Guan et al. (2005) have reported that the adsorption of myo-inositol hexakisphosphate (myo-IHP) on clay minerals resulted in an increase in the pH level due to the release of OH^- ions. Accordingly, the adsorption of myo-IHP may lead to a decreased sorption capacity of soils by either competing with orthophosphates for sorption sites or by reducing the sorption capacity by hydroxylation of the mineral surfaces. Ognalaga et al. (1994) observed that the adsorption of organic

phosphate and condensed phosphate shifted the zeta potential of the adsorbents from positive to negative, which could also affect the adsorption of orthophosphate.

1.1.4   Phosphorus Sorption as Affected by Chemical Characteristics of Highly Weathered Soils

According to von Uexkull & Mutert (1995), soil acidity affects up to 50 % of agricultural land throughout the world and, as a consequence, so does P availability. In the early 1970's, a great contingent of soil scientists from around the world, propelled by the need to incorporate soils of tropical zones into an agricultural perspective in terms of enhanced food production, made great advances in P chemistry by improving our knowledge of P reactions in highly weathered soils (Jensen, 1970; Barrow, 1974; Novais, 1977; Khasawneh et al., 1980). This allowed for better soil management practices and enhanced understanding of P availability. Nevertheless, there still is a lack of understanding of P reactivity, particularly, P interactions with organic matter. This is primarily true with respect to organic-based agriculture, which relies on the application of high amounts of organic materials, adding large amounts of carbon into the soil. This area has received great attention because, in spite of the high P sorption capacity of highly weathered soils, P losses from agricultural soils have been reported and frequently associated with agricultural lands receiving organic residues. This results in a rapid release of nutrients, which in turn, may facilitate nutrient losses and pose a potential harm to the environment, especially to natural water bodies.

Tropical soils are characterized by a high degree of weathering and have marginal fertility characterized by low cation exchange capacity (CEC), low pH, low organic matter content and high point of zero charge (PZC) and significant anion adsorption

capacity (AEC). These characteristics are due to the large amount of crystalline iron (Fe) and aluminum (Al) (hydr)oxides, predominantly goethite, hematite and gibbsite, and amorphous ferrihydrite and bohemite. Among the essential plant nutrients, P is the one that is most limiting due its high fixation on Fe- and Al-oxides.

 Since the PZC of these soils is generally high (commonly ranging from 7 to 10), the soils carry a net positive charge on which anionic species may bind either specifically, forming an inner-sphere complex, or electrostatically, forming an outer-sphere complex. The former has higher adsorption energy since the adsorbate forms a covalent bond directly with the mineral moiety, whereas the latter exhibits electrostatic character and the adsorbate is loosely bound. The adsorption of phosphate onto mineral oxides displays different modes of bonding, as mono and bidentate (when the phosphate is bound to one or two oxygens, respectively) besides forming mono or binuclear complexes (when the phosphate ion is bound to oxygen(s) in the corner of a single or two octahedrons, respectively) (Sparks, 2002).

1.1.5   Investigating Phosphorus Sorption Mechanisms on Soil Components

Much of the attention in the past devoted to sorption of P on soils and soil components was related to plant availability. Investigators related available P fractions to the total P in soils through the use of chemical extractants in an attempt to reflect the plant's ability to uptake this nutrient (Mehlich, 1953; Mehlich, 1984; Hedley, 1982; Tiessen & Moir, 1993). Most studies were, however, based on macroscopic observations that provided a limited understanding of the actual solid phases of P present in soils. Such studies are

devoid of mechanistic meaning, e.g., no information on the type of complex formed on the sorbent surface. There is a need to understand the mechanisms of P retention on soils, as this will provide a more definitive understanding of the environmental fate, transport and speciation of P as well as P bioavailability. Early investigations aiming at understanding P bioavailability and its relation to the formation of surface complexes were based on fitting sorption data to the Langmuir equation. Elucidation of the surface complexes was speculative and inferred from multiple linear portions of the Langmuir plot, which were ascribed to sites of varying reactivity (Fried & Shapiro, 1956; Olsen & Watanabe, 1957). A two-site Langmuir equation was used in an attempt to describe the low- and high-energy sites involved in the sorption reaction (Holford et al., 1974; Sui & Thompson, 2000). Even though these empirical models describe sorption data well, the parameters obtained are valid only for the conditions under which the experiment is conducted. Using these models to predict adsorption under changing environmental conditions such as solution concentration, ionic strength, and pH is problematic.

Because there often is a correlation between the amount of sorption and the surface characteristics such as surface complexation capacity, surface charge and capacitance density, surface complexation models (SCMs), which are chemical models based on a molecular description of the electric double layer that use equilibrium-derived data (Goldberg, 1992) have extensively been used to model sorption phenomena in soil components and soils. SCMs consider the charge of both the adsorbate ion and the adsorbent surface. The modeling is based on the assumption of a homogeneous surface with a single surface site, which is composed of a hydroxyl species bound to a central cation that can undergo protonation or deprotonation reactions. The sorbing species is

depicted as one that binds only at isolated sites. According to Goldberg (1995), these models are a significant advancement over empirical models. However, even with a molecular description of the double layer and experimental sorption data, parameter uncertainty is still a major concern. Yet, parameterization raises an additional issue: an array of adjustable parameters is often required to fit the experimental data, and thus it may not be surprising that equilibrium data will fit a number of models equally well (Sparks, 2002). Westall & Hohl (1980) applied acid-base titration data from a TiO2 system to the CCM (Constant Capacitance Model), TLM (Triple Layer Model), DDL (Diffuse Double Layer) and Stern model and they observed that each of the models fit the experimental data well (Sparks, 2002). In addition to the above, one of the greatest limitations in the use of SCMs is the fact that they do not consider surface precipitation of oxyanions, although it has been known for a long time that surface nucleation of metal hydroxides frequently occurs (Scheidegger et al., 1998; Roberts et al., 1999; Scheinost et al., 1999).

Sorption sites of variable reactivity have been of interest to investigators because of the so-called hysteresis effect that is often observed with P sorption. Long-term sorption studies with goethite show slow desorption, which was attributed to P migration within internal pores or surface precipitation. Since goethite undergoes little structural reordering into more crystalline forms under oxic conditions, incorporation of P into crystalline structural sites forming a solid solution should not represent an important mechanism by which P is retained on goethite. Alternatively, at high P concentrations, surface precipitation may be catalyzed leading to a new solid phase that is less readily dissolved or desorbed. One way of studying the formation of these structures is through

the use of molecular scale spectroscopic techniques that enable one to conduct experiments at realistic environmental conditions.

XAS is a powerful in situ technique that provides detailed information on the chemistry of an element in basically any matrix ranging from minerals to biological specimens and solutions. The XAS spectrum is conventionally divided in two energy regions: X-ray absorption near edge spectroscopy or near edge X-ray absorption fine structure (XANES or NEXAFS) and extended X-ray absorption fine structure (EXAFS) spectroscopy (Lombi & Susini, 2009). Because the absorption edge of an element is related to the chemical environment of the absorbing atom and its oxidation state, selecting appropriate energies of the incoming X-ray photon allows one to selectively study a given element and its varied oxidation states. XAS has been employed in environmental sciences to study the dynamics and reactivity of environmentally relevant soil and water contaminants. XANES has been particularly useful in examining the distribution, speciation and oxidation state of a number of heavy metals (Scheinost et al., 2002; Strawn & Baker, 2008) and plant nutrients (Beauchemin et al., 2003; Khare et al., 2004; Maguire et al., 2006; Lombi et al., 2006; Kruse & Leinweber, 2008) while EXAFS has been employed to assess bonding mechanisms and interatomic distances. Since X-ray wavelengths of about 10 pm (0.1 Å) are comparable to interatomic distances, X-ray scattering yields information about the surrounding local environment in short-range order materials (Gates, 2006) and EXAFS can thus be of great help in providing direct information on the surface complexes being formed at the atomic level.

In light of the great advantages of EXAFS over other spectroscopic techniques, which often require drying and high vacuum, EXAFS spectroscopy has been among the most

prominent techniques for studies on the partitioning of heavy metals ions at mineral/water interfaces (Scheidegger et al., 1997; Fendorf et al., 1997). It has been widely used in studies on the surface complexation of environmentally relevant elements formed at mineral oxide surfaces and is an effective technique for conducting in situ studies addressing the concentration (Spadini et al., 1994; Roberts et al., 2003; Arai, 2010), pH (Roberts et al., 2003; Arai et al., 2004; Arai, 2010) and residence time (Charlet & Manceau, 1992; Manning et al., 1998; Scheidegger et al., 1998; Arai & Sparks, 2002) effects on the formation of and differentiation between sorption complexes and surface precipitates. Major contributions have been made in the use of this technique in the study of high Z elements, virtually those up to Mn. Hayes et al. (1987) were the first to use EXAFS to provide structural information on Se complexation on the goethite/water interface. Hayes and his co-workers were able to examine the type of coordinating ligand for the nearest neighbor on the Se-goethite system, to distinguish between outer- and inner-sphere complexes, and to determine the type of bonding, e. g. monodentate or bidentate.

Rose et al. (1997) performed P-EXAFS measurements on liquid samples to determine the local environment of phosphorus during the hydrolysis of $FeCl_3$ in the presence of phosphate. In this study, P K-edge EXAFS spectroscopy was useful to confirm previous results obtained by EXAFS at the Fe K-edge as well as to describe more precisely the type of linkage between the PO_4 tetrahedron and the Fe octahedra. Rouff et al. (2009) also employed P-EXAFS to study the effect of protonation on structural disorder of P species in solution and solid phases including more complex mineral phases like hydroxylapatite and struvite.

To the best of our knowledge, no single P K-edge EXAFS study has been carried out to examine P sorption complex formation at the mineral/water interface.

1.1.6 Examining Phosphorus Sorption Mechanisms on Mineral Oxides by X-Ray Absorption Spectroscopy

Phosphorus bioavailability, transport potential and cycling are soil chemical processes that are strongly dependent upon the sorption mechanism. Phosphorus is predominantly sorbed in soils by 1:1 clay minerals, such as kaolinite, and amorphous and crystalline Fe and Al (hydr)oxides as well as in precipitate forms such as Fe-, Al- and Ca-phosphates and organic matter complexes. The major mechanisms by which P sorbs onto mineral surfaces are: ligand exchange (adsorption), precipitation, lattice diffusion and anion exchange, with ligand exchange being the most important one (Sparks, 2002).

Kinetic studies carried out on iron oxides have divided phosphate reactions into two time regions (Barrow, 1985; Torrent et al., 1992): an initial rapid reaction followed by slower uptake kinetics which have been attributed to solid state diffusion, diffusion through surface pores, migration from within aggregated particles to surface sites and precipitation of insoluble phosphates at the surface (Torrent, 1991). A number of studies have been conducted to elucidate the sorption mechanism and surface complexation/precipitation dependence on environmental conditions, particularly pH and P loadings, using titration calorimetry (Penn & Warren, 2009), X-ray absorption spectroscopy (Khare et al., 2005; Khare et al., 2007) and IR spectroscopy (Tejedor-Tejedor & Anderson, 1990; Arai & Sparks, 2001). Nevertheless, interpretations of surface complex structures, such as whether monodentate or bidentate complexes form are not clear. In terms of goethite, IR studies have suggested that an inner-sphere

bidentate binuclear surface complex may be the predominant mechanism at low pHs (Tejedor-Tejedor & Anderson, 1990; Luengo et al., 2006) and low surface loadings (Rahnemaie et al., 2007). Kwon & Kubicki (2004) employed MO/DFT calculations to model surface complexes and their findings corroborate the studies above. However, a monodentate mononuclear surface complex has also been suggested at low pHs (Persson et al., 1996) and at high P loadings (Rahnemaie et al., 2007). Arai & Sparks (2001) have suggested that bidentate binuclear surface complexes that formed at pH 4 to 6 were protonated and unprotonated complexes formed at pH $\geq$ 7.5. However, it is important to point out that the sorption mechanism, based on assignments from FTIR studies, was based on different FTIR techniques and different data analysis, which caused differences in the assigned surface complexes. Thus, although FTIR has been used to investigate chemical bonding types in a number of studies, it has limitations in terms of data interpretation.

A number of studies looking at heavy metals have been carried out employing EXAFS to assess the effects of aging, pH, and surface loading on the type of surface complex formed on various mineral oxides (Fendorf et al., 1994; Fendorf & Sparks, 1994; Elzinga et al., 2001; Arai et al., 2001). Sorption studies on As, conducted from 4 min to approximately 12 months, showed that As(V) sorption on goethite increased with time. Sorption was initially rapid, with over 90% As(V) being sorbed in a 24-h period at pH 4 to 6. However, no changes in the molecular environment could be observed from analysis of the As EXAFS from samples incubated for various periods (O'Reilly et al., 2001). Likewise, there has been a great deal of research that showed a dependence of sorption complex type on pH. Arai & Sparks (2002) found that As(V) exhibited a

biphasic sorption behavior when reacted with gibbsite for 3 days to 1 year reaction time, and that the pH impacted the time for the reaction to reach quasi-equilibrium. At pH 4.5, the reaction was nearly completed after 3 days. However, slow adsorption continued at pH 7.8 after 1 year. In addition, residence time also directly affected desorption such that the longer the residence time (3 days to 1 year), the greater the decrease in As(V) desorption at both pHs.

Surface loading has a more pronounced effect on the continuum between surface complexation and surface precipitation (Sparks, 2002). The dependence of surface loading on whether an adsorption complex or surface precipitation will predominate depends on pH and sorptive concentration. According to Sparks (2002), surface complexation tends to dominate at low surface coverages. As surface coverage increases, nucleation is operational and results in the formation of distinct entities or aggregates on the surface. As surface loadings increase further, surface precipitation becomes the dominant mechanism. However, surface precipitates may occur in systems that are undersaturated with respect to the (hydr)oxide species (Towle et al., 1997).

Numerous investigations aimed at distinguishing adsorption from precipitation complexes have been made on plant nutrients and environmental contaminants. However, only a few studies have employed XAS to study low Z elements. These studies have been based on the pre-edge spectral features of P-XANES (Franke & Hormes, 1995; Khare et al., 2005) and S-XANES (Prietzel et al., 2008). It has been shown that the pre-edge resonance features (e. g., energy position, intensity and line shape) are related to the number of nearest neighbors of an element, and they can, therefore, be employed to derive information on the geometrical structure of a surface complex (Franke &

Hormes, 1995). Khare et al. (2005) were able to distinguish adsorption from precipitation complexes based on the full width of the white-line peak broadening at its half maximum height. According to these authors, in a two-dimensional adsorbed phase, atomic orbitals of metal, oxygen, and phosphorus overlap to form discrete molecular orbitals resulting in sharper, more intense features (e. g., the white-line peak). Conversely, in a precipitate complex, atomic orbitals broaden into a band because a typical three-dimensional metal phosphate precipitate contains approximately 10^{22} atoms cm^{-3}, resulting in a nearly continuous distribution of energies.

Although useful information can be obtained via the XANES pre-edge features, this approach does not provide any information on atomic distances of neighboring atoms associated with the absorbing atom. Additionally, the spectral pre-edge features may be very subtle, making the interpretation and distinction between surface complexes rather challenging.

EXAFS analysis brings several advantages over the XANES pre-edge spectral features in analyzing P retention complexes. Since in EXAFS the photoelectron is scattered only by a single neighbor atom, it is a more reliable quantitative approach as one is able to more accurately assign surface complexes based on inter-atomic distances rather than relying on a single backscattering event. However, in XANES, all the scattering pathways, classified according to the number of scattering events, contribute to the absorption cross section. Having said that, since now one is able to do P-EXAFS analysis, it would, thus, be of great interest to collect data employing both techniques and relate XANES to EXAFS data in order to validate the XANES findings.

In this work, the continuum between adsorption and surface precipitation was addressed as a function of surface loading (Chapter 2) and pH and reaction time (Chapter 3). In Chapter 4, a XANES-based assessment of P reactivity, distribution and loss potential in some highly weathered soils of Southern Brazil was carried out in agricultural lands that have received consecutive application of swine and cattle manures over decades.

REFERENCES

Arai, Y. & Sparks, D. L. ATR-FTIR spectroscopic investigation on phosphate adsorption mechanisms at the ferrihydrite-water interface. J. Colloid Interf. Sci., 241: 317-326, 2001

Arai, Y. and D. L. Sparks. Residence time effects on arsenate surface speciation at the aluminum oxide-water interface. Soil Sci. 167:303-314, 2002

Arai, Y., Sparks, D. L., Davis, J. A. Effects of Dissolved Carbonate on Arsenate Adsorption and Surface Speciation at the Hematite−Water Interface. Environ. Sci. Tech., 38:817–824, 2004

Arai, Y. X-ray Absorption Spectroscopic Investigation of Molybdenum Multinuclear Sorption Mechanism at the Goethite−Water Interface. Environ. Sci. Tech., 44:8491–8496, 2010

Barrow, N. J. The slow reaction between soil and anions. 1. Effects of time, temperature and water content of a soil on the decrease in effectiveness of phosphate for plant growth. Soil Sci., 118:380-386, 1974

Beauchemin, S., Hesterberg, D., Chou, J., Beauchemin, M., Simard, R. R., Sayers, D. E. Speciation of phosphorus in P-enriched agricultural soils using XANES spectroscopy and chemical fractionation. J. Environ. Qual., 32:1809-1819, 2003

Celi, L., Lamacchia, S., Marsan, F. A., Barberis, E. Interaction of Inositol Hexaphosphate on Clays: Adsorption and Charging Phenomena. Soil Sci., 164:574-585, 1999

Charlet, L. & Manceau, A. X-ray absorption spectroscopic study of the sorption of Cr(III) at the oxide-water interface : II. Adsorption, coprecipitation, and surface precipitation on hydrous ferric oxide. J. Colloid Interf. Sci., 148: 443-458, 1992

Diskowski, H., Hoffmann, T. Phosphorus in Ullmann's Encyclopedia of Industrial Chemistry 2005, Wiley-VCH, Weinheim.

Elzinga, E. J., Peak, D., Sparks, D. L. Spectroscopic studies of Pb(II)-sulfate interactions at the Goethite-water interface . Geochim. Cosmochim. Acta, 65:2219-2230, 2001

Fendorf, S. E., & Sparks, D. L. Application of surface spectroscopies and microscopies to elucidate sorption mechanisms on oxide surfaces. Trans. of Int. Soc. Soil Sci., Vol. 3a, Commission II: 182-199, 1994

Fendorf, S. E., Eick, M. J., Grossl, P. R., Sparks, D. L. Arsenate and chromate retention mechanisms on goethite. 1. Surface structure. Environ. Sci. Technol. 31:315-320, 1997

Franke, R. & Hormes, J. The P K-near edge absorption spectra of phosphates. Physica B., 216:85- 95, 1995

Fried, C. R. & Shapiro, G. Phosphate supply pattern of various soils. Soil Sci. Soc. Am. Proc. 20:471–475, 1956

Gates, W. P. X-ray absorption spectroscopy. Handbook of Clay Science. Eds. Bergaya, F., Theng, B.K.G., Lagaly, G. In: Developments in Clay Science, Elsevier Ltd., Vol. 1, 2006

Giaveno, C., Celi, L., Cessa, R. M. A., Prati, M., Bonifacio, E., Barberis, E. Interaction of Organic Phosphorus With Clays Extracted From Oxisols. Soil Sci., 173:694-706, 2008

Goldberg, S. Use of Surface Complexation Models in Soil Chemical Systems, Advances in Agronomy, 27:233, 1992

Goldberg, S. Adsorption Models Incorporated into Chemical Equilibrium Models. SSSA Special Publication 42, p. 75-95, 1995. In: Chemical Equilibrium and Reaction

Models. Soil Science Society of America, American Society of Agronomy, Madison, WI, USA

Guan, X. H., Chen, G. H., Shang, C. Competitive Adsorption Between Orthophosphate and Other Phosphates on Aluminum Hydroxide. Soil Sci., 170:340-349, 2005

Harrison, A.F. Soil Organic P: A Review of World Literature. C.A.B. International, Wallingford, UK, 1987.

Hayes, K. F., Roe, A. L., Brown, G. E. Jr., Hodgson, K. O., Leckie, J. O., Parks, G. A. In situ X-ray absorption study of surface complexes: Selenium oxoanions on α-FeOOH. Science, 238:783–786, 1987

Hedley, M. J., Stewart, J. W. B., Chauhan, B. S. Changes in organic and organic soil phosphorus fractions induced by cultivation practices and laboratory incubations. Soil Sci. Soc. Am. J., 46:970–976, 1982

Holford, I.C.R., Wedderburn, R.W.M., Mattingly, G.E.G. A Langmuir two-surface equation as a model for phosphate adsorption by soils. J. Soil Sci. 25:242–255, 1974

Jensen, Phosphate potential and phosphate capacity of soils. Plant Soil, 33:17-29, 1970

Khare, N., Hesterberg, D., Beauchemin, S., Wang, S. L. Distribution of phosphate between Fe- and Al-oxides in mixed mineral systems. Soil Sci Soc of Am J., 68:460-469, 2004.

Khare, N., J. D. Martin, and D. Hesterberg. Phosphate bonding configuration on ferrihydrite based on molecular orbital calculations and XANES fingerprinting. Geochim. Cosmochim. Acta 71:4405-4415, 2007

Khasawaneh, F. E., Sample, E. C. & Kamprath, E. J. eds. The role of phosphorus in agriculture. Madison, American Society of Agronomy, 1980. p 591-615

Kruse, J. & Leinweber, P. Phosphorus in sequentially extracted fen peat soils: A K-edge X-ray absorption near-edge structure (XANES) spectroscopy study. Journal of Plant Nutrition and Soil Science, 171:613–620, 2008

Kwon, K. D. & Kubicki, J. D. Molecular Orbital Theory Study on Surface Complex Structures of Phosphates to Iron Hydroxides: Calculation of Vibrational Frequencies and Adsorption Energies. Langmuir, 20:9249-9254, 2004

Lombi, E., Scheckel, K. G., Armstrong, R. D., Forrester, S., Cutler, J. N., Paterson, D. Speciation and distribution of phosphorus in a fertilized soil: a synchrotron-based investigation. Soil Sci. Soc. Am. J., 70:2038–2048, 2006

Luengo, C., Brigante, M., Antelo, J., Avena, M. Kinetics of phosphate adsorption on goethite: Comparing batch adsorption and ATR-IR measurements. J. Coll. Interface Sci., 300:511-518, 2006

Maguire, R. O., Hesterberg, D., Gernat, A., Anderson, K., Wineland, M., Grimes, J. Liming poultry manures to kill pathogens and decrease soluble phosphorus. J. Environ. Qual., 35:849-857, 2006

Manning, B. A., Fendorf, S. E., Goldberg, S. Surface Structures and Stability of Arsenic(III) on Goethite: Spectroscopic Evidence for Inner-Sphere Complexes. Environ. Sci. Technol., 32:2383-2388, 1998

Mehlich, A. Determination of P, Ca, Mg, K, Na, and NH4. North Carolina Soil Test Division (Mimeo, 1953)

Mehlich, A. Mehlich-3 soil test extractant: A modification of Mehlich 2 extractant. Comm. Soil Sci. Plant An. 15:1409-1416, 1984

Mullins, G.G. Nutrient Management Plans-Poultry. In Natural Resource, Agriculture, and Engineering Service, Managing Nutrients and Pathogens from Animal Agriculture, NRAES-130, Ithaca, NY, 2000

Novais, R. F. Phosphorus supplying capacity of previously heavily fertilized soils. Raleigh, North Carolina State University, 1977. 153p (Ph D. Thesis)

Ognalaga, M., Frossard, E., Thomas, F. Glucose-1-phosphate and myo-inositol hexaphosphate adsorption mechanisms on goethite. Soil Sci. Soc. Am. J., 58: 332–337, 1994

Olsen, S. R. & Watanabe, F. S. A method to determine a phosphorus adsorption maximum of soils as measured by the Langmuir isotherm. Soil Sci. Soc. Am. Proc. 21:144–149, 1957

O'Reilly, S. E., Strawn, D. G., Sparks, D. L. Residence Time Effects on Arsenate Adsorption/Desorption Mechanisms on Goethite. Soil Sci. Soc. Am. J., 65:67–77, 2001

Penn, C. J. & Warren, J. G. Investigating Phosphorus Sorption onto Kaolinite Using Isothermal Titration Calorimetry. Soil Sci. Soc. Am. J., 73:560-568, 2009

Persson, P., Nilsson, N., Sjoberg. S. Structure and Bonding of Orthophosphate Ions at the Iron Oxide–Aqueous Interface. J. Colloid Interface Sci., 177:263–275, 1996

Prietzel, J., Thieme, J., Herre, A., Salome, M., Deichert, D. Differentiation between adsorbed and precipitated sulphate in soils and at micro-sites of soil aggregates by sulphur K-edge XANES. European J. Soil Sci., 59:730–743, 2008

Rahnemaie R., Hiemstra T., van Riemsdijk W. H. Geometry, Charge Distribution, and Surface Speciation of Phosphate on Goethite. Langmuir, 23:3680-3689, 2007

Roberts, D. R., Scheidegger, A.M., Sparks, D.L. Kinetics of mixed Ni-Al precipitate formation on a soil clay fraction. Environ. Sci. Technol., 33:3749-3754, 1999

Roberts, D.R., R.G. Ford and D.L. Sparks. Kinetics and mechanisms of Zn complexation on metal oxides using EXAFS spectroscopy. J. Colloid Interface Sci., 263:364-376, 2003

Rose, J., Flank, A. M., Masion, A., Bottero, J. Y., Pierre, E. Nucleation and growth mechanisms of Fe oxyhydroxides in the presence of PO4 ions. 2. P K-edge EXAFS study. Langmuir, 13:1827–1834, 1997

Rouff, A. A., Natchegaal, M., Rabe, S., Vogel, F. X-ray absorption fine structure study of the effect of protonation on disorder and multiple scattering in phosphate solutions and solids. J. Phys. Chem. A., 113:6895-903, 2009

Sanchez, P.A., & Buol, S.W. Soils of the tropics and the world food crisis. Science, 188:598-603, 1975

Scheidegger, A.M., Lamble, G. M., Sparks, D. L. Spectroscopic evidence for the formation of mixed-cation, hydroxide phases upon metal sorption on clays and aluminum oxides. J. Colloid Interface Sci., 186:118-128, 1997

Scheidegger, A. M., Strawn, D. G., Lamble, G.M., Sparks, D.L. The kinetics of mixed Ni-Al hydroxide formation on clay and aluminum oxide minerals: A time-resolved XAFS study. Geochim. Cosmochim. Acta, 62:2233-2245, 1998

Scheinost, A. C., Ford, R.G., Sparks, D. L. The role of Al in the formation of secondary Ni precipitates on pyrophyllite, gibbsite, talc, and amorphous silica: A DRS Study. Geochim. Cosmochim. Acta, 63:3193-320, 1999

Spadini, L., Manceau, A., Schindler, P. W., Charlet, L. Structure and Stability of Cd2+ Surface Complexes on Ferric Oxides: 1. Results from EXAFS Spectroscopy. J. Colloid Interface Sci., 168: 73-86, 1994

Sparks, D. L. Environmental Soil Chemistry. Second Edition. Academic Press, 2002, 368 pg.

Strawn, D. G., Baker, L. L. Speciation of Cu in a Contaminated Agricultural Soil Measured by XAFS, μ-XAFS, and μ-XRF. Environ. Sci. Technol., 42:37–42, 2008

Sui, Y. & Thompson, M. L. Phosphorus sorption, desorption, and buffering capacity in a biosolids-amended Mollisol. Soil Sci. Soc. Am. J., 64:164–169, 2000

Tejedor-Tejedor, M. I., & Anderson, M. A. The protonation of phosphate on the surface of goethite as studied by CIR-FTIR and electrophoretic mobility. Langmuir, 6:602–611, 1990

Tiessen, H & Moir, J. O. Characterization of available P by sequential extraction. In: Carter, M. R, editor. Soil Sampling and Methods of Analysis, Can. Soc. Soil Sci., Lewis Publishers, Boca Raton, 1993, p. 75–86

Torrent, J. Activation Energy of the Slow Reaction between Phosphate and Goethites of Different Morphology. Aust. J. Soil Res., 29:69-74, 1991

Towle, S. N.; Bargar, J. R.; Brown, G. E., Jr.; Parks, G. A. J. Surface Precipitation of Co(II)(aq) on Al2O3. J. Colloid Interface Sci., 187:62-82, 1997

von Uexktill, H. R. & E. Mutert . Global extent, development and economic impact of acid soils. Plant and Soil, 171:1-15, 1995

Westall, J. C., & Hohl, H. A comparison between electrostatic models for the oxide/solution interface. Adv. Colloid Interface Sci., 12:265-294, 1980

Chapter 2

USING EXTENDED X-RAY ABSORPTION FINE STRUCTURE SPECTROSCOPY TO DETERMINE THE BONDING CONFIGURATIONS OF ORTHOPHOSPHATE SURFACE COMPLEXES AT THE GOETHITE/WATER INTERFACE I: SURFACE LOADING EFFECTS

Abstract

To investigate the effect of P surface loading on the structure and kinetics of surface complexation at the goethite/water interface, goethite was reacted with orthophosphate at P concentrations of 0.1, 0.2, and 0.8 mmol L^{-1} at pH 4.5 for 5 days. The P concentrations were chosen to ensure that P loadings at the surface would allow one to follow the transition between adsorption and surface precipitation. EXAFS spectra were collected in fluorescence mode at the P K-edge at 2,150 eV. The structural parameters were obtained through the fits of the sorption data to single and multiple scattering paths using Artemis. EXAFS analysis revealed a continuum between adsorption and surface precipitation, with bidentate mononuclear (^{2}E), bidentate binuclear (^{2}C) and monodentate mononuclear (^{1}V) surface complexes as well as surface precipitates forming at the goethite/water interface under the studied conditions. The distances concerning the P – O (1.51 – 1.53 Å) and P – Fe (3.2 – 3.3 Å for bidentate binuclear and around 3.6 Å for mononuclear surface complexes) shells observed in our study were consistent with distances obtained via other spectroscopic techniques. The shortest P – Fe distance of 2.83 – 2.87 Å was indicative of bidentate mononuclear

bonding configuration. The coexistence of different surface complexes or the predominance of one sorption mechanism over others was directly related to surface loading.

2.1 Introduction

The combination of strong binding of phosphorus (P) in soils, leading to its limited availability to plants, particularly, in highly weathered soils of the tropics, and the dependence of agriculture upon such soils for food production has motivated researchers to examine the sorption mechanisms of P in soils and soil components. From an environmental standpoint, issues surrounding excess P, often due to the disposal of P-rich agricultural byproducts to agricultural lands, have also prompted researchers to address the chemical reactions controlling the reactivity and transport of this element.

The adsorption phenomenon involving oxyanions and soil mineral oxides was originally thought to be characterized by an exchange reaction which took place on the surface of soil minerals like Fe and Al (hydr)oxides. Early investigations aiming at understanding P bioavailability observed that phosphate exhibited some hysteresis and that behavior was attributed to the formation more thermodynamically stable quasichemical entities or surface complexes. Elucidation of the surface complexes was speculative and inferred from multiple linear portions of the Langmuir plot, which were ascribed to sites of varying reactivity (Fried & Shapiro, 1956; Olsen & Watanabe, 1957). Hingston et al. (1968, 1971, 1972, 1974) studied the sorption of several oxyanions, including P, As and S, on goethite and gibbsite and concluded that the elemental selectivity of sorption was indeed due to specific sorption. It was only with the help of molecular-scale techniques that the lack of molecular descriptions of the surface complexes was fulfilled, bonding configurations corresponding to the different sorption mechanisms were first observed and chemisorption reactions were shown to be involved (Parfitt & Atkinson, 1976).

Over the past decades, solid-phase speciation studies of P have relied largely on the use of spectroscopic techniques, especially Fourier transform infra-red (FTIR) (Tejedor-Tejedor & Anderson, 1990; Persson et al., 1996; Arai & Sparks, 2001; Elzinga & Sparks, 2007; Luengo et al., 2006; Antelo et al., 2010) and NMR (Bleam et al., 1991; Kim & Kirkpatrick, 2004; Li et al., 2010; Kim et al., 2011) spectroscopies. A number of studies have been conducted to elucidate the sorption mechanisms and surface complexation/precipitation dependence on environmental conditions, particularly pH and P loading. Overall, and regardless of the technique employed, there seems to exist a consensus that the possible bonding configurations between phosphate and Fe and Al (hydr)oxides include bidentate binuclear (^{2}C) and monodentate mononuclear (^{1}V) structures. Nevertheless, interpretations of surface complex structures, such as whether monodentate or bidentate complexes form, and the conditions at which they form are not clear. In terms of goethite, IR studies have suggested that an inner-sphere bidentate binuclear surface complex may be the predominant mechanism at low pHs (Tejedor-Tejedor & Anderson, 1990; Luengo et al., 2006) and low surface loading (Rahnemaie et al., 2007). Kwon & Kubicki (2004) employed MO/DFT calculations to model surface complexes and their findings corroborate the above studies. In a novel study employing NMR to address P sorption to Fe (hydr)oxides, Kim et al. (2011) studied the bonding mechanisms of P over a wide range of P concentration (0.1 – 3 mM) and pH (3 – 11) that encompasses most of the previous studies they observed that a bidentate binuclear complex was formed regardless of environmental conditions. However, a monodentate mononuclear surface complex has also been suggested at low pHs (Persson et al., 1996) and at high P loadings (Rahnemaie et al., 2007). IR studies on other Fe (hydr)oxides

include the work on ferrihydrite by Arai & Sparks (2001), in which the authors have suggested that bidentate binuclear surface complexes that formed at pH 4 to 6 were protonated and unprotonated complexes formed at pH $\geq$ 7.5, and Elzinga & Sparks (2007), working with hematite, observed the formation of bidentate binuclear structures at lower pHs at higher surface loadings in the 3.5–7.0 pH range whereas, at the highest pH values studied (8.5–9.0), monodentate mononuclear complex was present and its importance increased with increasing surface coverage at the high pH values. It is worth pointing out that the controversies surrounding the accurate determination of sorption mechanisms are due to the lack of direct evidence together with the reliance of the molecular assignments on the analytical approach, which has unavoidably led to questionable conclusions (Arai & Sparks, 2007, Carabante et al., 2010). An additional aspect that most of the early studies fail to precisely address is the formation of surface precipitates (Arai & Sparks, 2001) i.e., three dimensional entities formed when further increases in sorbate concentration exceeds a monolayer coverage on the mineral surface. A vast literature on this topic indicates that surface loading has a pronounced effect on the continuum between surface complexation and surface precipitation on a number of soil minerals and environmentally important elements (Charlet & Manceau, 1992; Fendorf, 1995; Scheidegger et al., 1997, 1998; Ford & Sparks, 2000; Roberts et al., 2003; Natchtegaal & Sparks, 2004). At high P concentrations, surface precipitation may be catalyzed leading to a new solid phase that is less readily dissolved or desorbed. According to Sparks (2002), surface complexation tends to dominate at low surface coverages. As surface coverage increases, nucleation is operational and results in the

formation of distinct entities or aggregates on the surface. As surface loadings increase further, surface precipitation becomes the dominant mechanism.

Synchrotron-based X-ray absorption spectroscopy (XAS) has been extensively applied to model systems to resolve molecular-level sorption mechanisms of a number of soil contaminants (Manning et. al., 1998; Arai et. al., 2001; Peak & Sparks, 2002). These tools can greatly improve our understanding of P reactions in soils and provide predictions on an atomic/molecular basis of mechanisms of P retention on soil minerals. Such data are useful in the development of molecular sorption models if one aims to relate P speciation to P mobilization. Furthermore, the combination of kinetics and spectroscopy to perform time-resolved *in-situ* sorption studies is ideal since spectroscopy can provide direct information on the type of species present at the surface of a solid and kinetics can provide insight into the processes that the sorbate and sorbent undergo as a steady state is approached.

It is noteworthy to mention that Hesterberg et al. (1999), Khare et al. (2005) and Khare et al. (2007) employed XANES to distinguish P adsorption from surface precipitation at mineral/water interfaces. However, in their studies, the authors relied on indirect observations to address the bonding configurations of the surface structures being formed on the mineral surface, namely, the full width at half maximum height (FWHM) concept and extended Hückel calculations. Therefore, to the best of our knowledge, our study is the first to employ EXAFS to collect direct information on the P sorption mechanisms formed at the mineral/water interface.

Accordingly, we combined the batch technique with EXAFS spectroscopy to examine the effects of surface loading and pH on the local atomic environment of sorbed P at the goethite/water interface.

2.2 Material & Methods

2.2.1 Mineral Synthesis

Goethite was synthesized according to the method of Schwertmann & Cornell (2000). Briefly, 200 mL of 1 M $Fe(NO_3)_3 . 9 H_2O$ were added to a plastic flask with continuous stirring and then 360 mL of 5 M KOH were carefully added. Four L of DDI water was added and the mixture was thoroughly mixed for more 30 min. The flask was sealed with Scotch duct tape and placed in an oven set at 70 °C for 4 days. After the 4th day, the supernatant solution was poured off and the goethite precipitate, which had settled to the bottom of the container, was washed with dialysis tubing for about one week until the electric conductivity matched that of the distilled deionized water ($\sim$ 0.95 $\mu S\ cm^{-1}$). The dialyzed mineral was transferred into 50 mL centrifuge tubes and centrifuged at 11 000 rpm for 30 min. The supernatant was removed with a syringe and the precipitate was freeze dried for approximately 60 h. Finally, the material was softly ground in a mortar and stored in a polystyrene bottle.

The specific surface area of the goethite, determined by a three point Brunauer-Emmett-Teller N_2 gas adsorption isotherm, was $40.0 \pm 0.6\ m^2\ g^{-1}$.

2.2.2 Sorption Experiments

The phosphate concentrations used in our study were, in general, higher than the concentration range used in similar studies employing other techniques. This was necessary due to the low detection limit for P using EXAFS.

Centrifuge tubes containing stock goethite suspensions of 20 g L^{-1} were placed in a rotating shaker set at 30 rpm at 298 K and equilibrated in 50 mmol L^{-1} KCl with the pH adjusted to 4.5 for 36 h prior to phosphate addition. The pH in the suspensions was monitored throughout the shaking period and adjusted to the target pH as needed by the addition of either NaOH or HCl. Thereafter, an aliquot of the suspension was transferred to a new centrifuge tube to yield a goethite suspension of 2 g L^{-1}, and a phosphate solution of 0.1, 0.2, and 0.8 mmol L^{-1} was added. This corresponded to surface coverages of 1.25, 2.5 and 10 µmol m^{-2}. The tubes were shaken and 5 mL aliquots from each tube were sampled on the 5th day.

Goethite dissolution (as determined by solution Fe) was determined before and after sorption experiments in which goethite was reacted with P at 0.1, 0.2 and 0.8 mmol L^{-1} at each pH, 3.0, 4.5, 6.0 and 7.5. For goethite reacted at pH 3.0, dissolved Fe concentrations were significantly higher ($\sim$ 95 mg L^{-1}) in comparison with the dissolved Fe concentrations at the other pHs ($\sim$ 56 µg L^{-1}), regardless of P concentration.

The phosphate concentrations were carefully chosen to ensure a range of surface coverages. The reaction time, 5 days, was shown to be sufficient to ensure that the bulk of the added P (> 95%) was associated with the surface.

2.2.3   XAS Sample Preparation and Analysis

At the outset, it is important to mention the difficulties associated with EXAFS analysis of low-Z elements. This, in large part, explains why there is an absence of studies on EXAFS investigations on P and other light elements. In studies with light elements, such as P, the resulting interference between the outgoing and backscattered electron waves shows up as a modulation of the measured absorption coefficient, thereby causing the oscillations shown in the EXAFS spectra. Collecting EXAFS data of low-Z absorbing atoms, such as P, may, therefore, presents a challenge (Lombi et al., 2006). The difficulties associated with data collection arise from either the absorbing atom as well as from the backscattering atom. In terms of low-Z absorbing atoms, one must consider that (i) fluorescence yield decreases with decreasing atomic number, and that (ii) in dilute samples, e.g., environmental samples, fluorescence attenuation is severely augmented especially in a dense, high-Z matrix such as goethite.

Apart from the technical difficulties for EXAFS analyses of low-Z elements mentioned above, sample preparation presents other challenges that one must be aware of. Special care must be taken to avoid the presence of sulfur (S) in samples. Sulfur contamination can cause the appearance of a S edge at ~ 2472 to 2484 eV (depending on the oxidation state of the S species present on the sample) and could interfere with the P-EXAFS measurements, resulting in distortions on $\chi(k)$. This is an issue even at very low concentrations of S because the Ge detector does not have the energy resolution to completely isolate the fluorescence of P from that of S. It is further complicated by the fact that the materials studied in this research have a high affinity for sulfate and are

excellent scavengers of any trace sulfate contamination in any of the reagents, pH buffers, or experimental apparatus.

Lastly, the absorber concentration may also represent a limitation to the acquisition of quality P-EXAFS data. We have successfully collected P-EXAFS data on samples in which P concentrations varied from as low as 100 µmol L^{-1} up to 800 µmol L^{-1}. The number of scans necessary for acquiring reasonable data is proportionally related to the P concentrations on the surface, varying from 10 up to 20 scans sample^{-1}. Besides the limitation of available experimental time, collecting more than 20 scans on a single sample becomes likely to cause adverse effects due to sample drying, possible radiation damage, and long-term stability of the X-ray source.

In terms of samples preparation, each sample was immediately filtered to pass through a 0.22 µm nitrocellulose membrane filter and washed three times with 3 mL of pH adjusted 50 mmol L^{-1} KCl to remove any entrained phosphate not associated with the surface. The cellulose membrane filter containing the mineral paste was sealed with 5-micron polypropylene XRF thin film (Ultralene®) and stored moist in a sealed sample box at 6 ºC until analysis. The samples were stored for no more than 24 h prior to analysis. Phosphorus K-edge spectra (2,151 eV) were collected at beamline X15B at the National Synchrotron Light Source (NSLS) at Brookhaven National Laboratory. The X15B sample chamber is a "hutch box" containing a He atmosphere at 1.001 atm. positive pressure.

EXAFS spectra were collected in fluorescence mode with samples mounted at 45° to the incident beam, using a liquid-nitrogen-cooled Canberra Ultra-Low-Energy Germanium detector positioned at 90°. X15B beamline optics consist of a collimating

and harmonic-rejection mirror, a monochromator utilizing Si (111) crystals to tune energy, and a focusing mirror to gather approximately 5×10^{11} photons sec^{-1}. into a 1-mm spot at the sample position. The fluorescence signal was normalized to incident beam intensity as measured using a windowless ionization chamber. XAS spectra were collected at photon energies between 2099 and 2750 eV with a minimum step size of 0.1 eV across the edge and gradually increasing step sizes up to 6 eV at 2750 eV. The collected spectra were processed using the Athena software in the computer package IFEFFIT (Ravel & Newville, 2005). Six to ten individual spectra were averaged for each sample.

2.2.4   EXAFS Data Analysis

The averaged spectra were normalized to an atomic absorption of one, and the EXAFS signal was extracted from the raw data using linear pre-edge and a quadratic spline post-edge, followed by subtraction of background using the Autobk algorithm (Newville et al., 1993). Data were converted from energy to photo electron momentum (k-space) and k-weighted by k^2. Fourier transforms (FT) of the k^2–weighted EXAFS were calculated over a k-range of 2.0 to between 10.1 and 10.6 to obtain the radial distribution function (RDF) in R-space. The FT of the EXAFS was fit with the predicted neighbor paths by varying the number of coordinating atoms (CN), their distance (ΔR), mean square displacement (δ^2) and passive electron reduction factor (S_0^2) in order to obtain the best fit between the experimental and predicted spectra.

First shell (P – O) bond distances were obtained from crystallographic data and were used in the fit and fixed at these values for higher shell fitting. We fixed the CN of the first oxygen shell at 4 as the regular coordination environment of PO_4 ions. Fits to second neighbor Fe shells were made by setting the degeneracy of each surface complex, CN = 2 for bidentate binuclear or CN = 1 for either bidentate mononuclear or mononuclear coordination, and fitting an amplitude factor describing the fraction of P in each configuration. Aqueous ($P_{(aq)}$) spectra was collected and fit to confirm the position of the multiple scattering (MS) within the PO_4 tetrahedron. The inclusion of MS improved the fit in the 1.6 – 2.8 Å region as strong MS within the PO_4 tetrahedron was expected. We included three MS paths in our fits: namely three-legged P – O1 – O2 – P triangular (MS_1), four-legged P – O1 – PO2 – P non collinear (MS_2) and four-legged P – O1 – P – O1 – P collinear (MS_3) paths.

The percentage of each of the surface complexes was determined based on the amplitude factor (S_0^2) obtained for a given surface complex. Since the overall amplitude factor must not exceed unit and the summation of the amplitudes of the individual Fe shells representing different complexes must equal the overall amplitude, i.e. first-shell amplitude, it is valid to state that each individual Fe shell's fraction of the overall amplitude represents the fraction of total phosphate present as that complex.

Several different models were employed to fit the MS path, including (i) correlating σ^2 MS to 2 times that of the single scattering (SS) path; and (ii) a direct correlation between σ^2 MS and that of the SS path (Rouff et al., 2009).

2.3 Results & Discussion

There have been a number of previous studies using spectroscopic techniques to characterize phosphate surface complexes forming on Fe(III)-, Al- and Ti (hydr)oxide mineral surfaces, including MO/DFT and ATR-FTIR, CIR-FTIR, NMR and XANES spectroscopies. Unlike IR spectroscopy, EXAFS analysis is insensitive to the protonation environment of surface complexes. Therefore, our discussion will be limited to the bonding configuration of the surface species. An inner-sphere surface complex via a ligand exchange mechanism has been shown to be the most prevalent sorption mechanism of orthophosphate sorption on mineral (hydr)oxides, such as goethite. In terms of bonding configuration, the bidentate configuration seems to be the most favorable P sorption complex formed at the (hydr)oxides surfaces (Table 1; Parfitt et al., 1975; Parfitt et al., 1976; Parfitt, 1977). Yet, what has not been established in the literature concerned to P bonding configurations at mineral surfaces are the environmental conditions which favor formation of a particular sorption complex mechanism. Additionally, the majority of the studies have employed NMR and IR techniques. There are no reports in the literature using EXAFS where detailed structural information, such as next nearest neighbor, bond distance and coordination numbers are reported. A list of relevant studies on P sorption mechanisms formed at mineral (hydr)oxides surfaces is shown in Table 1 and is aimed at assisting in the discussion of our results. Overall, both monodentate and bidentate bonding configurations are formed across a wide pH range (from 3 to approximately 13). With the exception of studies by Persson et al. (1996), Kim & Kirkpatrick (2004) and Rahnemaie et al. (2007), one can postulate that a monodentate bonding configuration occurs predominately at higher pHs.

41

On the basis of IR analysis, and as pointed out by Li et al., (2010) this could be an artifact due to the protonation state of sorbed P at low pHs which impacts the symmetry of P surface complexes and leads to band splitting. This, consequently, is a limitation of the IR technique. Persson et al. (1996), however, employed *ex situ* FTIR on dried goethite and, as the authors themselves indicate, those two factors may have contributed to significant shifts in band positions, which may have caused inappropriate molecular assignments. Kim & Kirkpatrick (2004) also performed their NMR experiments with vacuum-filtered and oven-dried samples. In order to rule out the possible effects that drying could have on the bonding configuration of P formed on the solid, the authors collected spectra from an undried γ-Al_2O_3 sample reacted with 0.1 M KH_2PO_4 at pH 5. The relatively high P concentration, at which the undried γ-Al_2O_3 reference sample was prepared could have favored the formation of the monodentate configuration and may have led to the observation of precipitates, even at the lowest P concentrations (10^{-4} mol P). In the work by Rahnemaie et al. (2007), MO/DFT calculations were performed to examine the presence of monodentate complexes at low pH without considering the presence of bidentate surface complexes, and that may be the reason why the monodentate complex was predicted under such conditions.

In terms of a bidentate bonding configuration, there seems to exist even more controversy surrounding the conditions at which the formation of such complexes is favored. However, it is believed, based on available literature, that orthophosphate forms only one type of bidentate configuration with (hydr)oxides surfaces, namely corner-sharing or bidentate binuclear (^2C) complexation.

2.3.1   P-EXAFS Spectra

Figure 2.1 shows the experimental $\chi(k)$ spectra of goethite spiked with P at surface coverages of 1.25, 2.5 and 10 μmol m^{-2} at pH 4.5. The radial distribution function (RDF) is a result of the Fourier transformation of the $\chi(k)$ function. The peaks shown in the experimental $\chi(k)$ spectra correspond to the coordination shells formed between P – O and P – Fe and reflect the interatomic distances within the material. For all samples, the E_0 ranged from -2.28 to 0.96 eV. The contributions of O were localized at P – O distances ranging from 1.51 to 1.53 and MS dominates at ~ 2.75 – 2.78 Å. The P – Fe shells are indicative of the existence of three different bonding configurations between P and the goethite surface and will be treated separately in the following discussion.
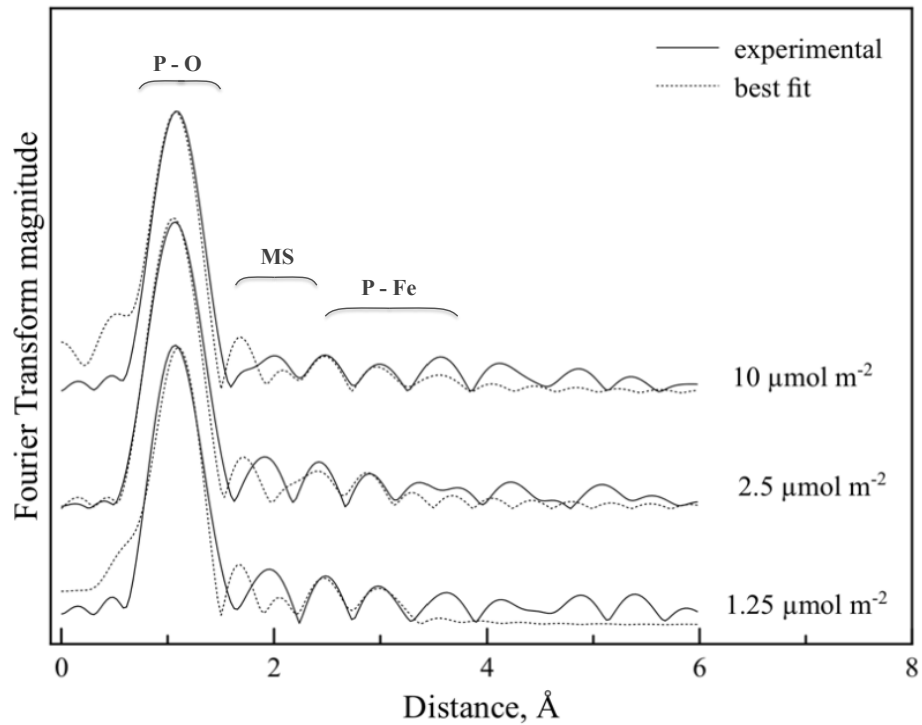
Figure 2.1   Experimental (solid line) and best fit (dashed line) Fourier transformed spectra of the phosphate surface complexes formed at the goethite/water interface at pH 4.5. A change in spectrum shape (R-space) followed by an increase in the phosphate loading indicates that the phosphate surface speciation changes with surface loading. Braces are intended to show the approximate region where the P – O, MS and P – Fe shells most significantly contribute in radial distance in the Fourier transformed spectra.
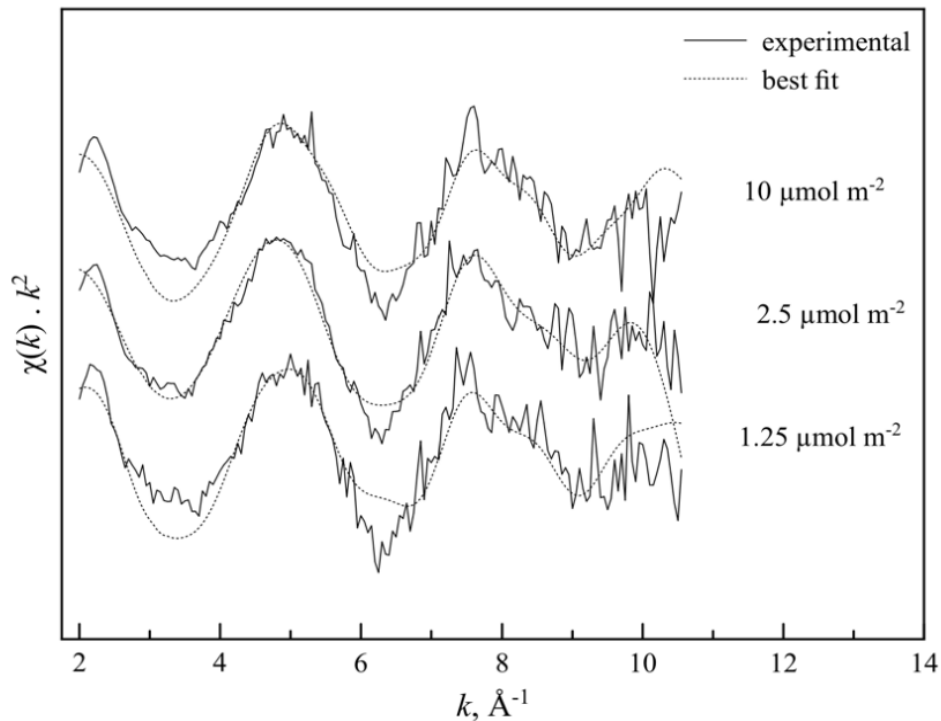
Figure 2.2.   Experimental (solid line) and best-fit (dashed line) k^2-weighted back transformed spectra of phosphate sorbed on goethite at 1.25, 2.5 and 10 μmol m^{-2} at pH 4.5.

2.3.2   Overall Formation of P Surface Complexes at the Goethite/Water Interface

We have identified the formation of three different phosphate surface complexes at the goethite/water interface, namely bidentate mononuclear (^{2}E), bidentate binuclear (^{2}C) and monodentate mononuclear (^{1}V) surface complexes. Additionally, surface precipitates were also observed, particularly, at higher P loadings.

The shortest P – Fe distances of 2.87 to 2.83 Å are indicative of a bidentate mononuclear configuration between P and Fe at low and intermediate surface loadings,

45

respectively. Intermediate P –Fe distances of 3.27, 3.2 and 3.3 Å were characteristic of a bidentate binuclear configuration between P and Fe at low, intermediate and high surface loadings, respectively. The most distant shell, 3.60 Å was indicative of a linear configuration between P and Fe. Table 2.2 shows the P – O and P – Fe bonding distances and corresponding P sorption mechanisms.

2.3.3 Adsorption Complexes

As indicated in Table 2.2, our results show that bidentate (^{2}C and ^{2}E) surface complexes are predominantly formed at low surface coverages and transition to monodentate configuration as surface coverage increases. This seems consistent with the literature that indicated that low surface coverages favor the formation of bidentate surface complexes (Parfitt et al., 1975a; Parfitt et al., 1975b; Parfitt et al., 1976; Parfitt & Atkinson, 1976; Parfitt, 1977; Tejedor-Tejedor & Anderson, 1990; Kim & Kirkpatrick, 2004; Elzinga & Sparks, 2007; Rahnemaie et al., 2007) and that the relative importance of bidentate binuclear species decreases as surface loading increases such that monodentate configuration would predominate at higher surface loadings (Tejedor-Tejedor & Anderson, 1990; Rahnemaie et al., 2007). However, on the basis of ATR-FTIR analysis, Antelo et al. (2005, 2010) observed that P adsorbs mainly as bidentate complexes at high phosphate loadings and that monodentate surface complexes begin to be important at low phosphate loadings and at high pHs. This was ascribed to bidentate species locating more charge at the surface than monodentate species, producing a lower electrostatic repulsion between the adsorbed species in the 1-plane. Interestingly, the

observation of Antelo et al. (2005, 2010) is consistent with the behavior of arsenic in its pentavalent form (As(V)), an analog of phosphate, having similar chemical and geometric properties, and present as the ionic species, $H_2AsO_4^-$ and $H_2PO_4^-$, respectively, at the typical pH range in the environment.

Because there has not been any EXAFS study on orthophosphate bonding on mineral (hydr)oxides, we compare our results to studies on As(V) sorption on mineral (hydr)oxides. EXAFS studies showed that As(V) can form three bonding configurations with mineral (hydr)oxides surfaces, similarly to what was observed in our study (Fendorf et al. (1997); Grossl et al. (1997)). However, counter to what was observed by these authors, our results show a predominance of the bidentate corner-sharing (^2C) surface complex at lower surface coverages and a transition to edge-sharing (^2E) and monodentate corner-sharing (^1V) as surface coverage increased to 10 μmol m^{-2}.

2.3.4 Bidentate Mononuclear Configuration

The shortest P – Fe distances, 2.83 and 2.87 Å, represent an edge sharing between the phosphate tetrahedra and the Fe octahedra. Thus, the only possible configuration for such a short distance would be an edge-sharing bidentate mononuclear configuration (^2E). Extended X-ray Absorption Fine Structure spectroscopy has indicated that a bidentate mononuclear configuration (^2E) can be formed between tri-, tetra- and penta-valent metals and (hydr)oxides surfaces, such as As(V) on goethite (Fendorf et al., 1997; Grossl et al., 1997), Se(IV) on HMO (Foster et al., 2003), As(III) on ferrihydrite and on

hematite (Ona-Nguema et al., 2005) and As(III) on maghemite (Morin et al., 2008) under different experimental conditions.

However, since the existence of a bidentate mononuclear surface complex between P and (hydr)oxide minerals has never been observed, we tried to rule out its existence by calculating it as forming a 120º angle. In this case, the P-Fe bond distance would be 3.15 Å. We also considered that MS contributions could be substantially affecting the RDF at those distances, but this hypothesis was promptly discarded after MS from an aqueous orthophosphate sample (10 mmol L^{-1} as KH_2PO_4 at pH 4.5) showed MS contributions at around ~ 2.74 Å.

Furthermore, the P – Fe distances observed in our study are comparable to those observed in the above-mentioned EXAFS studies, 2.83 – 2.87 Å and 2.87 – 3.08 Å, respectively (reported distances include uncertainties associated with the measure).

Figure 2.3 illustrates the bidentate mononuclear structure of phosphate sorbed to goethite based on the local coordination environment determined via EXAFS spectroscopy.
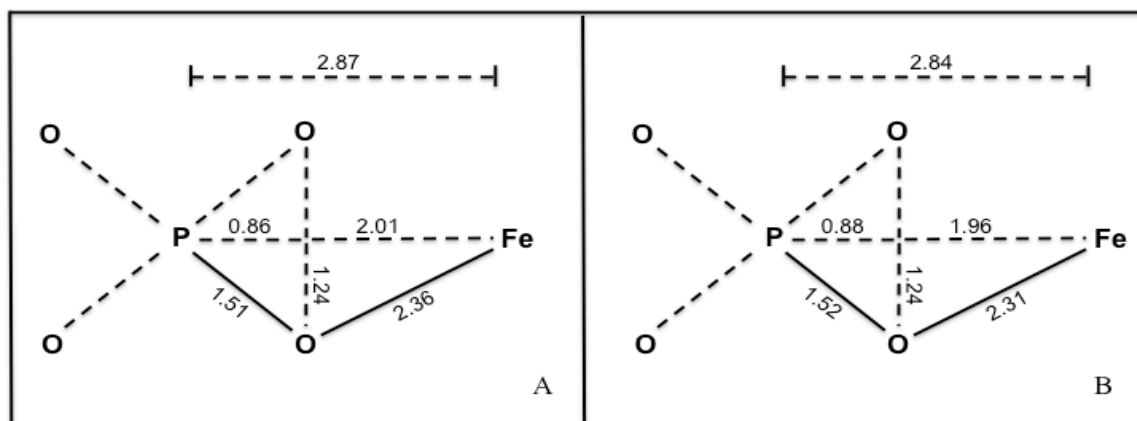
Figure 2.3   Schematic illustration of the two bidentate mononuclear P bonding configurations at the goethite/water interface.

2.3.5 Bidentate Binuclear Configuration

A bidentate binuclear configuration (^2C) of phosphate on (hydr)oxides has been shown to be the predominant sorption mechanism formed at lower surface coverages. In this study, the ^2C surface complex was present, although at different proportions, across the entire surface coverage range. The rationale for why ^2C predominates at lower surface coverages is that this configuration should be favored when the Fe/P ratio is smaller than unity. It follows that at low P concentration, the sorption sites compete with the PO_4 molecules at the same strength such that one PO_4 molecule must equally satisfy as many sorption sites as possible. Therefore, ^2C forms first and because it is strongly bound to high affinity sorption sites, it has a large thermodynamic stability, thus remaining associated with the surface even as solution P concentration increases. In addition, at low pHs, i.e., pH ~ 4.5, a higher positive surface charge induces a higher

49

adsorption capacity for anions like phosphate, because more negative charge can be brought to the surface for a given change in electrostatic potential (Hiemstra, 2010).

Table 2.2 shows the surface complex distribution as a function of surface loading. Following the surface complexe distribution across the loading range, one can show that the overall percent distribution of ^{2}C remains constant (~50%) when the surface coverage increases by a factor of 2.

2.3.6 *Monodentate Configuration*

Relatively few spectroscopic studies have reported P being attached to (hydr)oxide surfaces in a monodentate (^{1}V) configuration (Table 1). The studies in which a ^{1}V configuration has been observed were, in general, carried out employing P concentrations at relatively high surface coverages (Tejedor-Tejedor & Anderson, 1990; Elzinga & Sparks, 2007). Whereas the P – Fe distances for bidentate binuclear configuration are in good agreement with the work by Rahnemaie et at. (2007), who found P – Fe distances varying between 3.22 to 3.26 Å, the P – Fe distance for a monodentate configuration observed in our study was much larger, ~ 3.6 Å. Though, this is in agreement with the calculations performed by Kwon & Kubicki (2004), who found P – Fe bond distances generally longer for either configuration, if a ≥ 170º angle is formed by P – O – Fe suggesting a P – Fe bond distance of around 3.6 Å. EXAFS studies indicate that for As(V) these distances are generally in the order of 3.57 to 3.63 Å (Waychunas et al., 1993; Fendorf et al., 1997). Since P is a much lighter element than As, it is possible that the repulsion of P by the Fe atoms tend to maintain P farther apart

from Fe as possible, thus P – O – Fe forms preferentially a linear structure when a monodentate configuration is formed. Alternatively, the Fe – O bond distance may also be influenced by the repulsion and, accordingly, present a longer total Fe – P distance.

2.3.7   Surface Precipitate formation

The transition point from adsorption (or monolayer surface coverage) to precipitation (multilayer coverage or the formation of a separate phase) is not clearly defined (Corey, 1981). Torrent et al. (1990) estimated that, for monolayer coverage, the maximum P adsorption at the goethite surface should be 5 μmol m^{-2} for mononuclear bonding or 2.5 μmol m^{-2} for binuclear bonding. On the basis of their calculation, surface precipitates should have been observed at the two highest P loadings in our study. According to Dzombak & Morel (1990), the dissolution of iron from the mineral (hydr)oxide is a limiting factor for surface precipitation to occur, since surface precipitates are formed at the expense of dissolved material from the adsorbent surface. This might be the reason for the small degree of surface precipitation observed, given the relatively high phosphate loading employed in this study.

We observed surface precipitates in our study on the basis of calculations performed to the overall amplitude and the individual fractions of P in each bonding configuration in which we considered the relative distribution of monodentate and bidentate binuclear surface complexes.

2.4 Conclusions

We have successfully showed the applicability of EXAFS spectroscopy to shed light on the mechanisms by which P sorbs onto goethite under low pH and P surface loadings corresponding to 1.25, 2.5 and 10 µmol m^{-2}. Our results are in good agreement with the majority of studies on this topic. As such, bidentate surface (^{2}C and ^{2}E) complexes were the main bonding configuration formed at lower surface coverages, which transitioned to monodentate (^{1}V) configuration as surface coverage increased up to 100 µmol m^{-2}. Surface precipitates were observed on the basis of calculations performed to the overall amplitude and to the individual shells.

An edge-sharing bidentate mononuclear (^{2}E) surface complex was observed at relatively low to moderate surface coverages of 12.5 and 25 µmol m^{-2}. This surface complex has not been observed previously in the literature and showed that EXAFS is an important spectroscopic tool for obtaining more direct information on the local geometric structure of the surface structures formed at solid/water interfaces.

2.5 Acknowledgments

Table 2.1 Relevant studies on the P sorption mechanisms formed at mineral (hydr)oxide
surfaces using MO/DFT and ATR-FTIR, CIR-FTIR, NMR and XANES
spectroscopies.

Surface complex	Technique	pH	Sorbent	Reference
Monodentate				
	CIR-FTIR			
		6 – 8.4	goethite	Tejedor-Tejedor & Anderson, 1990
	ATR-FTIR			
		3- 13	goethite	Persson et al., 1996
		> 8.5	hematite	Elzinga & Sparks, 2007
		7	akaganeite	Deliyanni et al., 2007
	MO/DFT			
		~12.8	iron oxides	Kwon & Kubicki, 2004
		low pH	goethite	Rahmenaie et al., 2007
	NMR			
		3 - 11	boehmite, γ-Al$_2$O$_3$	Kim & Kirkpatrick, 2004
Bidentate				
	ex situ IR			
		3.4 and 10	goethite	Parfitt et al., 1975a
		4 and 10	goethite, hematite, lepidocrocite	Parfitt et al., 1975b

in situ IR			
	3.6 - 5.1	goethite	Parfitt & Atkinson, 1976
CIR-FTIR			
	< 6	goethite	Tejedor-Tejedor & Anderson, 1990
ART-FTIR			
	3 – 8.6	TiO_2	Connor & McQuillan, 1999
	4 – 7.5	ferrihydrite	Arai & Sparks, 2001
	4.5 - 9	goethite	Luengo et al., 2006
	< 7	hematite	Elzinga & Sparks, 2007
	4.5 - 9	nano ferrihydrite	Antelo et al., 2007
MO/DFT			
	4 - 6	iron oxides	Kwon & Kubicki, 2004
	high pH	goethite	Rahnemaie et al., 2007
NMR			
	4 - 10	boehmite	Li et al., 2010
	4.5 - 9	TiO_2	Kang et al., 2011
	3 - 11	goethite, akaganeite, lepidocrocite	Kim et al., 2011
	3 - 11	$\alpha\text{-}Al_2O_3$	Li et al., 2012

54

XANES			
	6	ferrihydrite	Khare et al., 2007
XPS			
	3 - 13	goethite	Martinez & Smart, 1987
Surface precipitates and undetermined inner-sphere bonding configuration			
ATR-FTIR			
	3.3	corundum	Del Nero et al., 2010
NMR			
	4 - 11	boehmite	Bleam et al., 1991
	5	non-xl Al(OH)$_3$	Lookmann et al., 1994
	4 – 8.5	γ-Al$_2$O$_3$	Johnson et al., 2002
	3 - 11	boehmite, γ-Al$_2$O$_3$	Kim & Kirkpatrick, 2004
	3.5 – 8.5	kaolinite, gibbsite	Van Emmerick et al, 2007

Table 2.2. P – O and P – Fe bonding distances, surface complex distribution and corresponding bonding configurations of P on goethite at three different surface coverages.

Surface loading	P - O		P - Fe									Surface precipitate
			Bidentate mononuclear			Bidentate binuclear			Monodentate			
μmol m^{-2}	R	σ^2	R	σ^2	fraction	R	σ^2	fraction	R	σ^2	fraction	fraction
	(Å)		(Å)		(%)	(Å)		(%)	(Å)		(%)	(%)
1.25	1.51	0.0021	2.87 (±0.03)	0.0032	48 (±32)	3.27 (±0.06)	0.0033	47 (±42)				
2.5	1.52	0.0004	2.83 (±0.04)	0.0052	77 (±60)	3.3 (±0.08)	0.0030	25 (±37)				
10	1.51	0.0004				3.3 (±0.05)	0.0002	18 (±12)	3.6 (±0.04)	0.0035	63 (±41)	20

R: radial structure function (RSF); σ^2: mean square displacement, ( ): uncertainties associated with parameter estimates
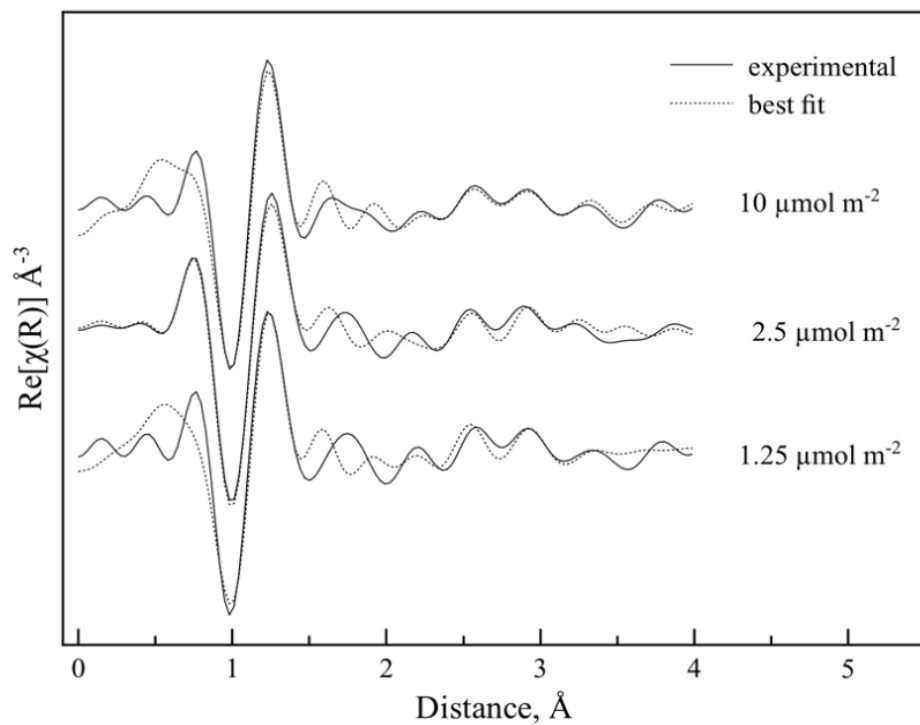
Figure 2.4a. Real (R) part of the Fourier Transform of P sorbed on goethite at three different surface coverages, 1.25, 2.5 and 10 µmol m^{-2}.
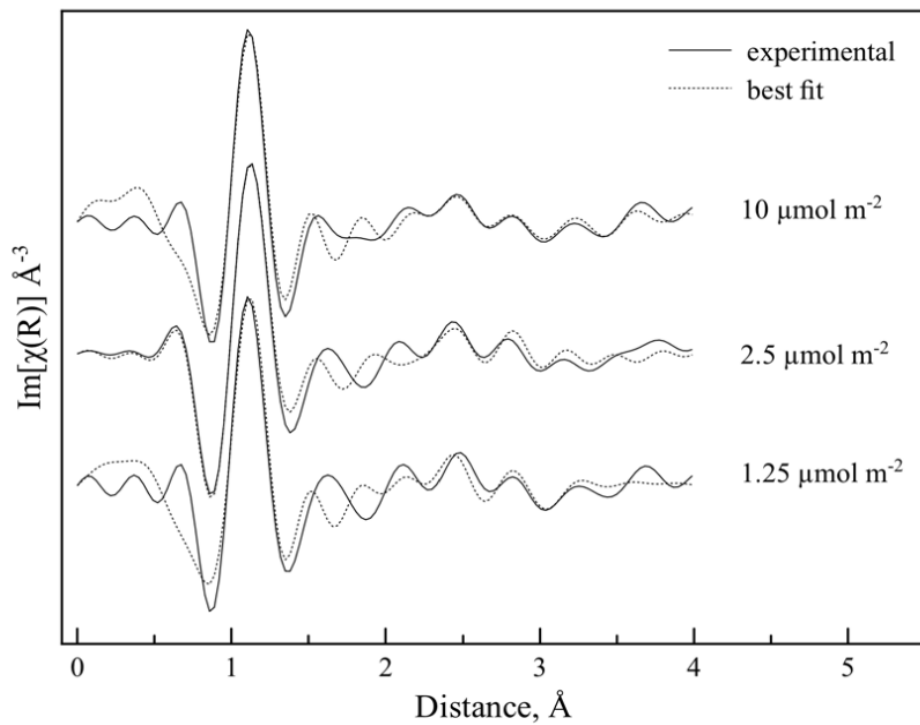
Figure 2.4b. Imaginary (R) part of the Fourier Transform of P sorbed on goethite at three different surface coverages, 1.25, 2.5 and 10 µmol m^{-2}.
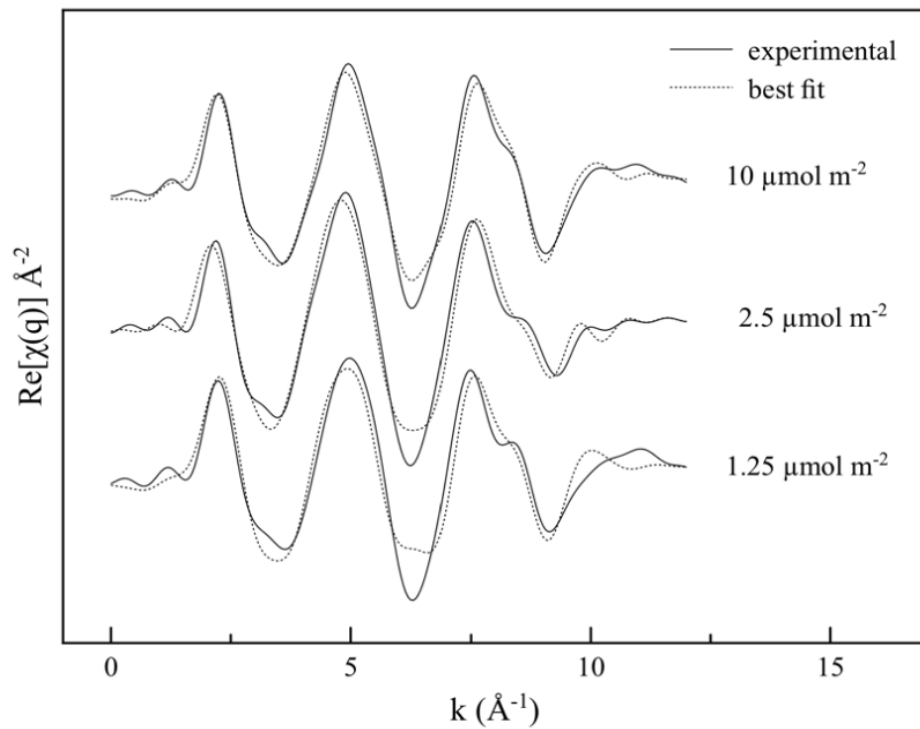
Figure 2.5a.   Real (q) part of the Fourier Transform of P sorbed on goethite at three different surface coverages, 1.25, 2.5 and 10 µmol m^{-2}.
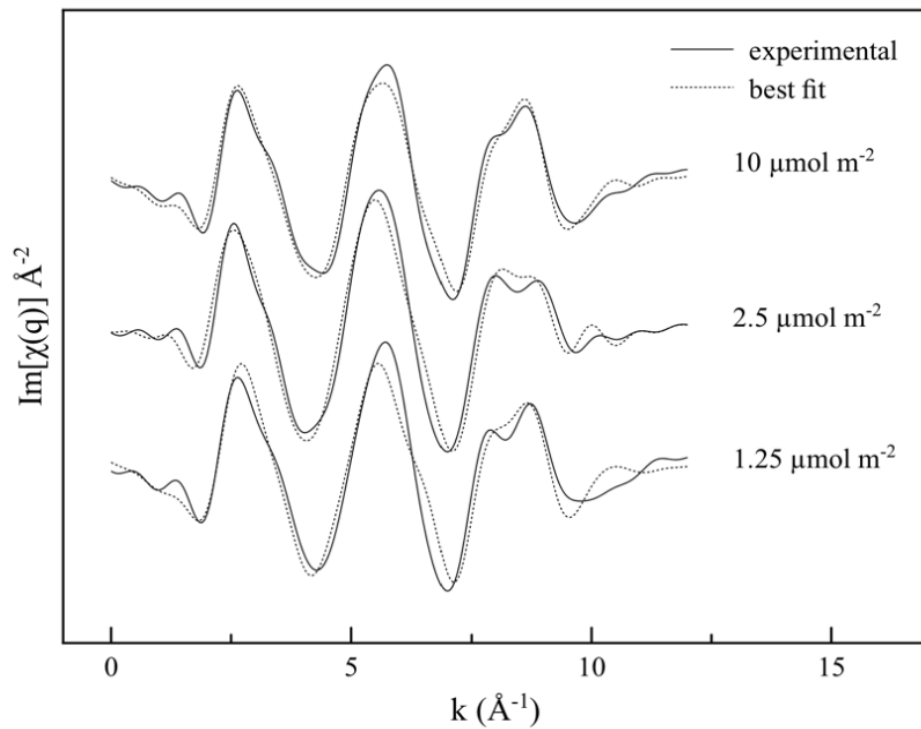
Figure 2.5b. Imaginary (q) part of the Fourier Transform of P sorbed on goethite at three different surface coverages, 1.25, 2.5 and 10 µmol m^{-2}.
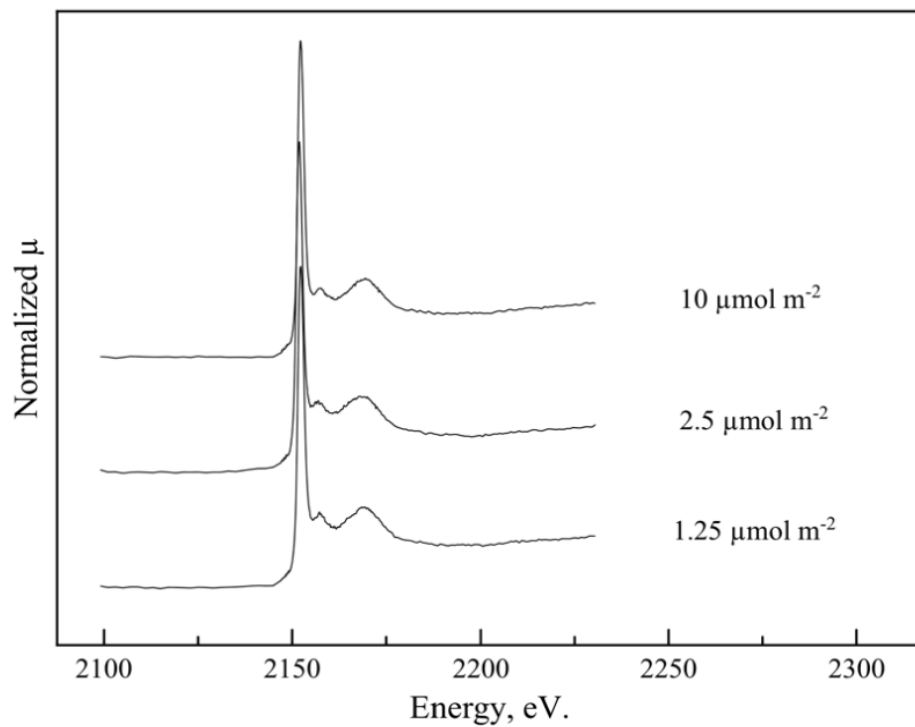
Figure 2.6. XANES spectra of P sorbed on goethite at three different surface coverages, 1.25, 2.5 and 10 µmol m^{-2}.

REFERENCES

Antelo, J., Avena, M., Fiol, S., Lopez, R., Arce, F. Effects of pH and ionic strength on the adsorption of phosphate and arsenate at the goethite– water interface. J. Colloid Interface Sci., 285:476–486, 2005

Antelo, J., Fiol, S., Pérez, C., Mariño, S., Arce, F., Gondar, D. López, R. Analysis of phosphate adsorption onto ferrihydrite using the CD-MUSIC model. J Colloid Interface Sci., 347:112-119, 2010

Antelo, J., Arce, F., Avena, M., Fiol, S. López, R., Macías, F. Adsorption of a soil humic acid at the surface of goethite and its competitive interaction with phosphate. Geoderma, 138:12-19, 2007

Arai, Y., Elzinga, E. J., Sparks, D. L. X-ray absorption spectroscopic investigation of arsenite and arsenate adsorption at the aluminum oxide-water interface. J. Colloid Interface Sci., 235:80-88, 2001

Arai, Y. & Sparks, D. L. ATR-FTIR spectroscopic investigation on phosphate adsorption mechanisms at the ferrihydrite-water interface. J. Colloid Interface Sci., 241: 317-326, 2001

Arai, Y. & Sparks, D. L. Phosphate Reaction Dynamics in Soils and Soil Minerals: A Multiscale Approach, *In* Advances in Agronomy, 94: 135-179, 2007

Bleam, W. F., Pfeffer, P. E., Goldberg, S., Taylor, R. W., Dudley, R. A 31P Solid-state Nuclear Magnetic Resonance Study of Phosphate Adsorption at the Boehmite/Aqueous Solution Interface. Langmuir, 7:1702–1712, 1991

Carabante, I., Grahn, M., Holmgren, A. Hedlund, J. In situ ATR-FTIR studies on the competitive adsorption of arsenate and phosphate on ferrihydrite. J. Colloid Interface Sci., 351:523-531, 2010

Charlet, L. & Manceau, A. X-ray absorption spectroscopic study of the sorption of Cr(III) at the oxide-water interface : II. Adsorption, coprecipitation, and surface precipitation on hydrous ferric oxide. J. Colloid Interface Sci., 148: 443-458, 1992

Corey, R.B. Adsorption vs. coprecipitation, (1981) pp.161-182. In: (Anderson, M.A. and Rubin, A.J. eds.) Adsorption of Inorganics at Solid-Liquid Interfaces, Ann Arbor Science, Ann Arbor Mich.

Dzombak, D. A., & Morel, F. M. M. Surface Complexation Modeling: Hydrous Ferric Oxide. Wiley-Interscience, 1990. New York, 393 pp.

Elzinga, E. J., & Sparks, D. L. Phosphate adsorption onto hematite: An in situ ATR-FTIR investigation of the effects of pH and loading level on the mode of phosphate surface complexation. J. Colloid Interface Sci., 308:53–70, 2007

Fendorf, S. Surface reactions of chromium in soils and waters. Geoderma 67:55–71, 1995

Fendorf, S. E., Eick, M. J., Grossl, P. R., Sparks, D. L. Arsenate and chromate retention mechanisms on goethite. 1. Surface structure. Environ. Sci. Technol. 31:315-320, 1997

Ford, R. G., & Sparks, D. L. The nature of Zn precipitates formed in the presence of pyrophyllite. Environ. Sci. Technol. 34:2479-2483, 2000

Foster A., Brown G. E. and Parks G. A. X-ray absorption fine structure study of As(V) and Se(IV) sorption complexes on hydrous Mn oxides. Geochim. Cosmochim. Acta, 67:1937–1953, 2003

Fried, C. R. & Shapiro, G. Phosphate supply pattern of various soils. Soil Sci. Soc. Am. Proc., 20:471–475, 1956

Grossl, P.R., Eick, M. J., Sparks, D. L., Goldberg, S., Ainsworth, C. C. Arsenate and chromate retention mechanisms on goethite. 2. Kinetic evaluation using a pressure-jump relaxation technique. Environ. Sci. Technol., 31:321-326, 1997

Hesterberg, D., Zhou, W., Hutchison, K. J., Beauchemin, S., Sayers, D. E. XAS study of adsorbed forms of phosphate. J. Synchrotron Rad., 6:636-638, 1999

Hiemstra, T. Surface complexation at mineral interfaces: Multisite and Charge Distribution approach. (Ph.D. thesis), Wageningen University, 2010

Hingston, F. J., Atkinson, R. J., Posner, A. M., Quirk, J. P. Specific adsorption of anions on goethite. Congr. Soil Sci. Soc. 9th (Adelaide), 669-678, 1968

Hingston, F. J., R. J., Posner, A. M., Quirk, J. P. Adsorption of selenite by goethite. Adv. Chem. Series, 79:82-90, 1968

Hingston, F. J., R. J., Posner, A. M., Quirk, J. P. Competitive adsorption of negatively charged ligands on oxide surfaces. Disc. Faraday Soc., 52:334-342, 1971

Hingston, F. J., R. J., Posner, A. M., Quirk, J. P. Anion adsorption by goethite and gibbsite. I. The role of the proton in determining adsorption envelops. J. Soil Sci., 23:177-192, 1972

Hingston, F. J., R. J., Posner, A. M., Quirk, J. P. Anion adsorption by goethite and gibbsite. II. Desorption of anions from hydrous oxide surfaces. J. Soil Sci., 25:16-26, 1974

Khare, N., D. Hesterberg, and J. D. Martin. Investigating phosphate surface precipitation in single and binary mixtures of Fe- and Al-oxide minerals using XANES. Environ. Sci. Technol., 39:2152-2160, 2005

Khare, N., J. D. Martin, and D. Hesterberg. Phosphate bonding configuration on ferrihydrite based on molecular orbital calculations and XANES fingerprinting. Geochim. Cosmochim. Acta, 71:4405-4415, 2007

Kim, Y. & Kirkpatrick, R. J. An investigation of phosphate adsorbed on aluminium oxyhydroxide and oxide phases by nuclear magnetic resonance. Eur. J. Soil Sci., 55:243–251, 2004

Kim, J., Li, W., Philips, B. L., Grey, C. P. Phosphate adsorption on the iron oxyhydroxides goethite (α-FeOOH), akaganeite (β-FeOOH), and lepidocrocite (γ-FeOOH): a ^{31}P NMR Study. Energy Environ. Sci., 4:4298-4305, 2011

Kwon, K. D. & Kubicki, J. D. Molecular Orbital Theory Study on Surface Complex Structures of Phosphates to Iron Hydroxides: Calculation of Vibrational Frequencies and Adsorption Energies. Langmuir, 20:9249-9254, 2004

Luengo, C., Brigante, M., Antelo, J., Avena, M. Kinetics of phosphate adsorption on goethite: Comparing batch adsorption and ATR-IR measurements. J. Colloid Interface Sci., 300:511-518, 2006

Li, W., Feng, J., Kwon, K. D., Kubicki, J. D. Phillips, B. L. Surface Speciation of Phosphate on Boehmite (γ-AlOOH) Determined from NMR Spectroscopy. Langmuir, 26:4753–4761, 2010

Manning, B. A., Fendorf, S. E., Goldberg, S. Surface Structures and Stability of Arsenic(III) on Goethite: Spectroscopic Evidence for Inner-Sphere Complexes. Environ. Sci. Technol., 32:2383-2388, 1998

Morin, G., Ona-Nguema, G., Wang, Y., Menguy, N., Juillot, F., Proux, O., Guyot, F., Calas, G., Brown Jr., G. E. Extended X-ray absorption fine structure analysis of arsenite and arsenate adsorption on maghemite, Environ. Sci. Technol., 42:2361–2366, 2008

Nachtegaal, M. & Sparks, D. L. Effect of iron oxide coatings on zinc sorption mechanisms at the clay-mineral/water interface. J. Colloid Interf. Sci. 276:13-23, 2004

Newville, M., Livins, P., Yacoby, Y., Rehr, J. J., Stern, E. A. Near-edge x-ray-absorption fine structure of Pb: A comparison of theory and experiment. Phys. Rev. B Condens. Matter 47:14126–14131,1993

Olsen, S. R. & Watanabe, F. S. A method to determine a phosphorus adsorption maximum of soils as measured by the Langmuir isotherm. Soil Sci. Soc. Am. Proc., 21:144–149, 1957

Ona-Nguema G., Morin, G., Juillot, F., Calas, G. Brown, G. E. EXAFS analysis of arsenite adsorption onto two-line ferrihydrite, hematite, goethite, and lepidocrocite. Environ. Sci. Technol., 39:9147–9155, 2005

Parfitt, R.L., R.J. Atkinson, and R. St.C. Smart. The mechanism of phosphate fixation by iron oxides. Soil Sci. Soc. Am. J., 39:837-841, 1975

Parfitt, R. L., Atkinson, R. J. Phosphate adsorption on goethite (α-FeOOH). Nature, 264:740-742, 1976

Parfitt, R.L., & Russell, J. D. Adsorption on hydrous oxides. IV. Mechanisms of adsorption of various ions on goethite. J. Soil Sci., 28:297-305, 1977

Peak, J. D. & Sparks, D. L. Mechanisms of selenate adsorption on iron oxides and hyroxides. Environ. Sci. Technol., 36:1460-1466, 2002

68

Persson, P., Nilsson, N., Sjoberg. S. Structure and Bonding of Orthophosphate Ions at the Iron Oxide–Aqueous Interface. J. Colloid Interface Sci., 177:263–275, 1996

Rahnemaie R., Hiemstra T., van Riemsdijk W. H. Geometry, Charge Distribution, and Surface Speciation of Phosphate on Goethite. Langmuir, 23:3680-3689, 2007

Roberts, D.R., R.G. Ford and D.L. Sparks. Kinetics and mechanisms of Zn complexation on metal oxides using EXAFS spectroscopy. J. Colloid Interface Sci., 263:364-376, 2003

Rouff, A. A., Natchegaal, M., Rabe, S., Vogel, F. X-ray absorption fine structure study of the effect of protonation on disorder and multiple scattering in phosphate solutions and solids. J. Phys. Chem. A., 113:6895-903, 2009

Scheidegger, A.M., Lamble, G. M., Sparks, D. L. Spectroscopic evidence for the formation of mixed-cation, hydroxide phases upon metal sorption on clays and aluminum oxides. J. Colloid Interface Sci., 186:118-128, 1997

Scheidegger, A. M., Strawn, D. G., Lamble, G.M., Sparks, D.L. The kinetics of mixed Ni-Al hydroxide formation on clay and aluminum oxide minerals: A time-resolved XAFS study. Geochim. Cosmochim. Acta, 62:2233-2245, 1998

Schwertmann, U., Cornell, R. M. Iron Oxides in the Laboratory: Preparation and Characterization; Wiley-VCH: Weinheim, Germany, 2000

Sparks, D. L. Environmental Soil Chemistry. Second Edition. Academic Press, 2002, 368 pg.

Tejedor-Tejedor, M. I., & Anderson, M. A. The protonation of phosphate on the surface of goethite as studied by CIR-FTIR and electrophoretic mobility. Langmuir, *6*:602–611, 1990

Torrent, J. Activation Energy of the Slow Reaction between Phosphate and Goethites of Different Morphology. Aust. J. Soil Res., 29:69-74, 1990

Ravel, B. & Newville, M. ATHENA and ARTEMIS: interactive graphical data analysis using IFEFFIT. J. Synchrotron Rad. 12:537–541, 2005

Waychunas G. A., Rea, B. A., Fuller, C. C., Davis, J. A. Surface chemistry of ferrihydrite. 1. EXAFS studies of the geometry of coprecipitated and adsorbed arsenate. Geochim. Cosmochim. Acta, 57:2251–2269, 1993

Chapter 3

USING EXTENDED X-RAY ABSORPTION FINE STRUCTURE SPECTROSCOPY TO DETERMINE THE BONDING CONFIGURATIONS OF ORTHOPHOSPHATE SURFACE COMPLEXES AT THE GOETHITE/WATER INTERFACE II: RESIDENCE TIME AND pH EFFECTS

Abstract

Identifying the mechanisms by which P is bound to soils and soil constituents is ultimately important as they provide information on the stability of bound species and their reactivity in the environment. EXAFS studies were carried out to provide information on how the local chemical environment of sorbed P changes as an effect of pH and time. Goethite was reacted with orthophosphate at a P concentration of 0.8 mmol L^{-1} P at pH 3.0, 4.5 and 6.0. The residence time effect on the mechanisms of P sorption on goethite was also evaluated for two different reaction times, 5 and 18 days, on goethite suspensions reacted at pH 4.5. The objective of this study was to understand how P sorption mechanisms change over a wide pH range when subjected to P concentrations above the P saturation ratio of goethite. Phosphorus K-edge EXAFS spectra were collected at 2,150 eV in fluorescence mode and the structural parameters were obtained through the fits of sorption data using Artemis. The monodentate surface complex was shown to be the predominant mechanism by which P sorbs at the goethite surface under the experimental conditions. The lack of a discrete Fe – P shell and the presence of highly

disordered structures, particularly, at R-space ≥ 4 suggested the formation of P surface precipitates at the goethite/water interface.

Keywords: surface complexation, surface precipitation, P K-edge EXAFS, P solid-phase speciation

3.1 Introduction

The reactions controlling the fate of oxyanion sorption in soils and soil components is intrinsically dependent upon the interaction between the sorbate species and the sorbent surface, e.g., phosphate (P) and goethite, respectively, and on the pH of the medium. This is because pH and contact time between these two entities has a profound effect on the molecular arrangement of the structures formed, (O'Reilly et al., 2001; Arai & Sparks, 2002), which will, eventually, determine the bioavailability, transport potential and cycling of chemicals in soils (Pignatello & Xing, 1995, Scheidegger et al., 1998; Strawn et al., 1998).

Phosphate, an essential plant nutrient and major culprit of eutrophication in fresh waters, is predominantly sorbed in soils by amorphous and crystalline Fe and Al (hydr)oxides through surface complexation or via formation of surface precipitates (McLaughlin et al., 1981; Borggaard, 1983; Parfitt, 1989). Goethite (α-FeOOH) is the most common Fe oxide in soils and has the highest P sorption capacity (~ 2.5 μmol m^{-2}, Borggaard, 1983; Torrent et al., 1990) among the crystalline Fe oxides.

From a macroscopic standpoint, the kinetics of P sorption on goethite is well established, characteirized by biphasic kinetics over two time regions (Barrow, 1985; Torrent et al., 1992): an initial rapid reaction followed by slower uptake kinetics which have been attributed, among others, to the formation of surface precipitates of insoluble phosphates at the mineral surface (Torrent, 1991) and surface complexation. The later includes the formation of bidentate binuclear (^{2}C) and monodentate mononuclear (^{1}V) structures (Parfitt & Russel, 1977; Tejedor-Tejedor & Anderson, 1990; Persson et al., 1996; Luengo et al., 2006; Rahnemaie et al., 2007; Kim et al., 2011). Several

spectroscopic techniques have been employed to address the sorption mechanisms of P in soils and soil components, primarily, vibrational spectroscopies, particularly IR. This is because the spectral information garnered from this technique represents a fingerprint of the molecular arrangement of a sample with absorption peaks corresponding to the frequencies of vibrations between the bonds of the atoms making up the material being analyzed.

In spite of the versatility of this technique, IR has some limitations in terms of data interpretation provided the lack of accuracy in determining the exact identity of surface structures due to the reliance of molecular assignments on the analytical approach used (Arai & Sparks, 2007).

Unlike IR, Extended X-Ray Absorption Fine Structure (EXAFS) spectroscopy offers relatively more straightforward information on coordination number, type of nearest neighbors and their distances to the absorbing atom (Fendorf et al., 1997; Scheidegger et al., 1998; O'Reilly et al., 2001; Arai & Sparks, 2002). In addition, it can provide a thorough depiction of interfacial reactions involved in the transition of the surface structures arising at the surface of the solid (Abdala, 2012).

In light of the great advantages of EXAFS over other spectroscopic techniques, which often require drying and high vacuum, EXAFS spectroscopy has been among the most prominent techniques for studies on the partitioning of heavy metals ions at mineral/water interfaces (Scheidegger et al., 1997; Fendorf et al., 1997). EXAFS has been widely used in studies on the surface complexation of environmentally relevant elements formed at mineral oxide surfaces and is an effective technique for conducting *in situ* studies addressing, among others, the residence time (Charlet & Manceau, 1992;

Manning et al., 1998; Scheidegger et al., 1998; O'Reilly et al., 2001; Arai & Sparks, 2002) effects on the formation of and differentiation between sorption complexes and surface precipitates.

The objective of this study was to examine the pH and the residence time effects on P surface complexes formed at the goethite/water interface across a wide pH range and at P concentrations commonly found in soil environments via EXAFS spectroscopy.

3.2   Material & Methods

3.2.1   Mineral Synthesis

Goethite was synthesized according to Schwertmann & Cornell (2000) and is described in details in Chapter 2.

3.2.2   Sorption Experiments

Goethite was spiked with orthophosphate at a P concentration of 0.8 mM L^{-1}, which is a P concentration equivalent to four times the sorption saturation capacity of goethite ($\sim$ 2.5 μmol m^{-2}, Borggaard, 1983; Torrent et al., 1990) to effect monolayer coverage. Goethite suspensions were reacted with P at the above-mentioned concentration across a wide range of pH, namely 3.0, 4.5 and 6.0. Goethite suspensions at pH 4.5 were also reacted for two different reaction times, 5 and 18 days.

Centrifuge tubes containing stock goethite suspensions of 20 g L^{-1} were placed in a rotating shaker set at 30 rpm at 298 K and equilibrated in 50 mmol L^{-1} KCl with pH

adjusted to either 3.0, 4.5 or 6.0 for 36 h prior to phosphate addition. The pH in the suspensions was monitored throughout the shaking period and adjusted to the target pH as needed. Thereafter, an aliquot of the suspension was transferred to a new centrifuge tube to yield a goethite suspension of 2 g L^{-1}, and phosphate solution to yield a P concentration of 0.8 mmol L^{-1} was added. At the end of the agitation period, 5 mL aliquots from each tube were sampled for analysis as described in the following session.

3.2.3 EXAFS Sample Preparation and Analysis

After sampling, each sample was immediately filtered to pass through a 0.22 μm nitrocellulose membrane filter and washed three times with 3 mL of pH adjusted 50 mmol L^{-1} KCl to remove any entrained phosphate not associated with the surface. The cellulose membrane filter containing the mineral paste was sealed with polypropylene XRF thin film (Ultralene®) and stored moist in a sealed sample box at 6 ºC until analysis. Phosphorus K-edge spectra (2,151 eV) were collected at beamline SXS at the Laboratório Nacional de Luz Synchrotron (LNLS), in Campinas, Brazil. EXAFS spectra were collected in fluorescence mode using a silicon drift detector. The beamline was equipped with a monochromator consisting of double crystal Si (111) and the electron storage ring was operated at 2.5 GeV with a current range of about 110 to 300 mA. In order to reject higher-order harmonics, one of the monochromator crystals was detuned 45% with respect to the other crystal. XAS spectra were collected at photon energies between 2100 and 2800 eV. with a minimum step size of 0.1 eV. between 2100 and 2155 eV. and larger step sizes varying from 0.75 to 6 between 2175 to 2800 eV. Thirteen to eighteen

76

individual spectra were averaged followed by subtraction of the background absorbance through the pre-edge region using the Autobk algorithm (Newville et al., 1993).

3.2.4   EXAFS Data Analysis

The averaged spectra were normalized to an atomic absorption of one, and the EXAFS signal was extracted from the raw data using linear pre-edge and a quadratic spline post-edge, and data were converted from energy to photo electron momentum (k-space) and k-weighted by k^2. EXAFS spectra were calculated over a typical k-space range with a Hanning window and 0.5 width Gaussian wings. Fourier transforms (FT) of the k^2–weighted EXAFS were calculated over a k-range between 10.3 and 10.6 and performed to obtain the radial distribution function (RDF) in R-space. We employed Artemis' quick first shell theory to fit the Fourier transformed EXAFS. The FT of the EXAFS was fit with the predicted function by varying the number of coordinating atoms (CN), their distance (ΔR), mean square displacement (δ^2) and passive electron reduction factor (S_0^2) in order to obtain the best fit between the experimental and predicted spectra.

A more detailed description of the fitting and data processing can be found in Chapter 2.

3.3   Results & Discussion

Studies addressing P sorption mechanisms on Fe and Al (hydr)oxides, particularly on goethite, have resulted in countless conflicting interpretations of binding mechanisms.

It is not unusual to find studies indicating that bidentate and monodentate configurations have been assigned to the formation of a phosphate surface complex under similar experimental conditions (see Table 2.1 from chapter 2 for a comprehensive list of references on this topic).

Previous studies dealing with the use of spectroscopic techniques to characterize phosphate surface complexes forming on (hydr)oxide mineral surfaces include MO/DFT and ATR-FTIR, CIR-FTIR, NMR and XANES spectroscopies. Unlike the above-mentioned spectroscopic techniques, EXAFS analysis is able to provide detailed information on the local coordination environment of an atom, such as interatomic distances, nearest neighbors and coordination numbers. The discussion that follows will be focused on the orthophosphate bonding configurations on the basis of interatomic distances and coordination numbers found within our orthophosphate/goethite systems.

3.3.1 P-EXAFS Spectra

Figure 3.1 shows the experimental $\chi(k)$ spectra of goethite spiked with P at a P concentration of 0.8 mmol L^{-1} at pH 3.0, 4.5 and 6.0. The radial distribution function (RDF) is a result of the Fourier transformation of the $\chi(k)$ function. The peaks shown in the experimental $\chi(k)$ spectra correspond to the coordination shells formed between P – O and P – Fe and reflect the interatomic distances within the material. For all samples, the E_0 ranged from 0.79 to 3.6 eV. The contributions of O were localized at P – O distances ranging from 1.51 to 1.54, being longer at the lowest pH, 1.54 Å, intermediate at pH 4.5, 1.53 Å, and shorter at pH 6.0, 1.51 Å, and MS dominated at ~ 2.75 – 2.79 Å. The P – Fe

shells indicated the existence of two predominant bonding configurations between P and

the goethite surface, bidentate binuclear and monodentate mononuclear.
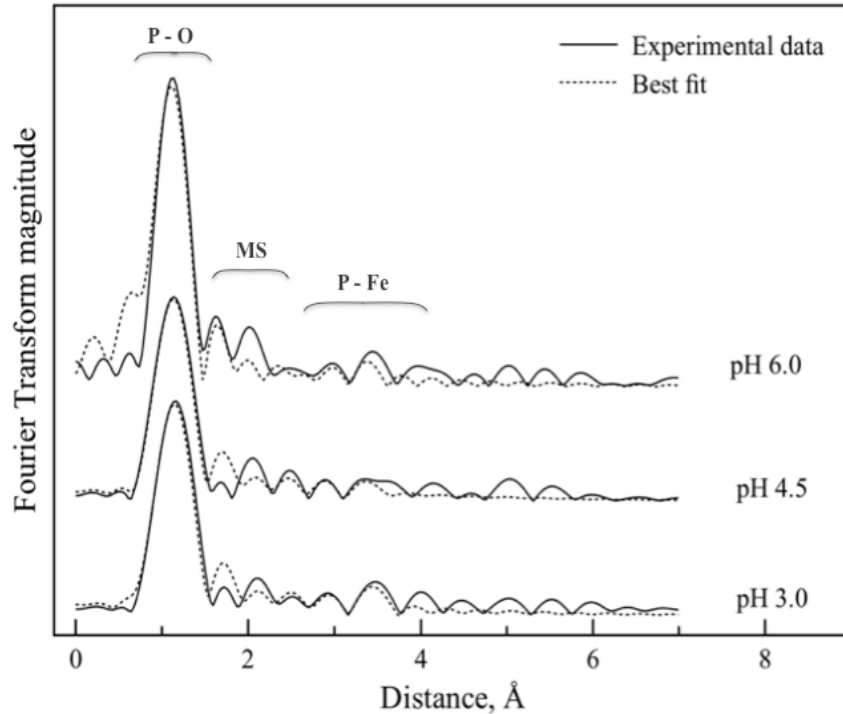
Figure 3.1   Fourier transformed spectra of experimental (solid line) and best fit (dashed line) of the phosphate surface complexes formed at the goethite/water interface at pH 3.0, 4.5 and 6.0. A change in spectrum shape (R-space) as a result of increasing pH from pH 3.0 to 6.0 indicates that the phosphate surface speciation is sensitive to pH. Braces are intended to show the approximate region where the P – O, MS and P – Fe shells most significantly contribute in radial distance in the Fourier transformed spectra.
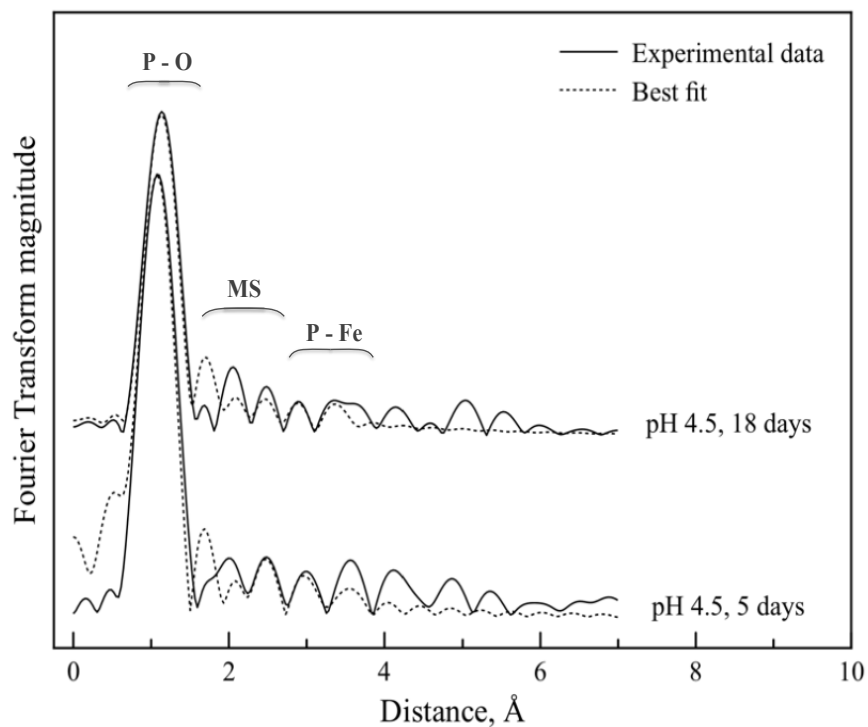
Figure 3.2   Fourier transformed spectra of experimental (solid line) and best fit (dashed line) of the phosphate surface complexes formed at the goethite/water interface at pH 4.5 at 5 and 18 days reaction time. Braces are intended to show the approximate region where the P – O, MS and P – Fe shells most significantly contribute in radial distance in the Fourier transformed spectra.
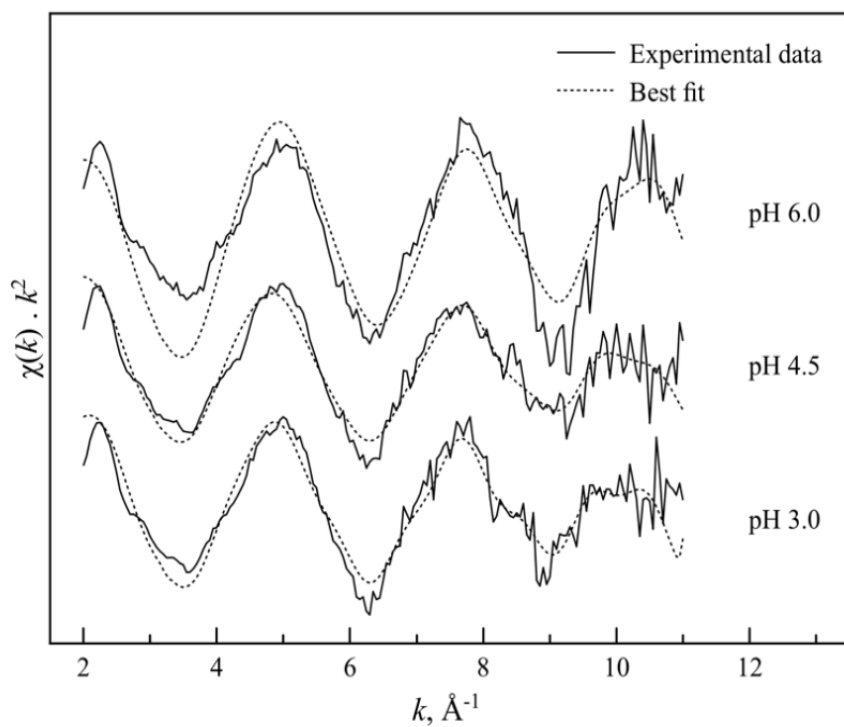
Figure 3.3   Experimental (solid line) and best-fit (dashed line) k^2-weighted back transformed spectra of phosphate sorbed on goethite at pH 3.0, 4.5 and 6.0.
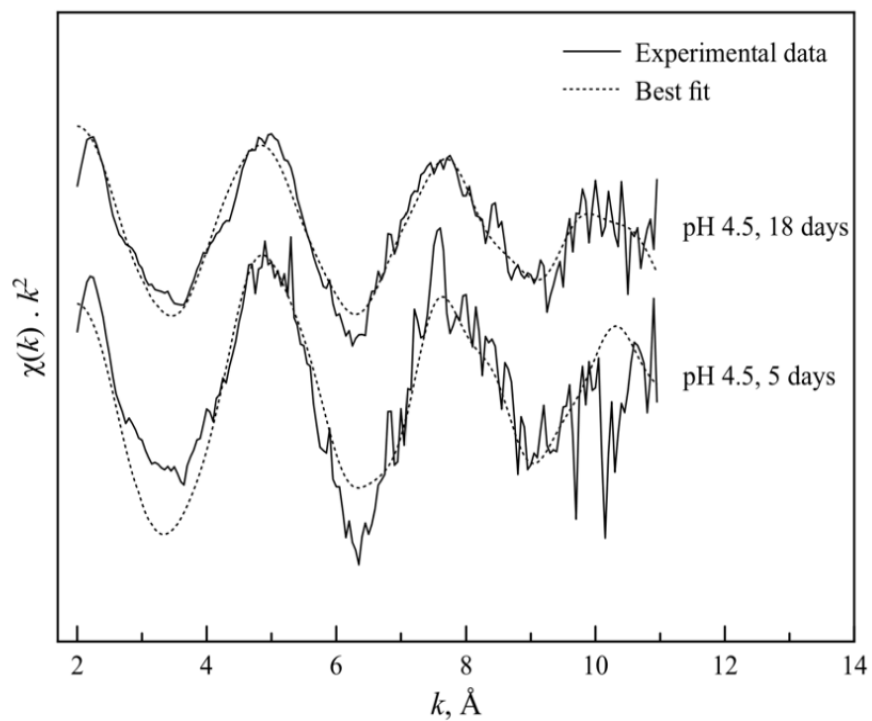
Figure 3.4   Experimental (solid line) and best-fit (dashed line) k^2-weighted back transformed spectra of phosphate sorbed on goethite at pH 4.5 at 5 and 18 days reaction time.

3.3.2   Overall Formation of P Surface Complexes at the Goethite/Water Interface

Two different phosphate surface complexes were identified at the goethite/water interface at the experimental conditions investigated, namely bidentate binuclear (^2C) and monodentate mononuclear (^1V) surface complexes. Additionally, analyzes of the Fourier transforms of sorption data suggests that surface precipitates were also present across all samples analyzed in our study.

The shortest P – Fe distances of 3.35, 3.27 and 3.26 Å were characteristic of a bidentate binuclear configuration between P and Fe across the pH range in our study, 3.0, 4.5 and 6.0, respectively. The most distant shells, occurring at ~ 3.60, 3.53 and 3.58 Å were indicative of a monodentate configuration between P and Fe. Table 3.2 shows the, P – O and P – Fe bonding distances and corresponding P sorption mechanisms. In terms of reaction time effects on P bonding configurations, no changes in the predominance of a surface complex over another were observed. However, our results showed that aging had a rather pronounced effect on bond lengths, suggesting that longer contact times favor shorter bond lengths, as evidenced by a shorter P – O bond at goethite reacted for 18 days, 1.51 Å, in comparison with a longer P – O bond of 1.53 Å for goethite reacted with orthophosphate for 5 days. On the basis of P – Fe bond lengths, residence time showed an even more significant effect on bond lengths, shortening P – Fe distances by as much as 7 Å on both surface complexes.

3.3.3 Adsorption Complexes

As indicated in Table 3.2, our results show that bidentate and monodentate surface complexes were present in all samples regardless of pH and reaction times. However, as indicated by the amp (S_0^2) values, a higher contribution of monodentate configuration was experienced at lower pHs that progressively decreased as pH increased from 3.0 to 6.0. The bidentate configuration was a minor contribution in the RDF, however, a bidentate path improved the fits significantly. This seems consistent with the literature that indicated that low surface coverages favor the formation of bidentate surface complexes (Parfitt et al., 1975a; Parfitt et al., 1975b; Parfitt et al., 1976; Parfitt & Atkinson, 1976; Parfitt, 1977; Tejedor-Tejedor & Anderson, 1990; Kim & Kirkpatrick, 2004; Elzinga & Sparks, 2007; Rahnemaie et al., 2007) and that the relative importance of bidentate binuclear species decreases as surface loading increases such that a monodentate configuration would predominate at higher surface loadings (Tejedor-Tejedor & Anderson, 1990; Rahnemaie et al., 2007). Antelo et al. (2005, 2010) on the basis of ATR-FTIR, have observed that P adsorbs mainly as bidentate complexes at high phosphate loadings and that monodentate surface complexes begin to be important at low phosphate loadings and at high pHs. This was ascribed to bidentate species locating more charge at the surface than monodentate species, producing a lower electrostatic repulsion between the adsorbed species in the 1-plane. Interestingly, the observation of Antelo et al. (2005, 2010) is consistent with the behavior of arsenic in its pentavalent form (As(V)), an analog of phosphate, having similar chemical and geometric properties, and present as the ionic species, $H_2AsO_4^-$ and $H_2PO_4^-$, respectively, at the typical pH range in the environment.

3.3.4 Bidentate Binuclear Configuration

A bidentate binuclear configuration (^{2}C) of phosphate on (hydr)oxides has been shown in the literature to exist over a wide range of pH (Table 1 from Chapter 2). In this study, the ^{2}C surface complex was present, although at different proportions, across the entire pH range in the study. As discussed in Chapter 2, a bidentate configuration should be expected to predominate at lower surface coverages as that configuration should be favored when the Fe/P ratio is smaller than unity. It follows that at low P concentration, the sorption sites compete with the PO_4 molecules at the same strength such that one PO_4 molecule must equally satisfy as many sorption sites as possible. Therefore, ^{2}C forms first and because it is strongly bound to high affinity sorption sites, it has a large thermodynamic stability, thus remaining associated with the surface even as solution P concentration increases. The higher proportion of a ^{2}C configuration was found to be in good agreement with the proposal by Hiemstra (2010) that at low pHs, a higher positive surface charge induces a higher adsorption capacity for anions like phosphate, because more negative charge can be brought to the surface for a given change in electrostatic potential.

Table 3.2 shows the surface complex distribution as a function of pH.

3.3.5 Monodentate Configuration

Overall, our results showed that a monodentate species is dominant over a broad pH range and high surface loadings whereas a bidentate species is particularly important at low pHs.

85

Our results were in good agreement with the relatively few spectroscopic studies that have reported P being attached to (hydr)oxide surfaces in a monodentate (^{1}V) configuration (see Table 2.1 from Chapter 2). The studies in which a ^{1}V configuration has been observed were, in general, carried out employing P concentrations at relatively high surface coverages (Tejedor-Tejedor & Anderson, 1990; Elzinga & Sparks, 2007). Residence time had a marked effect on bond lengths, with a P – Fe distance of 3.6 Å for goethite reacted for 5 days and 3.53 Å when reaction time was extended to 18 days.

Whereas the P – Fe distances for bidentate binuclear configuration are in good agreement with the work by Rahnemaie et al. (2007), who found P – Fe distances varying between 3.22 to 3.26 Å, the P – Fe distance for a monodentate configuration observed in our study was much larger, varying from 3.53 to 3.6 Å, though in agreement with the calculations performed by Kwon & Kubicki (2004), who found P – Fe bond distances generally longer for either configuration, if a $\geq$ 170º angle is formed by P – O – Fe, suggesting a P – Fe bond distance of around 3.6 Å. EXAFS studies indicate that for As(V) these distances are generally in the order of 3.57 to 3.63 Å (Waychunas et al., 1993; Fendorf et al., 1997). Since P is a much lighter element than As, it is possible that the repulsion of P by the Fe atoms tend to maintain P farther apart from Fe as possible, thus P – O – Fe forms preferentially a linear structure when a monodentate configuration is formed. Alternatively, the Fe – O bond distance may also be influenced by repulsion and, accordingly, resulting in a longer total Fe – P distance.

3.3.6   Surface Precipitate Formation

The transition point from adsorption (or monolayer surface coverage) to precipitation (multilayer coverage or the formation of a separate phase) is not clearly defined (Corey, 1981). Torrent et al. (1990) estimated that, for monolayer coverage, the maximum P adsorption at the goethite surface should be 5 μmol m^{-2} for mononuclear bonding or 2.5 μmol m^{-2} for binuclear bonding. On the basis of their calculation, surface precipitates should have been observed at the two highest P loadings in our study. According to Dzombak & Morel (1990), the dissolution of iron from the mineral (hydr)oxide is a limiting factor for surface precipitation to occur, since surface precipitates are formed at the expense of dissolved material from the adsorbent surface. This might be the reason for the small degree of surface precipitation observed, given the relatively high phosphate loading employed in this study.

We observed surface precipitates in our study on the basis of calculations performed to the overall amplitude and the individual fractions of P in each bonding configuration in which we considered the relative distribution of monodentate and bidentate binuclear surface complexes. Additionally, the presence of some modulation of short-range ordered structure, appearing at high RDF values (≥ 3.5 Å), associated with the lack of a discrete Fe shell, was interpreted as an indication of the formation of highly disordered surface precipitates structures.

3.4   Conclusions

A combination of strong X-ray attenuation, hence weak X-ray scattering by P, led to EXAFS spectra with poor signal-to-noise ratios. Accordingly, the uncertainties associated with the parameter estimates were somewhat high.

Aside from the technical limitations imposed by P-EXAFS measurements, we have successfully showed the applicability of EXAFS spectroscopy to shed light on the mechanisms by which P sorbs onto goethite across a wide pH range, relatively high surface loadings and reaction times.

Accordingly, the monodentate complex was observed across the entire pH range in study, indicating that pH does not seem to play a major role in surface complexation under the experimental conditions in which this study was carried out. The bidentate binuclear surface complex was also observed, particularly at lower pHs. It is important to mention that while the EXAFS spectra are dominated by monodentate bonding configuration, the presence of the bidentate complex shows that, regardless of environmental conditions, e.g., pH, surface loading and residence time, its formation is thermodynamically favorable (Chapter 2). It is also important to note that, even though the bidentate complex contribution is little, the dominance of the monodentate complex signal in the EXAFS spectra represents the 'average' local environment of P.

Residence time had a particular effect on P – Fe distances, in which longer exposure times resulted in shorter P – Fe distances for either monodentate or bidentate surface complexes. The shortening of P – Fe distances as reaction time increases seems to reflect some sort of instability of both surface complexes at short reaction times. The formation of shorter P – Fe bond distances at extended reaction times suggest that both

surface complexes become more stable as they are located closer to the surface. This suggests, therefore, that shorter exposure times may favor a greater reversibility of phosphate.

The ubiquitous presence of some modulation of short-range order structure, appearing at high RSF values (≥ 3.5 Å) associated with the lack of a discrete Fe shell could be an indication for the formation of highly disordered structures, such as surface precipitates.

Table 3.1. P – O and P – Fe bonding distances, surface complex distribution and corresponding bonding configurations of P on goethite at three different pHs.

pH	P - O		P - Fe			
			Bidentate		Monodentate	
	R $\overset{\circ}{A}$	σ^2	R $\overset{\circ}{A}$	σ^2	R $\overset{\circ}{A}$	σ^2
3.0	1.54 (±0.004)	0.0014 (±0.0007)	3.35 (±0.09)	0.01 (±0.01)	3.6 (±0.03)	0.0014 (±0.004)
4.5	1.53 (±0.005)	0.0018 (±0.0007)	3.25 (±0.06)	0.0012 (±0.008)	3.53 (±0.04)	0.0053 (±0.007)
6.0	1.51 (±0.007)	0.0001 (±0.0001)	3.27 (±0.06)	0.008 (±0.03)	3.58 (±0.09)	0.004 (±0.01)

R: radial structure function (RSF); σ^2: mean square displacement, S_0^2: passive electron reduction factor,

( ): uncertainties associated with parameter estimates

Table 3.2. P – O and P – Fe bonding distances, surface complex distribution and corresponding bonding configurations of P on goethite at two different reaction times.

Reaction time days	P - O		P - Fe			
			Bidentate		Monodentate	
	R $\overset{\circ}{A}$	σ^2	R $\overset{\circ}{A}$	σ^2	R $\overset{\circ}{A}$	σ^2
5	1.51 (±0.004)	0.0004 (±0.0009)	3.30 (±0.05)	0.0002 (±0.005)	3.6 (±0.04)	0.003 (±0.006)
18	1.53 (±0.005)	0.0018 (±0.0007)	3.25 (±0.06)	0.0012 (±0.008)	3.53 (±0.04)	0.0053 (±0.007)

R: radial structure function (RSF); σ^2: mean square displacement, S_0^2: passive electron reduction factor,

( ): uncertainties associated with parameter estimates

REFERENCES

Antelo, J., Avena, M., Fiol, S., Lopez, R., Arce, F. Effects of pH and ionic strength on the adsorption of phosphate and arsenate at the goethite– water interface. J. Colloid Interface Sci., 285:476–486, 2005

Antelo, J., Fiol, S., Pérez, C., Mariño, S., Arce, F., Gondar, D. López, R. Analysis of phosphate adsorption onto ferrihydrite using the CD-MUSIC model. J Colloid Interface Sci., 347:112-119, 2010

Arai, Y. & Sparks, D. L. Residence time effects on arsenate surface speciation at the aluminum oxide-water interface. Soil Sci., 167:303-314, 2002

Arai, Y. & Sparks, D. L. Phosphate Reaction Dynamics in Soils and Soil Minerals: A Multiscale Approach, *In* Advances in Agronomy, 94:135-179, 2007

Borggaard, O. K. The influence of iron oxides on phosphate adsorption by soil. J Soil Sci., 34: 333–341, 1983

Charlet, L. & Manceau, A. X-ray absorption spectroscopic study of the sorption of Cr(III) at the oxide-water interface : II. Adsorption, coprecipitation, and surface precipitation on hydrous ferric oxide. J. Colloid Interf. Sci., 148: 443-458, 1992

Corey, R.B. Adsorption vs. coprecipitation, (1981) pp.161-182. In: (Anderson, M.A. and Rubin, A.J. eds.) Adsorption of Inorganics at Solid-Liquid Interfaces, Ann Arbor Science, Ann Arbor Mich.

Dzombak, D. A., & Morel, F. M. M. Surface Complexation Modeling: Hydrous Ferric Oxide. Wiley-Interscience, 1990. New York, 393 pp.

Elzinga, E. J., & Sparks, D. L. Phosphate adsorption onto hematite: An in situ ATR-FTIR investigation of the effects of pH and loading level on the mode of phosphate surface complexation. J. Colloid Interface Sci. 308:53–70, 2007

Fendorf, S. E., Eick, M. J., Grossl, P. R., Sparks, D. L. Arsenate and chromate retention mechanisms on goethite. 1. Surface structure. Environ. Sci. Technol. 31:315-320, 1997

Hiemstra, T. Surface complexation at mineral interfaces: Multisite and Charge Distribution approach. (Ph.D. thesis), Wageningen University, 2010

Kim, Y. & Kirkpatrick, R. J. An investigation of phosphate adsorbed on aluminium oxyhydroxide and oxide phases by nuclear magnetic resonance. Eur. J. Soil Sci., 55:243–251, 2004

Kim, J., Li, W., Philips, B. L., Grey, C. P. Phosphate adsorption on the iron oxyhydroxides goethite (α-FeOOH), akaganeite (β-FeOOH), and lepidocrocite (γ-FeOOH): a ^{31}P NMR Study. Energy Environ. Sci., 4:4298-4305, 2011

Kwon, K. D. & Kubicki, J. D. Molecular Orbital Theory Study on Surface Complex Structures of Phosphates to Iron Hydroxides: Calculation of Vibrational Frequencies and Adsorption Energies. Langmuir, 20:9249-9254, 2004

Luengo, C., Brigante, M., Antelo, J., Avena, M. Kinetics of phosphate adsorption on goethite: Comparing batch adsorption and ATR-IR measurements. J. Coll. Interface Sci., 300:511-518, 2006

McLaughlin, J. R., Ryden, J. C. Sayers, J. K. Sorption of phosphate by iron and aluminum-containing compounds. J Soil Sci., 32:365-377, 1981

Manning, B. A., Fendorf, S. E., Goldberg, S. Surface Structures and Stability of Arsenic(III) on Goethite: Spectroscopic Evidence for Inner-Sphere Complexes. Environ. Sci. Technol., 32:2383-2388, 1998

Newville, M., Livins, P., Yacoby, Y., Rehr, J. J., Stern, E. A. Near-edge X-ray Absorption Fine Structure of Pb: A comparison of theory and experiment. Phys. Rev. B Condens. Matter, 47:14126–14131,1993

O'Reilly, S. E., Strawn, D. G., Sparks, D. L. Residence Time Effects on Arsenate Adsorption/Desorption Mechanisms on Goethite. Soil Sci. Soc. Am. J., 65:67–77, 2001

Parfitt, R. L. Phosphate reaction with natural allophane, ferrihydrite and goethite. J Soil Sci. 40:359-369, 1989

Parfitt, R. L., R. J. Atkinson, Smart, R. St. C. The mechanism of phosphate fixation by iron oxides. Soil Sci. Soc. Am. J. 39:837-841, 1975

Parfitt, R. L., Atkinson, R. J. Phosphate adsorption on goethite (α-FeOOH). Nature. 264:740-742, 1976

Parfitt, R.L., & Russell, J. D. Adsorption on hydrous oxides. IV. Mechanisms of adsorption of various ions on goethite. J. Soil Sci. 28:297-305, 1977

Persson, P., Nilsson, N., Sjoberg. S. Structure and Bonding of Orthophosphate Ions at the Iron Oxide–Aqueous Interface. J. Colloid Interface Sci., 177:263–275, 1996

Pignatello, J. J. & Xing, B. Mechanisms of Slow Sorption of Organic Chemicals to Natural Particles. Environ. Sci. Technol., 30:1-11, 1996

Rahnemaie R., Hiemstra T., van Riemsdijk W. H. Geometry, Charge Distribution, and Surface Speciation of Phosphate on Goethite. Langmuir, 23:3680-3689, 2007

Scheidegger, A.M., Lamble, G. M., Sparks, D. L. Spectroscopic evidence for the formation of mixed-cation, hydroxide phases upon metal sorption on clays and aluminum oxides. J. Colloid Interface Sci., 186:118-128, 1997

Scheidegger, A. M., Strawn, D. G., Lamble, G.M., Sparks, D.L. The kinetics of mixed Ni-Al hydroxide formation on clay and aluminum oxide minerals: A time-resolved XAFS study. Geochim. Cosmochim. Acta, 62:2233-2245, 1998

Schwertmann, U., Cornell, R. M. Iron Oxides in the Laboratory: Preparation and Characterization; Wiley-VCH: Weinheim, Germany, 2000

Strawn, D.G., Scheidegger, A. M., Sparks, D. L. Kinetics and mechanisms of Pb(II) sorption and desorption at the aluminum oxide-water interface. Environ. Sci. Technol., 32:2596-2601, 1998

Tejedor-Tejedor, M. I., & Anderson, M. A. The protonation of phosphate on the surface of goethite as studied by CIR-FTIR and electrophoretic mobility. Langmuir, *6*:602–611, 1990

Torrent, J. Activation Energy of the Slow Reaction between Phosphate and Goethites of Different Morphology. Aust. J. Soil Res., 29:69-74, 1990

Ravel, B. & Newville, M. ATHENA and ARTEMIS: interactive graphical data analysis using IFEFFIT. J. Synchrotron Rad. 12:537–541, 2005

Waychunas G. A., Rea, B. A., Fuller, C. C., Davis, J. A. Surface chemistry of ferrihydrite. 1. EXAFS studies of the geometry of coprecipitated and adsorbed arsenate. Geochim. Cosmochim. Acta, 57:2251–2269, 1993

Chapter 4

LONG-TERM MANURE APPLICATION EFFECTS ON PHOSPHORUS DESORPTION KINETICS AND DISTRIBUTION IN HIGHLY WEATHERED AGRICULTURAL SOILS

Abstract:

Phosphorus build up in agricultural soils to excessive levels has raised a worldwide concern as to the increased fertility status of natural waters and eventual threats it poses to soil and water quality. In order to assess the long-term effects of consecutive application of manures on P reactivity and distribution in highly weathered soils, we carried out a study in some agricultural soils of Paraná state, Brazil. Phosphorus K-edge XANES, along with sequential P chemical fractionation and desorption kinetics experiments, were employed to provide micro- and macro-scale information on the long-term fate of manure application on these soils. The manure rates applied to the soils over the years were typical of intensive agricultural areas in Brazil, varying from approximately 25 to 90 ton ha^{-1} year^{-1} on a dry weight basis. The soils have been cropped year round for 10, 20 and 40 years with different land management namely Tifton pastureland, no-tillage and conventional agriculture, respectively.

Soil test P (STP) values ranged from 3.7 up to 4.3 times as much higher than the reference soil. A sharp increase in amorphous Fe and Al amounts were observed as an effect of the consecutive application of manures. Whereas our results showed that the P

97

sorption capacity of some manured soils was not significantly affected, P risk assessment indices such as the DPS_{M-3}, DPS_{Ox}, PSS and PSR-II indicated that P losses should be expected, likely due to the excessive manure rates applied to the soils. The much higher contents of amorphous Fe and Al (hydr)oxides in manured soils seem to have counterbalanced the inhibiting effect of SOM on P sorption by creating additional P sorption sites. Accordingly, the newly created P sorbing surfaces were important to prevent an even larger P loss potential. This observation was in good agreement with desorption kinetics data, which showed that higher half-lives of P in manured soils might have been due to enhanced P sorption related to higher amorphous Fe and Al (hydr)oxide contents. Additionally, P in manured soils was shown to be associated with less labile pools. The shortest half-life and thus fastest P turnover in the adjacent forest soil might have been related to more labile P pools in the untreated soil. Although manure application led to an overall enlargement of P pools, reactive P was mainly associated with the less bioavailable ones, as evidenced by sequential P fractionation data.

4.1 Introduction

Soil and water quality impairments on intensive agricultural lands, such as reduced phosphorus (P) sorption capacity of soils with subsequent acceleration in eutrophication of surface waters, have frequently been linked to P in surface runoff (McDowell & Sharpley, 2001) and P leaching (Abdala et al., 2012). The buildup of soil test P (STP) to excessive levels can occur as a result of the over application of any P source, including commercial fertilizers and manures. This has led to an increased environmental rather than agronomic concern in many geographical areas around the world (Leinweber et al., 1997; Sharpley et al., 1999; Gosh et al., 2011; Abdala et al., 2012). However, the greatest concern today is with the land application of P as manures in intensive livestock (Mullins, 2000) and poultry production areas (Gosh et al., 2011; Abdala et al., 2012). Manure contains organic and inorganic P compounds at total P concentrations ranging from lower than 1 to greater than 3 %. The inorganic P pool in manures is large and has been reported to vary between 60 and 90 %. It is essentially quite soluble and, therefore, readily available to plants (Sharpley & Moyer, 2000). However, when it comes in contact with soil, various reactions take place. Those reactions make phosphate less soluble in water and less available to plants. Even though the cycling, transport potential and fate of P in soils are dependent on soil P species, solution concentration and pH among others, the P sorption/desorption reactions on mineral (hydr)oxide surfaces are the ultimate factor controlling soluble P levels in the environment.

In the normal pH range of agricultural soils of the tropics, P is mainly bound to Fe- and Al- (hydr)oxides and the sorption reactions involved include precipitation of metal phosphates and sorption/desorption processes occurring at aqueous/solid interfaces.

The application of manures to soils also delivers significant amounts of organic matter and other secondary nutrients, such as calcium (Ca), which can be important in stabilizing solution P into Ca-P secondary minerals as soil pH is raised. This can occur as a result of the liming effect that manures generally have on soils. The soluble organic matter, represented mainly by low molecular weight organic acids, such as citric, oxalic and malic acids, may alter the cycle of biologically active metals by means of various complexation reactions. It is widely documented that soluble organic constituents also enhance P solubility and mobility as well as represent important competitors with P for sorption sites (Grossl & Inskeep, 1991; Violante & Pigna, 2002). Notwithstanding, soluble organic matter is also known for its role in mineral dissolution (Kinder et al., 1986), particularly in the dissolution of Fe-(hydr)oxides, such as hematite (Hersman et al., 1995) and goethite (Holmén & Casey, 1996), which may otherwise enhance P sorption through the creation of highly-reactive amorphous (hydr)oxide minerals. The rates of Fe-(hydr)oxide dissolution by organic ligands are higher at lower pHs, and tend to attenuate as soil pH increases (Holmén & Casey, 1996). Highly weathered agricultural soils, to which continuous applications of manures are commonly applied as fertilizer to sustain plant growth, seem to represent such a scenario. This is because under those conditions, soils rich in Fe-(hydr)oxides with original acidic pH receive consecutive applications of manure which causes the pH gradually to increase over time. Therefore, Al- and Fe-(hydr)oxide dissolution in these systems may directly participate in complexation reactions with the copious amounts of P and organic matter added repeatedly in these soils, as well as being an important mechanism by which secondary P mineral phases are formed and stabilized in such soils.

The objective of this study was to assess the long-term effects of manure application on P sorption and reactivity via P K-edge XANES spectroscopy and conventional wet chemistry analysis in agricultural soils of Paraná State under different soil management systems that have received consecutive applications of manures over the last decades.

4.2 Material And Methods

4.2.1 Soil Characterization

Soil samples were collected from the topsoil layer, 0 to 10 cm depth, of benchmark agricultural areas of Paraná state, in Brazil, that have received periodic application of manures (swine and dairy) over the last decades. These soils have been cultivated with annual crops under different tillage systems, namely conventional cultivation, no-tillage and a Tifton pasture land, and have received annual application of manures for nearly 40, 20 and 10 years at manure rates of approximately 60, 25 and 90 ton ha^{-1} $year^{-1}$ on a dry weight basis, respectively. Particle size distribution in the soils included amounts of sand varying from 10 to 17 dag kg^{-1}, silt amounts varying from 16 to 22 dag kg^{-1} and clay amounts varying from 62 to 74 dag kg^{-1}. XRD analysis showed that kaolinite, goethite and gibbsite are the primary secondary minerals making up the clay fraction of these soils.

Table 4.1. shows some selected chemical characteristics of the soils.

4.2.2 Phosphorus K-Edge XANES Analysis

Solid-state characterization of P was carried out using P K-edge X-ray Absorption Near Edge Structure (XANES) spectroscopy at the Soft X-ray Spectroscopy (SXS) beamline at the Laboratório Nacional de Luz Synchrotron (LNLS), in Campinas, Brazil. Phosphorus K-edge XANES spectra were collected from air-dried soil samples that were ground in a ball-mill and passed through a 125-mesh sieve prior to analysis. The finely ground soil materials were uniformly spread on double coated carbon conductive tape, which was pre-tested for its P level and showed to be P-free, and mounted on a stainless steel sample holder. The spectrum was assigned a reference energy (E_0) value of 2,152 eV and scans were collected in energy ranging from 2,120 to 2,200 eV XANES data were collected with varying step sizes of 1.0 eV from 2,120 – 2,148 eV, 0.1 eV from 2,149 – 2,160 eV, 0.5 eV from 2,161 – 2,175 eV, and 1.0 eV from 2,176 – 2,200 eV. Low total P concentrations in samples, particularly those collected from adjacent sites, resulted in spectra with low quality and high noise. Therefore, each XANES spectrum was the result of merging 15 to 30 individual scans. The beamline was equipped with a monochromator consisting of double crystal Si (111) and the electron storage ring was operated at 2.5 GeV with a current range of about 110 to 300 mA. In order to reject higher-order harmonics, one of the monochromator crystals was detuned 45% with respect to the other crystal. Data analysis was performed using the Athena software in the computer package IFEFFIT. The background was corrected by fitting a first-order polynomial to the pre-edge region from 2,120 to 2,140 eV and the spectra were normalized over the reference energy of 2,152 eV.

Linear combination fitting (LCF) analysis of P-XANES spectra for the soil samples

was not performed. Instead, visual inspection of P-XANES spectra covered all of the spectral features for P species of interest in our study.

4.2.3 *Phosphorus Sequential Fractionation*

Soil P was sequentially fractionated using a modification of the Hedley (1982) fractionation method. Two grams of < 2mm-screen sieved soil were weighed into a 50-mL centrifuge tube and were sequentially extracted by adding 40 mL of either extractant solution. The extractant solutions were added in the following order: 1 M NH_4Cl, 0.5 M NH_4F (pH 8.2), 0.5 M $NaHCO_3$ (pH 8.5), 0.1 M NaOH + 1 M NaCl and 1 M HCl. In the two first extractions, the centrifuge tubes were shaken for 1 h in a reciprocating shaker set at 100 strokes per min. and for 18 h in the subsequent three extractions. After each extraction, the tubes were centrifuged at 8 000 rpm for 10 min., the supernatant was collected, filtered to pass through a 0.20 μm cellulose membrane filter and stored until analysis and the remaining soil was re-suspended for succeeding extractions. The P fractions obtained from this fractionation are a result of treating soils with solutions of increasing strength in order to solubilize P from more labile to more stable forms and are operationally defined as easily desorbable (1 M NH_4Cl), Al-associated (0.5 M NH_4F pH 8.2), easily mineralizable organic P ($NaHCO_3$ pH 8.5), Fe-bound P (0.1 M NaOH + 1 M NaCl) and Ca-bound P (1 M HCl). Reactive (P_{inorg}) was determined colorimetrically using the Murphy & Riley method (1962). Total P (P_t) concentrations in all extracts were determined after treating a 5 mL aliquot with a mixture of 0.2 g of potassium persulfate ($K_2S_2O_8$) + 0.2 mL of concentrated H_2SO_4 and overnight heated in an oven set at 110 ºC.

The resulting salt was re-suspended in deionized water and was analyzed by ICP-AES. Organic P (P_{org}) was calculated as the difference of $P_t - P_{inorg}$.

4.2.4   Desorption Study

Desorption experiments were carried out using a stirred-flow reactor equipped with a piston displacement pump designed for use in an HPLC system. A 12 mL stirred-flow chamber was used in these experiments to which 0.6 g of <2 mm-screen sieved soil samples were added. Ten mL of 1 M NH_4Cl desorbing solution were added to the chamber and a 25-mm diameter cellulose filter membrane with a 0.45 μm pore size was used in the reaction chamber. Upon sealing the reaction chamber, 1 M NH_4Cl solution was flowed through the chamber at a 1 mL min^{-1} rate and the suspension in the reaction chamber was stirred by a magnetic stir bar at ~ 300 rpm. Time zero was defined as the moment of entry of the first drop of effluent solution into the first tube of the fraction collector. The effluent was collected with a fraction collector set to collect 2 mL of solution per tube for 60 min. The desorption kinetics experiments were repeated in triplicate. Total desorbed concentrations of P, K, Ca, Mg and Fe were measured by ICP-AES.

The CurveExpert ® software was employed to adjust desorption data to a best-fit model. The rational power model, given by the math expression $y = a + bx + cx^2 + dx^3$, showed the best fits to our desorption data (Data not shown).

Average cumulative P desorption data were plotted as a function of time (mg kg^{-1} h^{-1}) and were calculated by multiplying the desorbed amount at each time per mass of soil

104

and volume of the reaction chamber. A single first-order exponential model was adjusted to average cumulative desorption data to describe elemental desorption kinetics and is shown in figure 2.

The integrated form of the exponential model can be written as

$$C_t = C_0{}^*(1 - e^{-kt}) \hspace{3cm} [1]$$

and the half-life of the evaluated elements in soil can be calculated by

$$C_{1/2} = \ln(2)/k \hspace{3cm} [2]$$

where C_t is the desorbed amount of a given element at time t, C_0 is the potential available element at time zero, and k is the apparent rate constant.

4.2.5   *Ammonium Oxalate Extractable Phosphorus, Aluminum and Iron*

Acid-oxalate extraction of soils is intended to quantify Fe and Al in poorly crystalline minerals (Jackson et al., 1986) because these matrix components are believed to have superior P sorption capacities in many soils (Breeuwsma & Silva, 1992; Novais & Smyth, 1999; Vilar et al., 2010).

The extraction procedure consisted of the addition of 500 mg of soil, which were previously ground to pass through a 100 mesh sieve and agitated with 30 mL of pH 5.5 1 M ammonium acetate for 2 h, according to the procedure described in Loeppert & Inskeep (1996). The tubes were centrifuged, decanted and the supernatant was collected, filtered through a 0.2 μm cellulose filter and analyzed for P by ICP-AES. The remaining soil was washed twice with deionized water to remove dissolved Ca and acetate before

being placed in an oven set at 40 ºC overnight. Thereafter, the soils were crushed to a suitable particle size in an agate plate before ammonium oxalate solution was added. Subsequently, each centrifuge tube containing the ground soil received 30 mL of pH 3.0 ammonium oxalate solution and was immediately shaken in a reciprocating shaker for 2 h in a light-proof container. The samples were then centrifuged, filtered through a 0.2 μm cellulose filter and diluted as appropriate with deionized water and analyzed for Al, Fe and P by ICP-AES. Oxalate extractable P (P_{Ox}) reported in this study is a summation of the amount of P extracted in the ammonium acetate extraction + P extracted in the ammonium oxalate extraction.

4.2.6   *Phosphorus Sorption Isotherms*

Phosphorus sorption isotherms were determined according to the procedure described by Alvarez & Fonseca (1990). Briefly, 25 mL of 10 mmol L^{-1} M KCl solution containing 0.0, 3, 6, 12, 24, 36, 48 or 60 mg L^{-1} of P were added to 0.5 g of soil in a 50-mL polypropylene centrifuge tube. The tubes were shaken for 24 hours on an orbital shaker at 25 ºC. After shaking, the soil was centrifuged and the supernatant was collected and filtered through a 0.2 μm syringe filter. The P concentration in solution was colorimetrically measured using the Murphy & Riley (1962) method. Sorption data were fitted to the Langmuir equation to determine the sorption maxima as follows:

$q = kbC/1+kC$ [3]

where q = sorbed P (mg kg^{-1})

k = adsorption affinity (L mg^{-1})

b = sorption maxima (mg kg^{-1})

C = P concentration in the equilibrium solution (mg L^{-1})

4.3 Results And Discussion

4.3.1 Manure Effects on Some Selected Soil Chemical Characteristics

In the following discussion, soil chemical changes will be interchangeably discussed from either a land management system or manure application rates standpoint due to the ambiguous nature of the effects that both can impart on soil chemical characteristics (Tables 1 and 2).

A sharp increase in soil pH was observed due to the application of manures with pH values ranging from 4.8 in the reference soil (Adjacent forest) to 6.1 in the Tifton pasture land (M 10+ yrs). Even though the agricultural land under conventional management had a longer history of application of manures, soil pH was intermediate between the reference soil and the systems where soil was minimally disturbed, i.e., no-tillage (M 20+ yrs) and Tifton pasture land. This observation also held true for soil organic matter (SOM), extractable Ca and Mg and percent base saturation values. Lower values of the above mentioned characteristics might be attributed to mixing of soil and transport of nutrients to deeper soil depths as an effect of plowing the topsoil in the conventional agriculture system (M 40+ yrs). Iron concentrations were inversely correlated to SOM contents, i.e., higher in the adjacent forest, followed by conventional agriculture, presumably because of its bare association to SOM in those soils. Aluminum

107

concentrations also decreased as a function of manure application with lower values particularly found under management systems favoring organic matter preservation/accumulation. The chelation effect that SOM has on Al is well documented in the literature and further observations and discussions on this topic can be found elsewhere. Soil K and P were nearly six and four times higher in conventional agriculture and Tifton pasture land in comparison to the reference soil, respectively. Interestingly, no-tillage showed K concentrations nearly the same as in the adjacent forest, likely due to K being easily transported along the soil profile of manured soils (Abdala et al., 2012) in comparison with P, that has generally limited mobility in soils.

4.3.2 Extractable P, Al and Fe and Calculated Sorption Indices

The purpose of performing Mehlich-3 and Ammonium oxalate extractions to determine the P sorption maxima ("*b*" coefficient of the Langmuir isotherm) on the soils was to yield some commonly used P sorption indices to relate the actual soil P status to P loss potential since this relationship is critical to understanding P contribution in causing eutrophication of surface waters.

The degree of P saturation (DPS) method was originally proposed by Van der Zee et al. (1988) as the molar ratio between P and the main sorbing matrix components of acidic soils, Fe + Al contents, and expressed as $P_{Ox}/(Fe_{Ox} + Al_{Ox})$. It is used to establish the degree of P saturation of soils, in which P_{Ox}, Fe_{Ox}, and Al_{Ox} were the soil contents of ammonium-oxalate extractable P, Fe, and Al, respectively. It was later proposed by Khiari et al. (2000) and Maguire & Sims (2002) and adopted by many researchers (Sims

et al., 2002; Sharpley et al., 2003; Nair et al., 2004; Ige et al., 2005) that routine soil testing extractants, such as the Mehlich-3 extractant solution, could be an alternative to the well established but time consuming DPS_{Ox} method and to simplify the measurement of the DPS. By calculating the DPS, one expresses the fraction of sorbent surface covered with P and the remaining soil's capability of retaining additional P.

In our study, we adopted a "α" value of 0.5 to calculate the DPS primarily for comparison with DPS values that have been used in the literature. When it comes to soils periodically fertilized with animal manures, P sorption may be regulated by additional sorbent phases other than Fe and Al only, namely soil contents of Ca, Mg, and organically complexed metals. The P sorption saturation (PSS) index is a measure that takes into account the overall P sorption capacity of a soil as it is based on the P sorption maxima of the Langmuir sorption isotherm (Sharpley, 1995). Additionally, the M3-PSR II method was evaluated in this study as it has shown great promise for identifying soils that represent an increased risk for P losses (Maguire & Sims, 2002).

4.3.3 Mehlich-3 and Ammonium Oxalate Extractable Phosphorus

Mehlich-3 and ammonium oxalate extractable P were significantly affected by application of manures (Table 3). Major increases in P_{M-3} concentrations were recorded by M 40+ yrs and M 10+ yrs, equivalent to 3.7 up to 4.3 times as much the P_{M-3} concentration in the adjacent forest soil, respectively. Increases in P_{Ox} concentrations, as effected by manure application, were also large, particularly in the M 40+ yrs and M 10+ yrs, with increases of 3.8 and 5 times as much the reference P value, respectively. The M

109

20+ yrs was the least affected by manure application, with P_{M-3} and P_{Ox} concentrations equivalent to 2 and 2.5 times as much the P concentration of the reference soil.

Compared with Oxalate, P_{M-3} represented a small percentage of the P_{Ox}, ranging from 16 % in the adjacent forest soil to only 12 % in the no-tillage soil.

The rating scale currently used in most states in Brazil for clayey textured soils recommends that agronomic optimum Mehlich-1 values of soil P vary between 8 and 12 mg kg^{-1} and excessive >12 mg kg^{-1} (CFSEMG, 1999). Based on the P_{M-3} concentrations found in this study, STP concentrations are considerably above the excessive threshold value, particularly in the soils receiving periodic application of M, with STP values ranging from 9 to 20 times as much greater than the excessive STP threshold values.

4.3.4 *Mehich-3 and Ammonium Oxalate Extractable Aluminum and Iron*

Mehlich-3 extractable Al and Fe did not significantly vary from the reference soil, with a mean Fe_{M-3} concentration of 124 ± 23 mg kg^{-1} in comparison to 156 mg kg^{-1} for the reference soil. Similarly, the mean Al_{M-3} concentration in the manured soils, 931 ± 88 mg kg^{-1}, did not vary significantly from the adjacent forest soil, 1089 mg kg^{-1}. However, Al_{Ox} and Fe_{Ox} were significantly affected by manure application, with mean Al_{Ox} and Fe_{Ox} concentrations of 6012 ± 429 mg kg^{-1} and 4378 ± 382 mg kg^{-1}, representing a percent increase of 55 % and 80 %, respectively, over the adjacent forest soil, with Al_{Ox} and Fe_{Ox} of 1991 and 3460 mg kg^{-1}, respectively. The marked increase in Al_{Ox} and Fe_{Ox} amounts as an effect of manure application indicates that the P sorption capacity of these

soils has been largely affected in view of the significant transformation of crystalline into highly-reactive amorphous Fe and Al minerals, hence increasing P sorption capacity.

In our study, Fe_{M-3} amounts represented between 10 and 13 % of the mean (Al_{M-3} + Fe_{M-3}), which was slightly higher than the values reported by Khiari et al. (2000) and Maguire & Sims (2002), which found that Fe_{M-3} made up a small percentage, 11.6 and 9 %, of the mean (Al_{M-3} + Fe_{M-3}) for acidic soils of Canada and the Mid-Atlantic United States, respectively. On the other hand, Fe_{Ox} amounts in the manured soils represented a much higher percentage of the mean (Al_{Ox} + Fe_{Ox}), varying from 40 to 44 % among manured soils and a lower percentage, 36 %, in the adjacent forest soil. The high percentage of mean $Fe_{Ox}/(Al_{Ox}$ + $Fe_{Ox})$ demonstrates that Fe_{Ox} is equally important to Al_{Ox} in the studied soils, regardless of land management, but particularly important with respect to soils periodically fertilized with manures.

In terms of manuring effects on Fe_{Ox} and Al_{Ox}, M 40+ yrs, M 20+ yrs and M 10+ yrs represented an increase of as much as 1.9, 2.2 and 2.4 times for Fe_{Ox} and of 1.8, 1.7 and 1.9 times for Al_{Ox}, respectively, greater than the reference value found in the adjacent forest soil. Putting it in terms of the $Fe_{Ox}:Al_{Ox}$ ratio, the equivalent ratios between each treatment were 1.1, 1.3 and 1.3, for M 40+ yrs, M for 20+ yrs and M for 10+ yrs, respectively. On the basis of Fe_{M-3} and Al_{M-3}, manure application did not lead to increases in Fe_{M-3} and Al_{M-3} values over the adjacent forest soil, but rather a fraction represented by 0.95, 0.65 and 0.78 for Fe_{M-3} whereas Al_{M-3} values were 0.92, 0.88 and 0.77, with corresponding $Fe_{M-3}:Al_{M-3}$ ratios of 1.03, 0.74 and 1.01, respectively. Altogether, it is valid to say that Fe_{Ox} represented a net percent increase of extractable Fe of 6.4, 43.1 and 22.3 % with respect to Fe_{M-3} concentrations along the treatments, respectively, if one is to

111

use the adjacent forest to represent a background value. It is also worthy to point out that the highest net increases in Fe_{Ox} amounts were associated with the M 20+ yrs, suggesting that no-tillage management may have favored the higher percentage of extractable Fe in comparison with the other soils.

Mehlich-3 extractable Fe and Al amounts also represented a small percentage of the Fe_{Ox} and Al_{Ox}, particularly for Fe, which ranged between 2 and 8 % among all soils. Mehlich-3 extractable Al represented the largest percentage of the Al_{Ox}, accounting for 13% in the Tifton pastureland and 17 % in both conventional agriculture and no-tillage systems, and an even larger percentage of Al_{M-3}, 55 %, in the adjacent forest soil. The much higher Al_{Ox} and Fe_{Ox} amounts in the manure amended soils reflect their high SOM content, as organic matter can increase the amorphous nature of these matrix components (Hersman et al., 1995; Holmén & Casey, 1996), and hence extractability (Maguire et al., 2000).

4.3.5 Degree of Phosphorus Saturation, Phosphorus Sorption Saturation and Phosphorus Saturation Ratio Indices

Overall, M 40+ yrs and M 10+yrs are likely to be experiencing P losses at some degree, regardless of the P risk loss assessment method used. The reference DPS values found in the literature suggest that DPS_{Ox} values above 25 % are indicative of greater potential of P loss (Nair et al., 2004; Pautler & Sims, 2000; Breeuwsma et al., 1995; Abdala et al., 2012). Notwithstanding, the calculated DPS_{M-3} values for M 40+yrs and M 10+ yrs, 35 and 50 %, respectively, indicate the greater P loss potential of those soils, in agreement with the literature values of $DPS_{M-3} \geq 20$ % (Maguire & Sims, 2002; Abdala et

al., 2012). Even though the P_{M-3} concentration of the adjacent forest soil (55 mg kg^{-1}) is above the threshold STP value, it should not pose a risk for P loss to the environment. The M 20+ yrs presented a P_{M-3} concentration of 105 mg kg^{-1}, which is equivalent to 9 times as much greater than the excessive STP threshold value for Brazilian soils. Nevertheless, all P risk loss assessment indices indicate that the P loss potential associated with that soil should not represent a concern. Indeed, several studies have demonstrated that Mehlich-3 STP values should not be used as isolated measures to relate the amount of dissolved P in soils that are subject to loss (Breeuwsma & Silva, 1992; Maguire & Sims, 2002; Nair et al., 2004; Abdala et al., 2012). Rather, more reliable P risk loss assessment tools, such as the DPS, PSS, PRS and WSP values, should be used as predictors of P loss from a soil.

The PSC of the soils was not significantly affected by the application of manures, except for the M 10+ yrs, that presented a marked decrease of 49 % with respect to the adjacent forest soil (Table 3). Several studies have shown the effect of organic matter decreasing the PSC of soils (Iyamuremye & Dick, 1996; Abdala et al., 2012). In our study, the competitive sorption between organic matter and phosphate for P sorption sites was apparently minor with respect to the effect that organic matter played on the transformation of crystalline to amorphous Al and Fe (hydr)oxides, thus increasing the PSC of the soils (Borggaard et al., 1990; Pizzeghello et al., 2011).

Percent decreases of 49 % in PSC observed in the M 10+ yrs were likely due to the much higher labile C acting directly by decreasing the P sorption sites. Jan Verburg et al. (2012) carried out a study on the effects of manure application on C lability on the same soils used in this study. A significant linear relationship between the PSC calculated in

our study and labile C obtained in the above study was given by labile C = 5.53 − 0.025 PSC*, R^2 = 0.48. The negative slope of the equation denotes the effect that labile C played on the PSC of those soils.

Overall, the PSC of the soils exhibited a good coefficient of determination on the basis of related STP and P sorption indices (Table 5).

Since the ammonium oxalate extraction is sensitive to the changes in mineral crystallinity and it reflected well the effect that C-rich materials played on the transformation of originally crystalline into poorly crystalline Fe(III)-minerals, thus representing the creation of additional P sorption sites, it is valid to reason that whereas Fe_{M-3} values account for little in calculating P sorption indices, Fe_{Ox} is a relevant quantity to pursue as it provides a measure of sorption capacity generated as an effect of manure application.

Finally, the PSR II provided the most modest sorption saturation values, though in good agreement with all the other indices (Table 5). The highest R^2, 0.99, obtained from the relationship between PSR-II and $DPS_{M-3,}$ expresses the small contribution of Fe_{M-3} on the DPS_{M-3} calculation. This is partly because Mehlich-3 was a poor extractant for Fe relative to Al, in comparison with the oxalate extract. Therefore, Mehlich 3 may not be useful for measuring the P saturation ratio in manured soils or other soils where Fe oxides play an equivalent or more important role in P sorption than Al.

PSR-II values were nearly identical to the PSC, except for M 10+ yrs, due to PSS being more sensitive to the PSC than the other methods.

4.3.6 Sequential Chemical Phosphorus Fractionation

Phosphorus in the adjacent forest soil was primarily associated with Fe-(hydr)oxide minerals ((NaOH + NaCl)-P fraction), accounting for as much as 44% of the total, followed by Al-P (NH_4F-P), 33%, biologically active ($NaHCO_3$-P), 14%, which was slightly higher than in soils receiving application of manures probably due to P being associated with more humified SOM, Ca-P (HCl-P), 9%, and readily available (NH_4Cl-P) P accounting for < 1% (Table 2). Except for NH_4F-P, in which reactive P accounted for up to 85% of the total, the reactive P percentages in all other fractions was more modest, varying between 60 and 67%. The share of reactive P in the adjacent forest was found to follow the order: NH_4F > NH_4Cl > $NaHCO_3$ > HCl > NaOH + NaCl.

Sequential chemical fractionation of soil P showed that there was an overall increase in the amount of P in all fractions following the consecutive application of manure, with a predominance of reactive over unreactive P. This substantiates the higher association of reactive P with Al-, Ca- and Fe- minerals whereas implies unreactive P being apparently connected to rapid to slowly decomposable organic molecules (Negassa & Leinweber, 2009). This observation is in good agreement with literature elsewhere (Hountin et al., 2000, He et al., 2004). Reactive P concentrations in manure amended soils followed the order NH_4F > HCl > $NaHCO_3$ > NaOH + NaCl > NH_4Cl, indicating that although manure application led to an overall enlargement of P pools, reactive P is mainly associated with the less bioavailable pools. Not surprisingly, the distribution of P within the different pools is in good agreement with literature data for soils with acidic or moderately acidic pH receiving cattle or swine manures, in which P is mainly incorporated into the NaOH fraction (Tran & N'dayegamiye, 1995; Leinweber et al.,

1997; Hountin et al., 2000). Unreactive P was primarily associated with the Fe-bound fraction, which supports the findings that Fe-bearing minerals are important components of soils in retaining organic forms of P (Zhang et al., 1994; Hountin et al., 2000; Lehmann et al., 2005), accounting for around 30% of unreactive P in manured soils. Provided the majority of P in these soils was shown to be associated with Al- and Fe-(hydr)oxide minerals, one can argue that the individual contribution of either sorbent must vary significantly, especially because of the larger proportion of Al_{Ox} in relation to Fe_{Ox}, representing 1.4 to 1.7 fold. Therefore, in order to address the individual contribution of Al- versus Fe-bound P, we included an additional step (NH_4F extraction) to the conventional sequential fractionation procedure so we could evaluate the partitioning of P between these two distinct sorbing phases.

One advantage of the NH_4F extraction is that Al-bound P can be assessed separately from Fe-bound P. This is particularly advantageous when one is aiming to assess the partitioning of P between these two important sorbing phases (e.g, Al and Fe), which is worth doing in studies looking at land use changes, in which P shows relatively fast turnover rates. However, in most studies relying on sequential chemical fractionation of P, Al- and Fe-bound P are obtained from a single extraction, e.g., NaOH extraction, thus making comparisons somewhat limited.

The application of manures caused a shift in P solid-phase partitioning, from Fe- to Al-bound P minerals as the major solid-phases controlling P solubility in the soils. This has an important environmental consequence in view of the greater P bioavailability of Al-P minerals in soil environments (Novais & Smyth, 1999, Hesterberg, 2010). The NH_4F-P was the fraction that was particularly enriched, accounting for as much as 44, 38

116

and 42% of P associated in that pool for M 40+ yrs, M 20+ yrs and M 10+ yrs, respectively, in which nearly 90% of P was in the inorganic form. Our P K-edge XANES data support this observation, as noted by the virtual absence of a high energy pre-white-line diagnostic feature denoting crystalline Fe(III)-bonded P in manured soils (Figure 1).

4.3.7   Desorption Kinetics Experiments

Total desorbed amounts of P, Ca, K, Mg and Fe and calculated half-lives can be found in table 4. Figure 2 shows the breakthrough curves (i.e., outlet concentration versus time) for average cumulative desorption kinetics of P, Ca, K, Mg and Fe.

Desorption kinetics data of Ca and Mg for all soils obeyed first-order kinetics, with R^2 values ranging from 0.95 to 0.99. First-order kinetics plots of K desorption showed R^2 values ranging from 0.9 to 0.98. Phosphorus and Fe showed the lowest R^2 values for the first-order kinetics plots, with R^2 values ranging from 0.6 to 0.98 for P and from 0.47 to 0.88 for Fe.

The exponential first-order equation was found to provide good agreement between experimental data and the equation-predicted values as expressed by the R^2 values (data not shown).

Half-lives of P varied largely among the studied soils, ranging from 19 min. in the adjacent forest soil up to 124 min. in the no-tillage soil. Conventional agriculture and Tifton pastureland yielded intermediate half-lives, 66 and 93 min., respectively. The higher amounts of amorphous Fe and Al (hydr)oxides in the manured soils (Table 3) might have enhanced the sorption of P, hence the higher half-lives in manured soils in

117

comparison with the adjacent forest soil. The shortest half-life and thus fastest P turnover, 19 min., in the adjacent forest soil, might have been related to more labile P pools, as evidenced by sequential P fractionation data. Similarly, kinetic data of Fe half-lives showed a large variation among land management systems, with adjacent forest soil presenting the shortest half-life, 52 min., and no-tillage with the longest half-life, 267 min. Conventional agriculture and Tifton pasture land showed intermediate half-lives, with a slight variation between them, 55 and 48 min., respectively.

Calcium, K and Mg half-lives did not vary much among soils, varying from 9 to 13 min., respectively.

Total desorbed P, Ca, Mg, K and Fe amounts varied largely as a function of manure application rates (Table 3). Overall, the adjacent forest soil presented the highest amount of desorbed Fe and lowest desorbed amounts of P, Ca and Mg. Desorbed K was second lowest in the adjacent forest soil, 153 mg kg^{-1}, behind M 20+ yrs, with total K desorbed of 133 mg kg^{-1}. M 10+ yrs showed the highest desorbed amounts of P, 42 mg kg^{-1}, Ca, 2326 mg kg^{-1}, and Mg, 599 mg kg^{-1} and lowest Fe, 4 mg kg^{-1}. Desorbed P varied between 3 and 42 mg kg^{-1}, being highest in the M 10+ yrs and lowest in the adjacent forest soil. Intermediate values of 12 and 22 mg kg^{-1} were found for M 20+ yrs and M 40+ yrs, respectively. Overall, desorbed P, Ca, K, Mg and Fe values were greater than the Mehlich-3 extractable values provided in Table 1. Although the desorbing solution employed in the desorption experiments (1 M NH_4Cl) was of relatively lower strength than Mehlich-3, the stirred-flow technique allows the constant removal of reaction products, therefore enhancing desorption of easily desorbable phases.

Among all the soils, M 10+ yrs was the one that exhibited the best linear fit for a first-order kinetics plot for P desorption. Coincidently, this soil also showed the highest plant available P concentration, regardless of the method of extraction, and highest labile C content (Jan Verburg et al., 2012). It is likely that the majority of P being desorbed in M 10+yrs comes from easily desorbable P pools contained in organic matter. However, anion competition cannot be ignored, as it substantiates the theory that competition between organic matter and P for the same sorption sites on (hydr)oxide surfaces enhances the lability of soil P. The initial deviation from linearity of the first-order kinetics plots for P desorption suggests that stronger bonds prevented P from being readily desorbed in M 20+ yrs and in the adjacent forest soil. The angular coefficient, R^2, of the kinetics plots were in conformity with this assumption, being highest for M 10+ yrs, (R^2 = 0.98), second for M 40+ yrs (R^2 = 0.95) and lowest for adjacent forest soil (R^2 = 0.6) and M 20+ yrs (R^2 = 0.78).
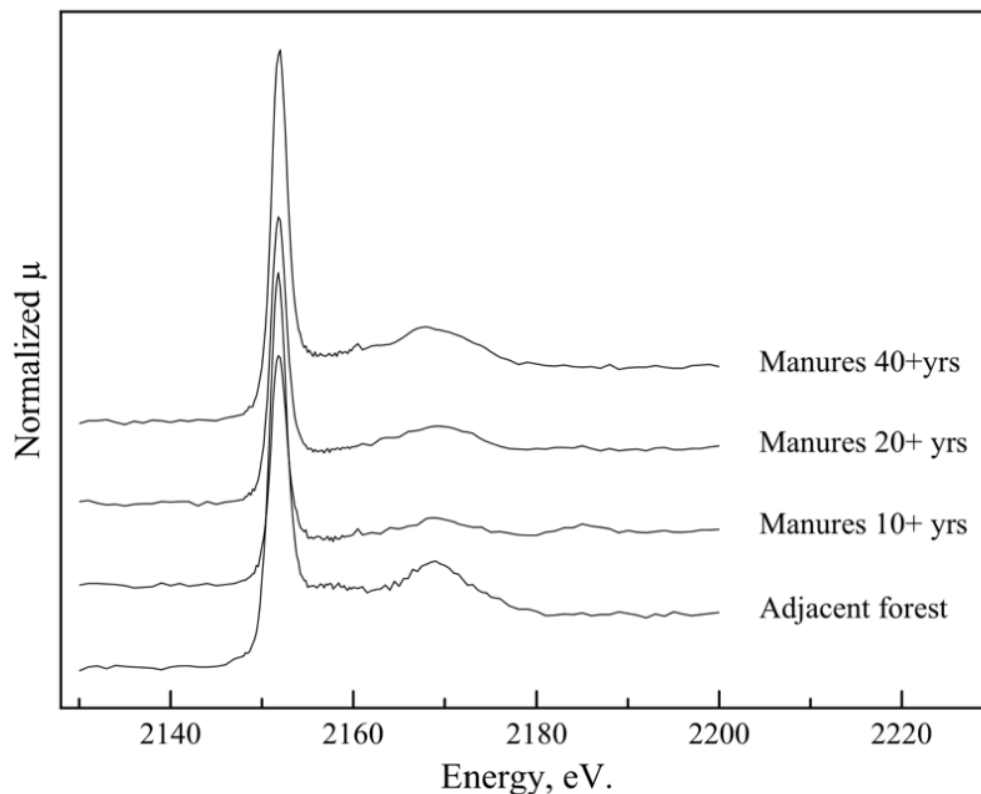
Figure 4.1   P K-edge XANES of soils treated with swine manures with different application history and under different land management systems in Paraná State, Brazil.

4.3.8   Phosphorus K-edge XANES analysis

Linear combination fits of the XANES spectra were not performed. Therefore, the discussion and conclusions made throughout this session were based on visual inspection of the spectra and comparison with mineral standards as well as with spectra of manures that are available in the literature.

120

The P K-edge XANES spectra of all phosphate minerals in this study had absorption edge energies around 2152 eV. Additional pre-edge or post-edge features were also observed, indicating that mineral crystallinity and a variety of elements were associated with the features. The differences in pre- and post-edges of the P K-edge XANES analysis clearly showed the effect that long-term manure application had on XANES K-edge spectra of manured soils as they resembled manure-like XANES K-edge spectra found elsewhere in the literature (Figure 1).

A pre-edge feature around 2148 eV is characteristic of crystalline Fe phosphates (Hesterberg et al., 1999; Khare et al., 2005; Ingall et al., 2011) and it is more prominent in crystalline than non-crystalline minerals (Hesterberg et al., 1999; Kruse & Leinweber, 2008). Likewise, the reference soil from Paraná state, showed a small pre-edge, indicating that crystalline Fe-containing minerals are originally found in those soils and that the repeated application of manure led to the formation of non-crystalline minerals, which can be denoted by the virtual absence of a pre-edge in the manured soils. As a matter of fact, organic matter coupled to Fe(III) reduction is a thermodynamically favorable process that may lead to the formation of amorphous Fe(III)/(II)-containing minerals (Anderson, 2004).

The nutrient content of manured soils from Paraná state was generally much higher than it was in the adjacent forest, especially in P, K and Mg (Table 1). The appearance of spectral features around 2167 eV and 2170 eV present in the manured soils may be due to the much larger contents of K and Mg concentrations in those soils, suggesting the presence of potassium phosphates or magnesium phosphates, such as struvite [$NH_4MgPO_4 \cdot 6H_2O$] (Rouff et al., 2009).

In view of the similarities between our work and the research carried out by Sato et al. (2005) (manure types and application history), comparisons will be made when appropriate. Conversely to what was observed by Sato et al. (2005), Ca-P minerals were not observed in our study. Calcium phosphates usually display a diagnostic shoulder on the high-energy side of the absorption edge (Hesterberg et al., 1999; Kruse & Leinweber; Ingall et al., 2011) and the prominence of this feature seems to be a measure of the Ca abundance in the mineral (Ingall et al., 2011). This feature was virtually absent in all spectra. It is interesting because the manure application history in the work by Sato et al. (2005) is comparable to ours, although the rates may vary. Even though the rates of animal manures applied in our soils were moderate, some of the soils have received manure application for several decades and the accumulated amounts of manures should be taken into account. Manures were applied at rates varying from 5 to 10 ton ha^{-1} year^{-1}. The calcium content in these materials usually ranges from 3 to 4 %, which is equivalent to an application of 150 to 400 kg ha^{-1} year^{-1}.

It is evident that, in the work by Sato et al. (2005), a combination of higher soil pH and soil Ca concentrations and much lower extractable Fe contents provided the ideal conditions for the formation of Ca-P secondary minerals, whereas in our study, the relatively lower pH together with the much higher extractable Fe contents favored the formation of Fe-P secondary minerals.

4.4 Conclusions

Since STP concentrations tested extremely high in some of the soils, along with DPS_{M-3}, DPS_{Ox} and PSR-II indices, it is no doubt safe to predict that drainage water from M 40+ yrs and M 10+ yrs are causing and/or sustaining eutrophication of water bodies nearby those areas.

Storing organic matter in soils, particularly in highly weathered soils of the tropics is ultimately desirable, as it improves soil fertility and enhances crop yields. However, managing agricultural soils towards increasing SOM contents via application of P-rich materials may significantly affect soil and water quality at the expense of increased P losses and eventual eutrophication of water bodies. Soluble organic matter content seems to especially be a determinant factor as to whether soils will present an enhanced or lowered capacity towards fixing P.

Decreases in P sorption capacity of the soils as an effect of the application of large amounts of C and eventual blockage of P sorbing sites was offset by the transformation of crystalline into highly-reactive amorphous Fe and Al minerals, representing new sorbing sites for P. Accordingly, the net effect of manure application on the soil PSC was insignificant for most soils. M 10+ yrs presented the lowest PSC among all soils, with greater P loss potential as indicated by the P risk assessment indices employed in our study. Coincidently, this soil presented the highest total C, labile C and carbon management index (CMI) values (Jan Verburg et al., 2012) among all soils, indicating that managing soils towards increasing SOM may represent a tradeoff between P loss potential and enhancement of C storage in soils.

The main contrasting characteristics between the work carried out by Sato et al. (2005) and this work lies in the much higher M-3 extractable Fe (mean ~ 131 mg kg^{-1}) and much lower Ca (mean ~ 886 mg kg^{-1}) contents in Brazilian soils compared to the lower Fe (mean ~ 19 mg kg^{-1}) and Ca (mean ~ 5872 mg kg^{-1}) contents of NY soils. In addition, soil pH was also a factor in that it favored the higher Fe and Al activity towards controlling P solubility in the more acidic Brazilian soils as opposed to Ca being the main cation to which P was sorbed in the circumneutral pH range of the NY soils.

The consecutive application of animal manures was shown to have an effect on the transformation of crystalline into amorphous Fe- and Al-containing minerals, as evidenced by ammonium oxalate extractions of Fe and Al and confirmed by visual inspection of XANES spectra, showing the presence of the diagnostic pre-edge feature of crystalline Fe(III)-minerals in the adjacent area and its absence in manured soils. Accordingly, the highly reactive non-crystalline Fe-containing minerals formed are presumably the main surfaces to which P from the animal manures is held.

Finally, the much higher Mg and K concentrations found in M 10+ yrs along with the higher cycling rates of those elements, as shown by the desorption kinetics data, seemed to be due to the formation of relatively soluble Mg and K phosphates in that soil, as shown by diagnostic features in the XANES spectra.

Table 4.1. Selected soil chemical characteristics of the soils in analysis.

Treatment	pH[a]	SOM[b]	P[c]	K[c]	Ca[c]	Mg[c]	Fe[c]	Al	CEC	Base sat.
		(%)			mg kg^{-1}				cmol$_c$ kg^{-1}	(%)
M 40+ yrs	5.5	14	201	364	1049	291	148	1007	14	60
M 20+ yrs	5.9	15	105	65	1256	456	101	953	14	71
M 10+ yrs	6.1	17	237	331	1401	478	122	835	16	73
Adjacent forest	4.8	9	55	66	378	101	156	1089	9	32

[a] pH in water. [b] loss on ignition. [c] elements extracted using the Mehlich-3 extractant solution.

Table 4.2. Sequential Phosphorus fractionation of the soil samples

	NH$_4$Cl			NH$_4$F			NaHCO$_3$			NaOH + NaCl			HCl		
	P$_{inorg}$	P$_{org}$	Total	P$_{inorg}$	P$_{org}$	Total	P$_{inorg}$	P$_{org}$	Total	P$_{inorg}$	P$_{org}$	Total	P$_{inorg}$	P$_{org}$	Total
	-- mg kg^{-1} --														
M 40+ yrs	6	5	12	514	76	590	120	37	157	298	135	435	130	15	145
	54*	*46**	*1***	*87**	*13**	*44***	*76**	*24**	*12***	*69**	*31**	*32***	*89**	*11**	*11***
M 20+ yrs	2	1	4	283	36	323	72	26	98	231	94	326	95	11	106
	64*	*36**	*0***	*89**	*11**	*38***	*74**	*26**	*11***	*71**	*29**	*38***	*89**	*11**	*12***
M 10+ yrs	13	16	29	639	58	697	159	44	201	323	154	477	216	38	245
	45*	*55**	*2***	*92**	*8**	*42***	*78**	*22**	*12***	*68**	*32**	*29***	*85**	*15**	*15***
Adjacent forest	1	0	1	98	18	116	32	17	48	92	62	154	19	11	30
	66*	*34**	*0***	*85**	*15**	*33***	*66**	*34**	*14***	*60**	*40**	*44***	*63**	*37**	*9***

Pinorg: reactive P; Porg: unreactive P

italic*: reactive/unreactive partitioning percentage of P with respect to the total within a pool;

italic**: represents the total percentage of P within a pool out of the total.

Table 4.3. Mehlich-3 and ammonium oxalate oxalic acid extractable phosphorus, aluminum and iron and calculated P sorption indices.

Treatments	P_{M-3}	P_{Ox}	Fe_{M-3}	Fe_{Ox}	Al_{M-3}	Al_{Ox}	PSC (b)	DPS_{M-3}	DPS_{Ox}	PSS	PSR
	---------------------------- mg kg^{-1} ----------------------------							------------------- % -------------------			
M 40+ yrs	201	1304	148	3863	1007	5820	912	35	27	22	20
M 20+yrs	105	864	101	4454	953	5712	1027	20	17	10	11
M 10+ yrs	237	1762	122	4817	835	6503	579	50	31	41	28
Adjacent forest	55	348	156	1991	1089	3460	1139	9	13	5	5

M-3: Mehlich-3 extractable P, Al and Fe; Ox: Ammonium oxalate oxalic acid extractable P, Al and Fe;

PSC: sorption maxima coefficient "b" of the Langmuir isotherm. $DPS_{Ox} = P_{Ox}/[\alpha(Al_{Ox} + Fe_{Ox})] \times 100$;

$DPS_{M-3} = P_{M-3}/[\alpha(Al_{M-3} + Fe_{M-3})] \times 100$; $PSS = (P_{M-3}/ PSC) \times 100$; $PSR = P_{M-3}/(Al_{M-3})$;

M-3 PSR II = $(P_{M-3}/ Al_{M-3}) \times 100$.

Table 4.4. Total desorbed amounts and half-lives of P, Ca, K, Mg and Fe in the studied soils.

Element	M 40+ yrs		M 20+ yrs		M 10+ yrs		Adjacent forest	
	Total desorbed	Half-life	Total desorbed	Half-life	Total desorbed	Half-life	Total desorbed	Half-life
	mg kg^{-1}	min.	mg kg^{-1}	min.	mg kg^{-1}	min.	mg kg^{-1}	min.
P	22	66	12	124	42	93	3	19
Ca	1418	11	1595	10	2326	11	511	10
K	535	10	133	10	432	10	153	13
Mg	345	9	496	9	599	12	107	9
Fe	6.5	55	6.3	267	4.4	48	15	52

Table 4.5. Relationship between phosphorus sorption capacity and related STP and P sorption indices.

	Intercept	Slope	R^2	Significance
DPS$_{M-3}$	93.9	-0.072 PSC	0.94	**
DPS$_{Ox}$	51.23	-0.032 PSC	0.85	**
PSR-II	52.8	-0.04 PSC	0.93	**
Desorbed P	82.75	-0.069 PSC	0.99	**
NH$_4$Cl P	58.73	-0.052 PSC	0.99	**

** Significance at P <0.01 level by F-test.

Ct = 12.42*(1 - exp^{-0.012 t})   R² = 99
Ct = 43.99*(1 - exp^{-0.003 t})   R² = 99
Ct = 7.538*(1 - exp^{-0.014 t})   R² = 99
Ct = 26.92*(1 - exp^{-0.013 t})   R² = 99

Ct = 346.8*(1 - exp^{-0.077 t})   R² = 99
Ct = 497.5*(1 - exp^{-0.079 t})   R² = 99
Ct = 612.2*(1 - exp^{-0.059 t})   R² = 99
Ct = 105.8*(1 - exp^{-0.077 t})   R² = 99

Ct = 532.7*(1 - exp^{-0.071 t})   R² = 99
Ct = 133.2*(1 - exp^{-0.054 t})   R² = 98
Ct = 431.3*(1 - exp^{-0.07 t})   R² = 99
Ct = 153.5*(1 - exp^{-0.054 t})   R² = 99
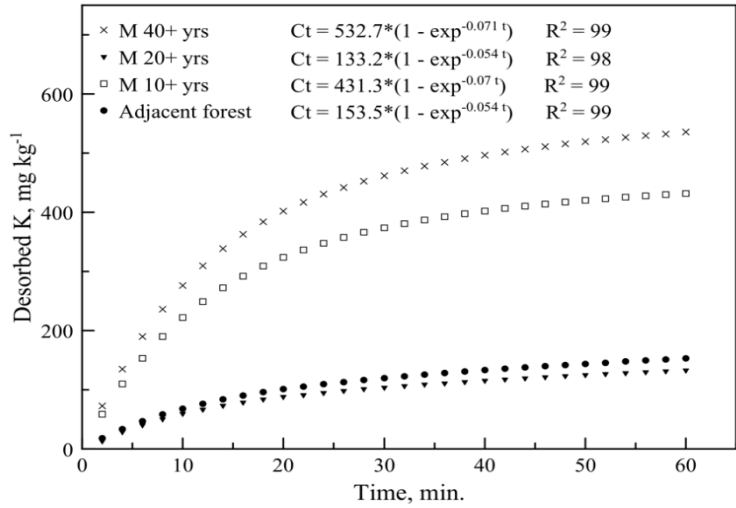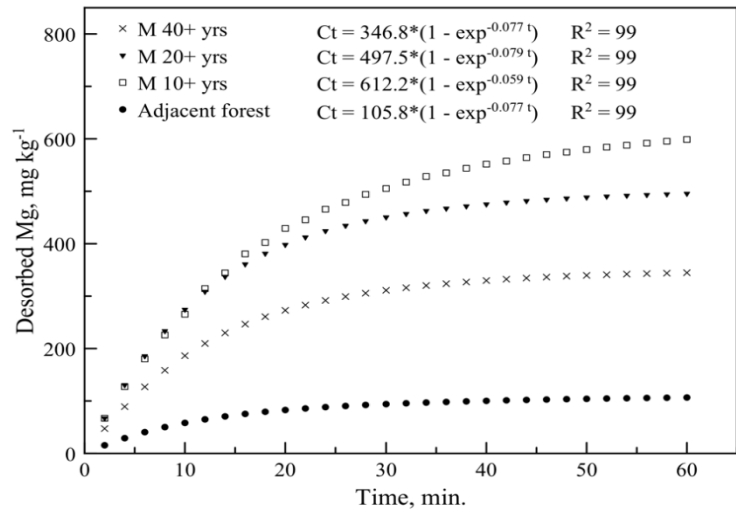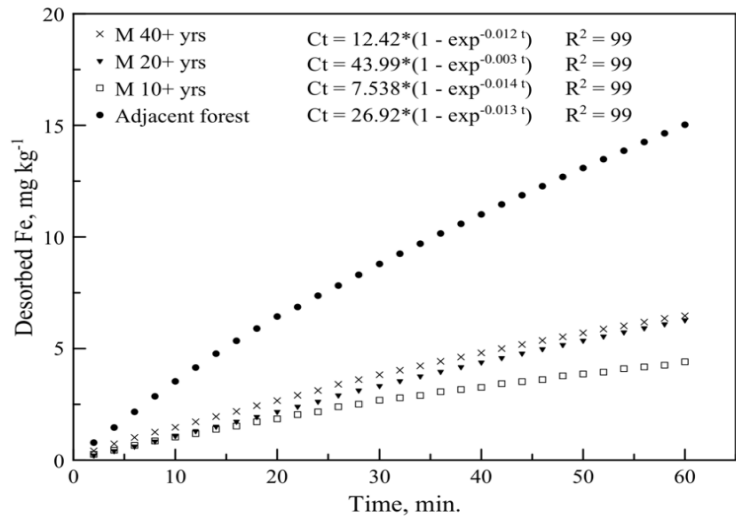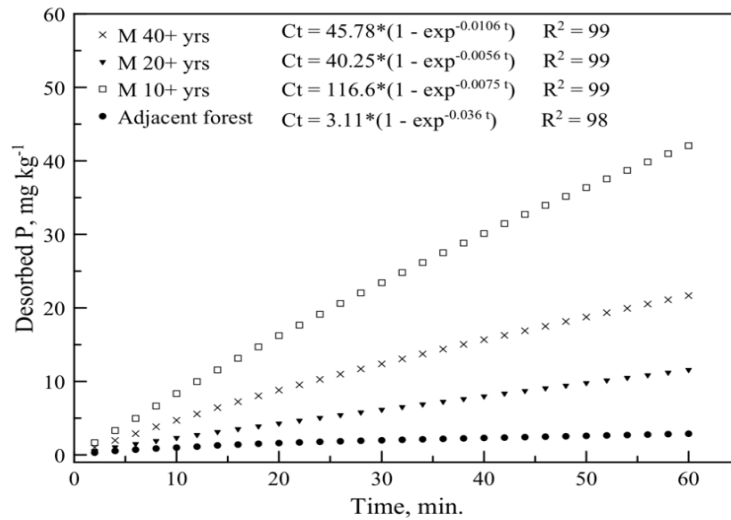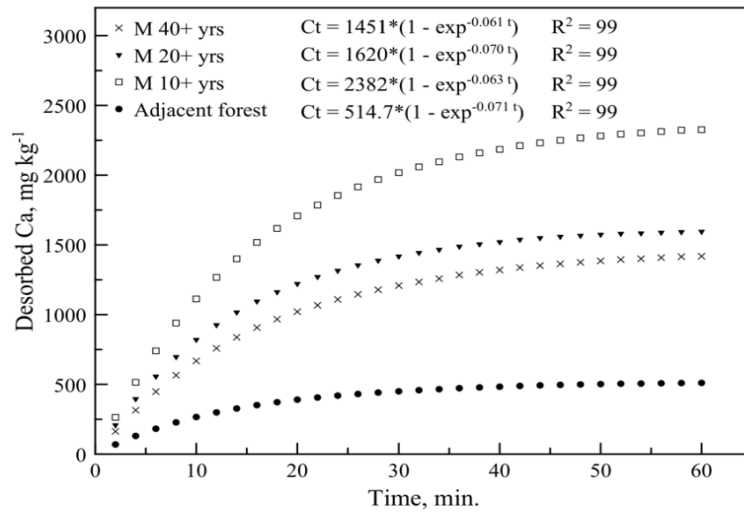
Figure 4.2.   Average cumulative desorption kinetics of P, Ca, K, Mg and Fe of soils subjected to varied manure application rates and different land management systems.

REFERENCES

Abdala, D. B., Ghosh, A. K., da Silva, I. R., Novais, R. F., Alvarez V., V. H. Phosphorus saturation of a tropical soil and related P leaching caused by poultry litter addition. Agr Ecosyst Environ., 162:15–33, 2012

Alvarez V., V. H. & Fonseca, D. M., Definição de doses de fósforo para determinação da capacidade máxima de adsorção de fosfatos e para ensaios de casa de vegetação. Rev. Bras. Ciên. Solo, 14:49–56, 1990

Borggaard, O. K. Dissolution and adsorption properties of soil iron oxides. Doctoral dissertation. The Royal Veterinary and Agricultural University, Copenhagen. 1990

Breeuwsma, A., & Silva, S. Phosphorus fertilization and envi- ronmental effects in the Netherlands and the Po region (Italy). Rep 57. Agric. Res. Dep., The Winand Staring Centre for Integrated Land, Soil and Water Res., Wageningen, the Netherlands, 1992

Breeuwsma, A., Reijerink, J. G. A., Schoumans, O. F. Impact of manure on accumulation and leaching of phosphate in areas of intensive livestock farming. p. 239–249. In K. Steele (ed.) Animal waste and land-water interface. Lewis Publ., Boca Raton, FL, 1995

COMISSÃO DE FERTILIDADE DO SOLO DO ESTADO DE MINAS GERAIS – CFSEMG. Girassol. *In:* Ribeiro, A.C., Guimarães, P.T.G., Alvarez V., V.H., eds. Recomendações para o uso de corretivos e fertilizantes em Minas Gerais, 5ª Aproximação. Viçosa, MG, 1999. p. 310

Dao, T. H. Polyvalent cation effects on myo-inositol hexakis dihydrogenphosphate enzymatic dephosphorylation in dairy wastewater. J. Environ. Qual., 32:694–701, 2003

Gosh, A. K., Barbosa, J. da Silva, I. R. An Environmental Threshold of Soil Test P and Degree of P Saturation of Brazilian Oxisols. CLEAN – Soil, Air, Water, 39:421-427, 2011

Grossl, P.R. & Inskeep, W.P. Precipitation of dicalcium phosphate dihydrate in the presence of organic acids. Soil Sci. Soc. Am. J., 55:670 – 675, 1991

He, Z., Griffin, T. S., Honeycutt, C. W. Enzymatic hydrolysis of organic phosphorus in swine manure and soil. J. Environ. Qual., 33:367-372, 2004

Hedley, M. J., Stewart, J. W. B., Chauhan, B. S. Changes in organic and organic soil phosphorus fractions induced by cultivation practices and laboratory incubations. Soil Sci. Soc. Am. J., 46:970–976, 1982

Helga, W. & Lukas, K. Eds. The World of Organic Agriculture – Statistics and Emerging Trends 2009. International Federation of Organic Agriculture Movements (IFOAM), DE-Bonn, Research Institute of Organic Agriculture, FiBL, CH-Frick and International Trade Centre ITC, Geneva, 2009

Hesterberg, D., Zhou, W., Hutchison, K. J., Beauchemin, S., Sayers, D. E. XAS study of adsorbed forms of phosphate. J. Synchrotron Rad., 6:636-638, 1999

Hersman, L., Lloyd, T., Sposito, G. Siderophore-promoted dissolution of hematite. Geochim. Cosmochim. Acta, 16:3327–3330, 1995

Hesterberg, D. Macro-scale chemical properties and x-ray absorption spectroscopy of soil phosphorus. p. 313-356. In B. Singh and M. Gräfe (Ed.) Synchrotron-based techniques in soils and sediments. Developments in Soil Science, Vol. 34. Elsevier, Burlington, MA., 2010

Holmén, B.A. & Casey, W.H. Hydroxamate ligands, surface chemistry, and the mechanism of ligand-promoted dissolution of goethite [α-FeOOH(s)]. Geochim. Cosmochim. Acta, 60:4403–4416, 1996

Houtin, J. A., Karam, A., Couillard, D., Cescas, M. P. Use of a fractionation procedure to assess the potential for P movement in a soil profile after 14 years of liquid pig manure fertilization. Agri Ecosyst Environ., 78:77-84, 2000

Ige, D. V., Akinremi, O. O., Flaten, D. N. Environmental index for estimating the risk of phosphorus loss in calcareous soils of Manitoba. J. Environ. Qual., 34:1944–1951, 2005

Ingall, E. D., Brandes, J. A., Diaz, J. M., de Jonge, M. D., Paterson, D., McNulty, I., Elliot, W. C., Northrup, P. Phosphorus K-edge XANES spectroscopy of mineral standards, J. Synchrotron. Radiat., 18:189-197, 2011

Jackson, M.L., Lim, C. H., Zelazny, L. W. Oxides, hydroxides, and aluminosilicates. p. 101–150. In A. Klute (ed.) Methods of soil analysis. Part 1. 2nd ed. Agron. Monogr. 9. ASA and SSSA, Madison, WI., 1986

Jan Vergurg, E. E., Oliveira, D. M. S., Borges, S. B., Mayrink, G. C. V., da Silva, I. R. Carbono orgânico total, carbono lábil e índice de manejo de carbono em Latossolo Vermelho-Escuro sob diferentes manejos intensivos. *In:* XIX Reunião Brasileira de Manejo e Conservação do Solo e da Água. Lages, SC. 2012

Khare, N., D. Hesterberg, and J. D. Martin. Investigating phosphate surface precipitation in single and binary mixtures of Fe- and Al-oxide minerals using XANES. Environm. Sci. Technol., 39:2152-2160, 2005

Khiari, L., Parent, L. E., Pellerin, A., Alimi, A. R. A., Tremblay, C., Simard, R. R., Fortin, J. An agri-environmental phosphorus saturation index for acid coarse-textured soils. J. Environ. Qual., 29:1561–1567, 2000

Kruse, J. & Leinweber, P. Phosphorus in sequentially extracted fen peat soils: A K-edge X-ray absorption near-edge structure (XANES) spectroscopy study. J. of Plant Nutrit. Soil Sci., 171:613–620, 2008

Lehmann, J., Lan, Z., Hyland, C., Sato, S., Solomon, D., Ketterings, Q. M. Long-Term Dynamics of Phosphorus Forms and Retention in Manure-Amended Soils. Environ Sci. Technol., 39:6672-6680, 2005

Leinweber, P., Haumaier, L., Zech, W. Sequential extractions and ^{31}P-NMR spectroscopy of phosphorus forms in animal manures, whole soils and particle-size separates from a densely populated livestock area in northwest Germany. Biol. Fertil. Soils, 25:89–94, 1997

Loeppert, R.H. & Inskeep, W. P. Iron. p. 639–664. In Methods of soil analysis. Part 3. SSSA Book Ser. 5. SSSA, Madison, WI., 1996

Maguire, R.O. & Sims, J. T. Measuring agronomic and environmental soil phosphorus saturation predicting phosphorus leaching with Mehlich 3. Soil Sci. Soc. Am. J., 66:2033–2039, 2002

Maguire, R.O., Sims, J. T., Coale, F. C. Phosphorus solubility in biosolids amended farm soils in the mid-Atlantic region of the USA. J. Environ. Qual., 29:1225–1233, 2000

McDowell, R.W., & Sharpley, A. N. Approximating P release from soils to surface runoff and subsurface drainage. J. Environ. Qual., 30:508–520, 2001

Murphy, J., & Riley, J. R. A modified single solution method for the determination of phosphate in natural waters. Anal. Chim. Acta, 27:31–36, 1962

Nair, V.D., K.M. Portier, D.A. Graetz, and M.L. Walker. 2004. An environmental threshold for degree of phosphorus saturation in sandy soils. J. Environ. Qual. 33:107-113, 2004

Negassa, W., Leinweber, P. How does the Hedley sequential phosphorus fractionation reflect impacts of land use and management on soil phosphorus: A review. J. Plant Nutr. Soil Sci., 172:305-325, 2009

Novais, R. F. & Smyth, T. J. Fósforo em Solo e Planta em Condições Tropicais. Viçosa, UFV, DPS, 1999. 399p.

Pautler, M. & Sims, J. T. Relationship between soil test phosphorus, soluble phosphorus, and phosphorus saturation In Delaware soils. J. Soil Sci. Soc., Am. 64:765-773, 2000

Pizzeghello, D., Berti, A., Nardi, S., Morari, F. Phosphorus forms and P-sorption properties in three alkaline soils after long-term mineral and manure applications in north-eastern Italy. Agriculture, Ecosystems and Environment, 141:58–66, 2011

Rouff, A. A., Natchegaal, M., Rabe, S., Vogel, F. X-ray absorption fine structure study of the effect of protonation on disorder and multiple scattering in phosphate solutions and solids. J. Phys. Chem. A., 113:6895-903, 2009

Sato, S., Solomon, D., Hyland, C., Ketterings, Q. M., Lehmann, J. Phosphorus Speciation in Manure and Manure-Amended Soils Using XANES Spectroscopy. Environ. Sci. Technol., 39:7485–7491, 2005

Sharpley, A. N. Dependence of runnoff phosphorus on extractable soil phosphorus. J. Environ. Qual., 24:920-926, 1995

Sharpley, A.N., Daniel, T. C., Sims, J. T., Lemunyon, J., Stevens, R. A., Parry, R. Agricultural phosphorus and eutrophication. USDA-ARS Rep. 149. U.S. Gov. Print. Office, Washington, DC., 1999

Sharpley, A. N. & Moyer, B. Phosphorus forms in manure and compost and their release during simulated rainfall. J. Environ. Qual., 22:597–601, 2000

Sharpley, A. N., Weld, J. L., Beegle, D. B., Kleinman, P. J. A., Gborek, W. J., Moore, P. A., Mullins, G. Development of phosphorus indices for nutrient management planning strategies in the United States. Journal of Soil and Water Conservation, 58:137-152, 2003

Shober, A. L., Sims, T. J. Evaluating phosphorus release from biosolids and manure-amended soils under anoxic conditions. J. Environ. Qual., 38:309–318, 2009

Sims, J. T., Maguire, R. O., Leytem, A. B, Gartley, K. L., Pautler, M. C. Evaluation of Mehlich-3 as an agri-environmental soil phosphorus test for the Mid-Atlantic United States of America. Soil Sci. Soc. Am. J., 66:2016-2032, 2002

Tran, T. S., N'dayegamyie, A. Long-term effects of fertilizers and manure application on the forms and availability of soil phosphorus. Can. J. Soil Sci., 75:281-285, 1995

Toor, G.S., Hunger, S., Peak, J. D., Sims, J. T., Sparks, D. L. Advances in the Characterization of Phosphorus in Organic Wastes: Environmental and Agronomic Applications, *In* Advances in Agronomy, 89:1-72, 2006

Turner, B. T. & Leytem, A. Phosphorus compounds in sequential extracts of animal manures: chemical speciation and a novel fractionation procedure. Environ. Sci. Technol., 38:6101-6108, 2004

van der Zee, S. E. A. T. M., & Van Riemsdijk, W. H. Model for long-term phosphate reaction kinetics in soil. J. Environ. Qual., 17:35–41, 1988

Vilar, C.C., Costa, A. C. S., Hoepers, A., Souza Jr., I. G. Capacidade máxima de adsorção de fósforo relacionada a formas de ferro e alumínio em solos subtropicais. Rev. Bras. Ciên. Solo. 34:1059-1068, 2010

Violante, A. & Pigna, M. Competitive sorption of arsenate and phosphate on different clay minerals and soils. Soil Sci. Soc. Am. J., 66:1788-1796, 2002

Yamuremye, F., Dick, R. P., Bahan, J. Organic amendments and phosphorus dynamics: III phosphorus Speciation. Soil Sci., 161:444-451, 1996

Zhang, Y. S., Werner, W., Scherer, H. W. Sun, X. Effect of organic manure on organic phosphorus fractions in two paddy soils. Biol Fert Soils, 17:64-68, 1994